Gholamreza Joodaki

Earth Mass Change Tracking Using GRACE Satellite Gravity Data

Thesis for the degree of Philosophiae Doctor

Trondheim, January 2014

Norwegian University of Science and Technology
Faculty of Engineering Science and Technology
Department of Civil and Transport Engineering

NTNU – Trondheim
Norwegian University of
Science and Technology

NTNU
Norwegian University of Science and Technology

Thesis for the degree of Philosophiae Doctor

Faculty of Engineering Science and Technology
Department of Civil and Transport Engineering

ISBN 978-82-326-0002-1 (printed ver.)
ISBN 978-82-326-0003-8 (electronic ver.)
ISSN 1503-8181

Doctoral theses at NTNU, 2014:34

Printed by NTNU-trykk

Abstract

This project is dealing with the estimation of present-day Earth's mass transport and its redistribution by using observations from Gravity Recovery and Climate Experiment (GRACE) satellite mission. GRACE measures the gravity fluctuations which are primarily related to redistribution of water around the globe. GRACE data has yield profound new insights into melting rates of ice sheets and mountain glaciers, land hydrology, ocean circulation, and sea level rise.

In this project, first, the ice melting rate in the Greenlandic ice sheet is studied. This is done by analyzing the time series of monthly GRACE release 04 gravity field solutions from three different data sets, CSR (Center for Space Research), GFZ (Geoforschungszentrum), and JPL (Jet Propulsion Laboratory) with respect to their long-term temporal changes. The data are de-striped by applying a non-isotropic filter. Also, a method for reducing the leakage effects is developed. As an example, the ice mass balance is estimated of -163 ± 20 Gt/yr based on the CSR release 04 and smoothing by a parameter of $a = 10^{13}$ during April 2002 to February 2010. The results also show that the spatial distribution of the ice mass loss is changing with time and the ice mass loss is accelerating. For example, its acceleration is a rate of –32±6 Gt/yr^2 during 2002 to 2011.

The second part of this project is concern with the determination of water mass changes in the Nordic Seas. It is determined by analyzing the time series of monthly GRACE level 2 release 04 data from GFZ during October 2002 to October 2010. The striping errors are reduced by using a non-isotropic filter and the data are smoothed by a parameter of $a = 10^{14}$ according to Gaussian smoothing radius of 530 km. The time

series of water mass changes are used to study the steric sea height variations over the Nordic Seas during the same period of study. This is done by analyzing the time series of monthly sea level anomaly from ENVISAT (Environmental Satellite) altimetry data, cycles 10 to 93, among the time series of water mass changes. The results show that the interdisciplinary nature of the GRACE measurements have opened up the unique opportunity to enhance our knowledge on the interaction between Earth system components and their response to climate variability.

In the last part of this project, variations of the continental total water storage, total groundwater storage, and anthropogenic contributions across the Middle East are studied. By using a mascon analysis method and GRACE level 2 release 05 data from CSR during February 2003 to December 2012, the time series of total water storage, total ground water storage and anthropogenic contributions are estimated over this region. The region is subdivided to seven mascons including Iran, Iraq, Syria, eastern Turkey (east of 35^{o} longitude), northern and southern Saudi Arabia (north and south of 25^{o} latitude), and the region immediately west of Caspian Sea. The total groundwater storage, and anthropogenic contributions are separated from the total water storage by using the CLM4.5 (version 4.5 of the Community Land Model) hydrological model. The results show that Iran with a rate of 25±6 Gt/yr has the most groundwater loss rate during February 2003 to December 2012 in this region. The Iran's rate of groundwater loss from the GRACE data is supported by an analysis of in situ well data from across Iran. The results also show that the GRACE mission is able to monitor monthly water storage changes within river basins and aquifers that are 200,000 km^2 or larger in area, and, can contribute to water management at regional and national scales, and to international policy discussions as well.

Acknowledgements

I sincerely thank my supervisor Prof. Hossein Nahavandchi for his support, trust and confidence in my abilities to do this PhD research. He has always supported my ideas and helped me by his constructive discussions, reviews, and comments on my articles.

I would like to express special thanks to Prof. John Wahr for his hospitality and supervision during my extended visit in Colorado University. With his great knowledge in applications of Gravity Recovery and Climate Experiment (GRACE) satellite mission, John taught me how to analysis the GRACE data to study the continental water storage changes. John has also put a lot of efforts and enthusiasm into the manuscript: Joodaki et al. (2013).

I am grateful to all staffs in the division of Geomatics at Norwegian University of Science and Technology (NTNU) for their hospitality and memorable working environment.

Finally, and most of all, I am indebted to my amazing wife, Zohreh, and my beloved daughter, Taranom, for their love, patience and dedications all the way through my PhD study.

This PhD study was funded by Norwegian University of Science and Technology (NTNU).

Table of Contents

List of Figures

List of Tables

Chapter 1

Introduction

The main goal of this Ph.D. study is a monitoring and understanding of the Earth's mass change and its distribution in ocean, continental water storages such as groundwater, and ice sheets with seasonal, annual and inter-annual contributions as well as secular trends.

1.1 Motivation:

In recent years the public concern about future of the Earth, its climate, its environment and shortage of its natural resources has been more than ever before. According to the 4th Intergovernmental Panel on Climate Change (IPCC) report (Solomon et al., 2007), the climate changes are influenced by man-made effects. Understanding of the Earth's mass changes as a result of climate changes is one of the key parameters to major decisions facing human societies. The Earth's mass distribution is constantly changing. Variations in the distribution of mass might be happened due to tides in the ocean and solid earth, atmospheric disturbing with synoptic storms, seasonal climatic changes, and etc. Variations in the mass distribution cause temporal changes in the Earth gravity filed. The mass changes and its redistributions are reflected in small amplitudes, but they manifest themselves with large scale changes of gravity and the geoid, which are observable by satellites or ground-based instrumentations. Figure 1.1 shows the interrelation of gravity and its variations with the mass transport and its redistribution. The most permanent mass transport and its redistribution are occurred by ocean

circulation, water fluxes between various terrestrial water storages, ice melting, and sea level changing. In addition, mass variability is also happened by the mantel convection. This process which has large amplitudes compared to those associated with climatic variability, occurs slowly relative to human timescales through the whole of mantel. Instrument accuracy has in the past been insufficient to measure the small changes in the gravitational acceleration, caused by changes in water storage, but nowadays thanks to satellite gravity missions with very precise sensors, this obstacle has been overcome. Satellite gravity observations also have a global coverage and it can fill gaps in data of ground-based instrument. Gravity Recovery and Climate Experiment (GRACE) satellite mission provides a record of time-variable gravity with a resolution from global scales down to a few hundred kilometers. GRACE observations have sufficient resolution and accuracy to study variations in total terrestrial water storage, including snow, surface water, soil moisture and groundwater.

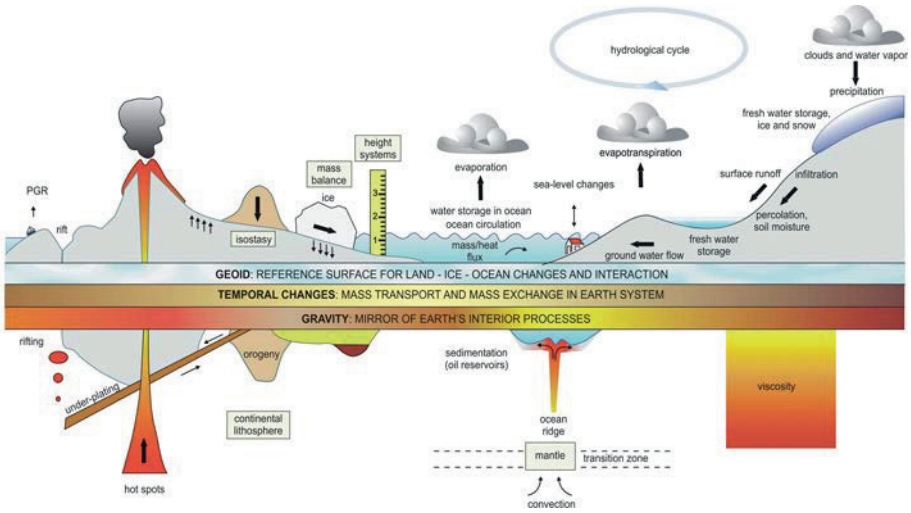

Figure 1.1. Interrelation of gravity, gravity variations, mass transport and distribution (Ilk et al., 2005)

Many research groups have used GRACE data to estimate rates of the Earth's mass change, for example Ice mass change in polar regions (Joodaki and Nahavandchi, 2012a; Nahavandchi and Joodaki, 2012; Sørensen and Forsberg, 2010; Baur et al., 2009; Velicogna and Wahr, 2005), depletion of groundwater (Famiglietti et al., 2011; Rodell et al., 2009; Tiwari et al., 2009), reservoir storage changes (Wang et al., 2011; Swenson

and Wahr, 2009), and ocean mass change (Joodaki et al., 2013; Chambers and Schroter, 2011; Morison et al., 2007).

1.2 Scientific objectives

In this thesis, the state of the art research concerning the Earth's mass variations, caused by changes in water storage will be outlined. Results for Ice sheet melting, groundwater depletion and ocean mass variations will be summarized. In the fact, the scientific objectives in this thesis are threefold. First, it is to derive a mass balance of the Greenland ice sheet. Second, it is to extract natural and anthropogenic changes in the distribution of water stored in the soil and sub- soil layers of the Earth in the Middle East. Third, it is to estimate mass variations in Nordic seas. Besides determining the mass changes, spreading and acceleration of ice mass loss in Greenland ice sheet, steric sea level variations in Nordic seas and temporal variations of Iranian groundwater estimates based on in situ observations of well levels will be also presented.

1.3 Scientific method

For this project, the mass change estimation is derived using the gravity satellite mission GRACE data. The observed spatio-temporal gravity changes are associated with mass re-distribution in the atmosphere and in and on the Earth. A challenge when using this method is to separate the signals contributing to the gravity signature, such as hydrology, Glacial Isostatic Adjustment (GIA) and present-day mass changes. The change in gravity caused by the mass changes can be isolated by modeling the other contributing signals, and hence the mass change can be determined from the gravity changes by forward modeling.

1.4 Structure of Thesis

This thesis is based on six papers which are described in the following and they are enclosed in App. A-F. The thesis contents are supplementary to the contents of these six papers. The thesis structure has been shown in Figure 1.2.

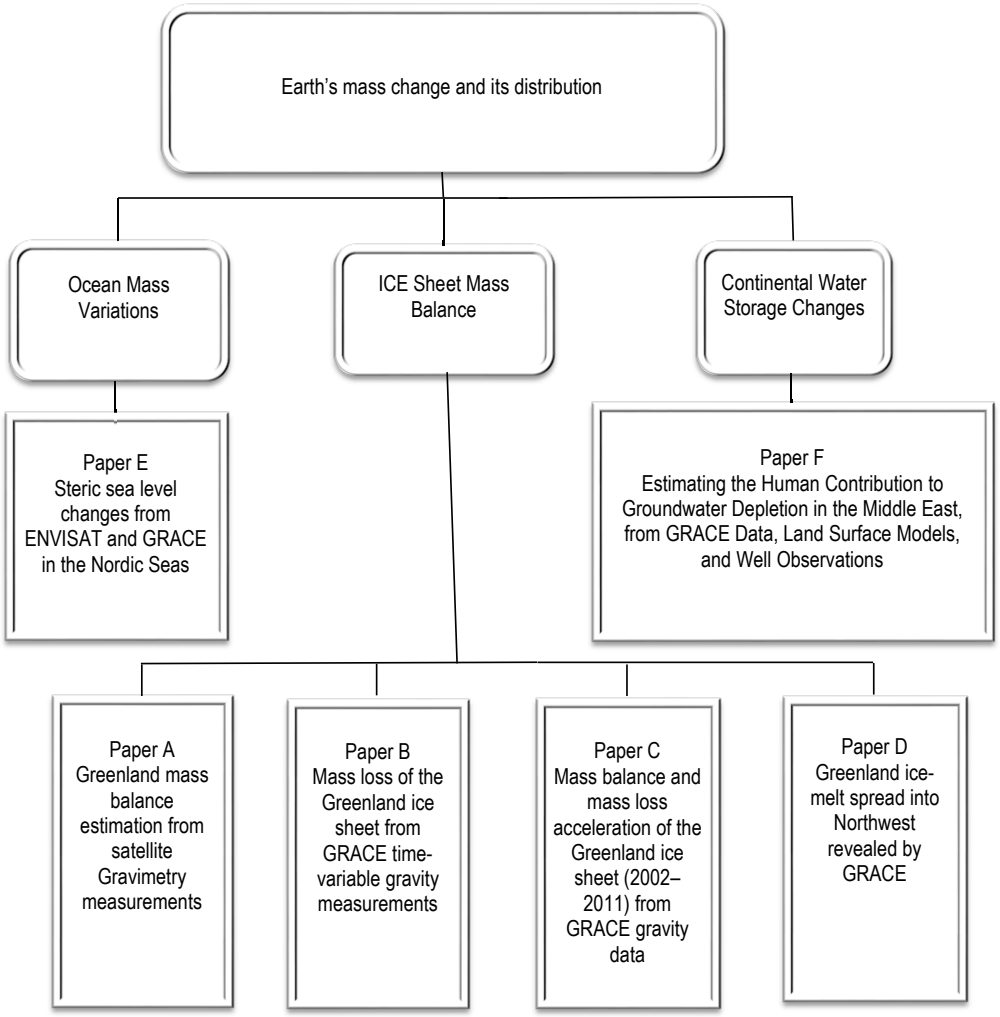

Figure 1.2. Structure of the thesis

1.5. Scientific Papers

The papers listed below are the scientific works which have been carried out in this Ph.D. project.

Paper A

Gholamreza Joodaki and Hossein Nahavandchi, (2010), Greenland mass balance estimation from satellite gravity measurements, ESA Living Planet Conference, ESA Special Publication SP-686.

This paper is based on the results of the first attempt to compute the mass balance of the Greenland ice sheet in this Ph.D. project. It addresses the ice mass balance on the Greenland ice sheet using 2002 – 2010 GRACE level 2 release 04 data. The GRACE data was from the Center for Space Research at the University of Texas (CSR) which its high frequency noise had been filtered out in three different smoothing cap radiuses by a non-isotropic filter. In this study C_{20} coefficients of the spherical harmonic solutions were substituted with those obtained from satellite laser ranging (SLR) and for separation of leakage effects, the appropriate reduction model was used. To estimate the time series of mass changes using the GRACE data and its necessary corrections, a software package had been developed. Taking the average over all smoothing radiuses, we found the total Greenland mass balance of 155 $Gtyr^{-1}$ from the CSR data.

Paper B

Gholamreza Joodaki and Hossein Nahavandchi, (2012), Mass loss of the Greenland ice sheet from GRACE time-variable gravity measurements, Stud. Geophys. Geod., 56, 197-214, DOI: 10.1007/s11200-010-0091-x.

In this paper, the total Greenland mass loss was estimated by using the GRACE level 2 release 04 data from three different processing centers, Center for Space Research (CSR), German Research Center for Geosciences (GFZ) and Jet Propulsion Laboratories (JPL). The data time span was April 2002 to February 2010. Striping effects in the GRACE data had been filtered out using a non-isotropic filter in three different smoothing radiuses. The monthly SLR estimates for C_{20} coefficient were used

to replace the estimates from GRACE. For separation leakage effects, a method based on the GRACE data had been used. We found mass losses of -163 $Gtyr^{-1}$, -161 $Gtyr^{-1}$, and -84 $Gtyr^{-1}$ based on CSR, GFZ, and JPL data respectively and a degree of smoothing corresponds to a Gaussian filter with a radius of 340 km. It was also concluded that there was some significant spread of the results among different processing centers of GRACE solutions.

Paper C

Gholamreza Joodaki and Hossein Nahavandchi, (2012), Mass balance and mass loss acceleration of the Greenland ice sheet (2002– 2011) from GRACE gravity data, Journal of Geodetic Science, 2(2), 156-161 DOI: 0.2478/v10156-011-0032-9.

In this paper the magnitude and acceleration of the Greenland ice sheet mass loss between 2002 and 2011 were examined. Using monthly observations of time-variable gravity from the GRACE satellite gravity mission, the time series of the Greenland mass changes were estimated. Such as paper A and B, the C_{20} coefficient was substituted with those obtained from the SLR and the leakage effects were reduced by the method which has been described in the paper B. We also used a non-isotropic filter whose degree of smoothing corresponds to a Gaussian filter with a radius of 340 km. It was concluded that the Greenland mass loss during this time period was not a constant, but accelerating with time. Fitting a quadratic trend to the monthly time series, we found the mass loss increased from -121 $Gtyr^{-1}$ in 2002 – 2003 to -210 $Gtyr^{-1}$ in 2006 – 2007 and -271 $Gtyr^{-1}$ in 2010 – 2011 with an acceleration of -32±6 $Gtyr^{-2}$ in 2002 – 2011.

Paper D

Hossein Nahavandchi and Gholamreza Joodaki, (2012), Greenland ice-melt spread into Northwest revealed by GRACE, Kart og Plan, Volume 72, Annual 105, 234-240.

It addresses to spread the Greenland ice melting from the southern region to the northwest region in the period of 2007-2010. In this study the 2002-2010 GRACE level 2 Release04 data from CSR were used that they had been filtered out with a non-isotropic filter whose degree of smoothing corresponds to a Gaussian filter with a radius of 340 km and the C_{20} coefficient was replaced by the monthly SLR estimates for it.

The method which has been described in paper B was used to reduce the leakage effects. It was concluded that a rapid mass loss of the Greenland icecap was spread from southern portions to northwest Greenland coast in 2007-2010. It was also concluded that the ice sheet was losing mass nearer to the ice sheet margins than in the interior portions.

Paper E

Gholamreza Joodaki, Hossein Nahavandchi, and Kourosh Ghazavi (2013), Steric sea level changes from ENVISAT and GRACE in the Nordic Seas, 20 years of Progress in Radar Altimetry symposium, ESA publication SP-710.

In this paper, steric sea level changes were estimated over the Nordic Seas using altimetry and gravity data. The data were based on the monthly GRACE solution from GFZ and the Environmental Satellite (ENVISAT) altimetry during October 2002 to October 2010. The paper includes two parts. The first part is dealt with ocean mass changes using the GRACE data and the second part is related to the sea level anomaly estimation. The data reconciliation is important in the combination of satellite altimetry with the GRACE data. GRACE data do not include degrees 0 and 1 spherical harmonic coefficients and the C_{20} coefficient has not been well observed by GRACE. GRACE data also have no atmospheric and oceanic mass signals effects. In the process of the GRACE data, the atmospheric mass and ocean barotropic variations are removed, meanwhile it is necessary for comparison with the altimetry data. In this study using the proper models, the GRACE data were reconciled with the altimetry data. After reconciling the data, the time series of the ocean mass changes and the sea level anomaly were computed. Subtracting the ocean mass changes from the sea level anomaly, the steric sea level changes were derived over the Nordic Seas for October 2002 to October 2010.

Paper F

Gholamreza Joodaki, John Wahr, and Sean Swenson (2013), Estimating the Human Contribution to Groundwater Depletion in the Middle East, from GRACE Data, Land Surface Models, and Well Observations, Water Resources Research, under review.

The Gravity Recovery and Climate Experiment (GRACE) satellite data is used to evaluate monthly freshwater storage trends in the Middle East during February 2003 to December 2012. The results show a large negative trend in the total water storage estimates, centered over western Iran and eastern Iraq. Removing contributions from the Caspian Sea and from two large lakes, Tharthar and Urmiah, in the region and combining the GRACE data with a modified version of the CLM4.5 hydrological model to remove natural variability, we conclude that most of the long-term, sub-surface water loss in this region is due to a decline in groundwater storage. By dividing the entire region into seven mascons outlined along national boundaries, including Iran, Iraq, Saudi Arabia, Turkey, Syria and the region immediately west of the Caspian Sea and fitting them to the Stokes coefficients, we find an alarming rate of groundwater depletion in Iran with 25±6 Gt/yr during the study period. The conclusion of significant groundwater loss is supported by the in situ well data from across Iran. Furthermore, anthropogenic groundwater trends are estimated across the region by removing the natural variations in groundwater from the CLM4.5 hydrological model. Though over half of the groundwater loss in Iran (14±6 Gt/yr) may be the anthropogenic contributions, the results show that in most places of this region the naturally occurring groundwater loss is larger than the anthropogenic loss.

Chapter 2

Gravity Recovery and Climate Experiment (GRACE) Satellite Mission

2.1. Mission Objectives and Follow on

Gravity Recovery and Climate Experiment (GRACE) satellite mission has two satellites which were launched in March 17th 2002 by a joint project between the US National Aeronautics and Space Administration (NASA) and German Aerospace Center (DLR) (Figure 2.1). The primary objective of the project was to provide with unprecedented accuracy, global and high-resolution models of the Earth's gravity field, of both the static and time varying component (Tapley et al., 2004). The precise geoid determination in conjunction with satellite altimetry and in-situ data will allow to significant advances in the oceanographic community studies such as ocean heat flux (Song and Colberg, 2011), long term sea level change (Chen et al., 2005), upper oceanic heat content (Jayne et al., 2003), and the absolute surface geostrophic currents (Dobslaw et al., 2004). Usage of GRACE to accurate determination of the time variations in the Earth’s gravity field is beneficial to many areas of scientific research such as oceanography, hydrology, glaciology or solid Earth sciences.

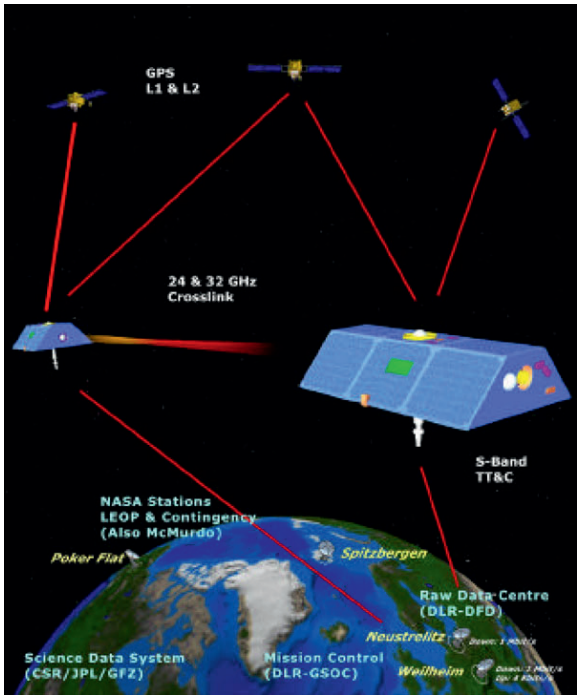

Figure 2.1. GRACE satellite mission (Dunn et al., 2003)

Study of the time varying component of the Earth's gravity field will help to better understanding of time variable processes like deep ocean current changes (Wahr et al., 2002), large-scale evapotranspiration (Ramillien et al., 2006), soil moisture changes (Swenson et al., 2008), mass balance of ice sheets and glaciers (Joodaki and Nahavandchi, 2012b; Velicogna and Wahr, 2005), changes in the storage of water and snow of the continents (Swenson and Wahr, 2002), mantle and lithospheric density variations, postglacial rebound or solid Earth's Isostatic response (Velicogna and Wahr, 2002). The secondary objective was to record globally distributed profiles of the GPS signal excess delay caused by the atmosphere and ionosphere which can be converted to total electron content and/or refractivity, respectively (Beyerle et al., 2006).

Though the planned lifetime of the GRACE mission was originally 5 years, the satellites are still operating today. In June 2010 NASA and DLR signed an agreement to extent the mission to 2015 (Buis, 2012). Recognizing the importance of extending this long term dataset, NASA has approved the development and launch of the GRACE

Follow On mission. This project will be jointly with Germany, and the mission will be launched in August 2017 (Watkins, 2013).

2.2. Measurement principle

The twin satellites of GRACE are flying at an altitude of 450- 500 km in a near polar orbit with an inclination of 89.5^{o}. The satellites have been separated by a distance of approximately 220 km. GRACE satellites are tracking each other in a low Earth orbit (LEO), so GRACE is called Low-Low satellite to satellite tracking (LL-SST) mission. The estimation of gravity fields using LL-SST mission is a relatively new development, and GRACE is in fact the first mission of its kind. When the GRACE satellites pass over a mass anomaly on or near the surface of the Earth, the leading satellite senses the anomaly first as it causes a small perturbation in the orbit. Shortly after, the trailing satellite feels the exact same perturbation caused by the same anomaly, only slightly displaced in time. This perturbation is observed as a change in distance between the two satellites. Using observed changes in the inter-satellite distance, position and acceleration of each satellite, the Earth's gravity field can be determined. Changes in the inter-satellite distance are the mission data, while acceleration and position are made for each satellite. The position of each satellite is precisely determined by the GPS (Global Positioning System) satellites. The resolution of the gravity field which can be recovered from the tracking data depends on the orbital height. The lower the orbit, the better the resolution, but also the more drag on the satellites and the shorter life time.

2.3. GRACE Instrumentation

Micron- level measuring the range and rate range between the satellites is the key scientific element of GRACE. An extremely precise microwave ranging system (within 10 μm), named K/K_a-band Ranging System (KBR) placed at the center of mass of each satellite, measures the inter-satellite distance (Dunn et al., 2003). Additionally each spacecraft carries three instruments: a GPS receiver, a precision accelerometer and a star camera. The precise accelerometer, with a precision of 0.1 nanometer per second squared, is used to measure the non-gravitational accelerations of the satellites (ibid.). The GPS receivers on-board the satellites enable precise time-tagging and positioning with accuracy on the cm level (ibid.). The GPS receivers can track up to 14 GPS

satellites with dual- frequency data quality comparable to precision geodetic ground receivers. High precision inertial orientation of the satellites is measured by the star tracker with a precision of 25 arc seconds (0.0075 degrees) (ibid.).

2.4. GRACE gravity data levels

Extraction of Earth gravity models is being handled by the three processing centers within the GRACE project Science Data System (SDS): the Center for Space Research at the University of Texas, Austin (UTCSR), Jet Propulsion Laboratory (JPL) at Pasadena, USA and the Geoforschungszentrum in Potsdam, Germany (GFZ). After validation, the SDS delivers monthly models of Earth gravity field, and distributes it to public via Physical Oceanography, Distributed Active Archive Center (PO.DAAC) at JPL and Information Systems and Data Center (ISDC) at GFZ. The GRACE data is divided into three levels which are explaining in the following (Figure 2.2).

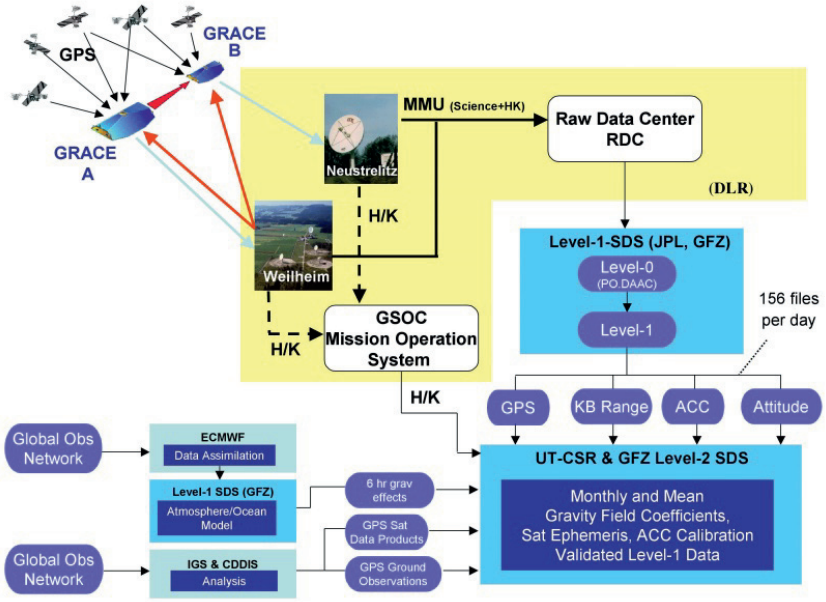

Figure 2.2. GRACE mission data flow (courtesy to UTCSR)

2.4.1. Level-0 DATA:

The raw stream data from each GRACE satellite is received at the Mission Operation System (MOS) twice per day using its Weilheim and Neustrelitz tracking antennae. The level-0 data are the GRACE raw data which are stored in two appropriate files, science instrument and housekeeping data by the Raw Data Center (RDC) of the MOS located in Neustrelitz/Germany (Bettadpur, 2003). The SDS centers retrieves these files and extracts and reformats the corresponding instrument and ancillary housekeeping data like GPS navigation solutions, space segment temperatures or thruster firing events. Afterwards the data is transferred to the SDS permanent archives (Bettadpur, 2007). The interesting data for gravity field estimations are the inter satellite range-rate measurements (μm/s), but also accelerometer data and attitude and positioning data are important.

2.4.2. Level-1 DATA:

Level-1 data are the preprocessed, time-tagged and normal-pointed instrument data including the K-band ranging, accelerometer, star camera and GPS data of both satellites. As shown in Figure 2.3, processing of level-1 products are done primarily at JPL with supporting from GFZ (e.g. accelerometer data preprocessing), and in case of hardware or network problems, there is an identical processing system (hardware/software) in GFZ to serve as a backup system. The level-1 data are divided into level-1A and level-1B. Level-1A data are the raw data which have been calibrated and time-tagged in a non-destructive sense as the data can be reversed to obtain the original level-0 data if desired, except for bad data packets. Level-1A data products are not distributed to public. Level-1B data products include among others, the inter-satellite range, range-rate, range-acceleration, the non-gravitational accelerations from each satellite, the pointing estimates, the orbits, etc. After validation, level-1B data products are released to the public through PO.DAAC at JPL and ISDC at GFZ. These products are processed to produce the monthly gravity field estimates in form of spherical harmonic coefficients. The leve-1B data is possibly irreversible (Bettadpur, 2007).

2.4.3. Level-2 DATA:

Level-2 data are the monthly and mean gravity field derived from calibrated and validated GRACE level-1 data products among the precise orbits of both GRACE satellites and ancillary data sets (temperature and pressure fields, ocean bottom pressure, and hydrological data) which are necessary to eliminate time variabilities in gravity field solutions. All level-2 products are archived at JPL's PODAAC and at GFZ's ISDC and are available 60 days after data taking. The level-2 processing software is developed independently by all the three processing centers using already existing but completely independent software packages which are upgraded for GRACE specific tasks. Routine processing is done at UTCSR and GFZ, while JPL only generates level-2 products at times for verification purposes (Figure 2.3).

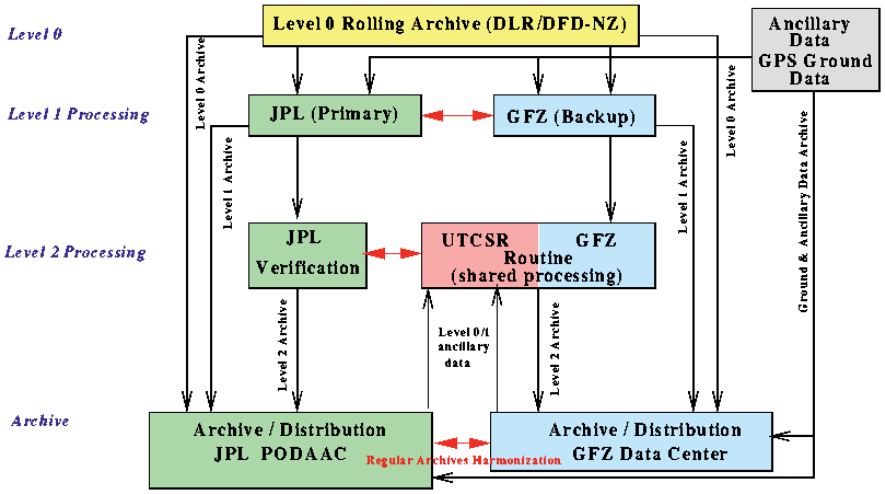

Figure 2.3. GRACE SDS products (courtesy to GFZ)

The GRACE level-2 data are provided as sets of fully normalized spherical harmonic coefficients, C_{lm}, S_{lm}, also called Stokes coefficients. The degree and order of the coefficients are up to 60, 120, and 120 for CSR, GFZ, and JPL respectively. The coefficients are distributed on the level-2 data archives as GAC, GAD and GSM files

(GAC, GAD and GSM are file extensions). The GSM files contain spherical harmonic coefficients representing the gravity field of the Earth. The atmospheric and oceanic mass signals effects have been removed from these coefficients. The GAC and GAD files include the modeled atmospheric and oceanic contributions to the GSM coefficients. The GAC files include the global atmospheric and oceanic effects and the GAD files represent ocean bottom pressure variations. The latest version of the data is release 05 from CSR, GFZ, and JPL which is more accurate. Figure 6 shows the time span of the GRACE level-2 data for the three processing centers, CSR, GFZ, and JPL. As shown in Figure 2.4, there are some missing data for the GRACE level-2 data products for instance, for all three data sets, the months June-July 2002 and June 2003 are missing due to missing accelerometer data. The months January 2011 and October 2012 are missing for all three data sets as well. The data of the month January 2003 is missing only for GFZ processing center.

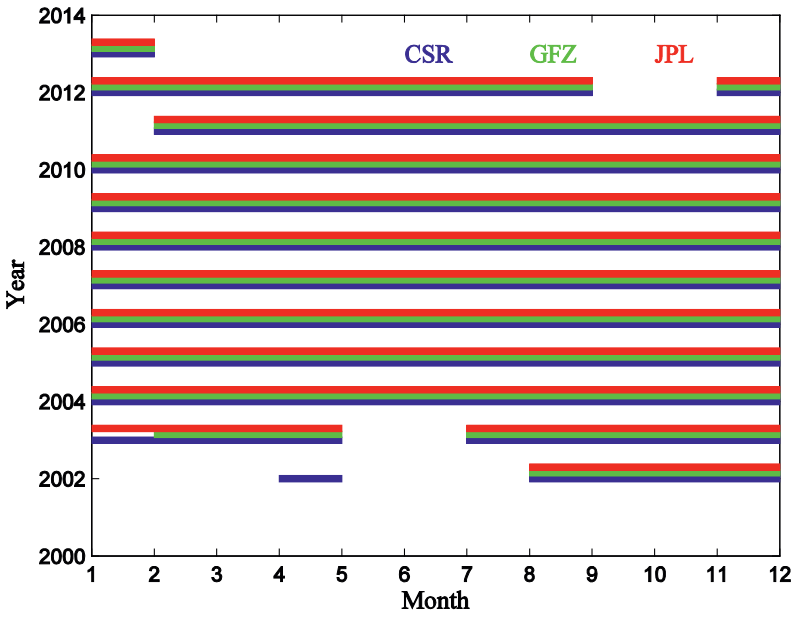

Figure 2.4. Time span of the GRACE level-2 data for the three processing centers, CSR in blue, GFZ in green, and JPL in red

Chapter 3

Surface Mass Changes from GRACE

3.1. Basics

According to Newton's gravitational law, the gravitational potential U at any field point r_0 in the exterior of the body which has the mass density distribution $\rho(r)$ is:

$$U(r_0) = G\int \frac{\rho(r)}{|r - r_0|}\mathrm{d}V \qquad (1\text{-}3)$$

where G is the gravitational constant, r locates the mass element in dV, and the integration is over the entire volume V of the body. Invoking the multi-pole expansion in spherical coordinates and using surface harmonic functions and their complex conjugation, we can write equation (1-3) in following form:

$$U(r_0) = G\sum_{l=0}^{\infty}\sum_{m=-l}^{l}\frac{4\pi}{2l+1}\Gamma_{lm}\frac{1}{r_0^{l+1}}Y_{lm}^{*}(\Omega_0) \qquad (2\text{-}3)$$

where Ω_0 is an abbreviation for the latitude and longitude (φ_0, λ_0) and Y_{lm}^{*} is the complex conjugation of surface harmonic function of degree l and order m, defined by

$$Y_{lm}^{*}(\Omega)=(-1)^{m}\left(\frac{(2l+1)}{4\pi(l+m)!}\right)^{1/2}P_{lm}(\sin\varphi)\exp(im\lambda) \tag{3-3}$$

and the complex-valued coefficients

$$\Gamma_{lm}=\int\rho(r)r^{l}Y_{lm}(\Omega)\mathrm{d}V \tag{4-3}$$

are the multi-pole moments of the density distribution $\rho(r)$. It is customary to express $U(r_0)$ in the following form:

$$U(r_0)=\frac{GM}{r_0}\sum_{l=0}^{\infty}\sum_{m=0}^{l}\left(\frac{a}{r_0}\right)^{l}\tilde{P}_{lm}(\sin\varphi_0)\left(C_{lm}\cos m\lambda_0+S_{lm}\sin m\lambda_0\right) \tag{5-3}$$

where M is the total mass of the body, $\tilde{P}_{lm}$ is the normalized associated Legendre function:

$$\tilde{P}_{lm}=\left(\frac{(2-\delta_{m0})(2l+1)(l-m)!}{(l+m)!}\right)^{1/2}P_{lm} \tag{6-3}$$

where P_{lm} is the associated Legendre function and δ is the Kronecker delta function. Comparing the two equivalent equations (2-3) and (5-3), and using the relation $Y_{l,-m}(\Omega)=(-1)^{m}Y_{lm}^{*}(\Omega)$ as well as a similar relation for Γ_{lm}, one gets

$$C_{lm}+iS_{lm}=\left(K_{lm}\big/Ma^{l}\right)\Gamma_{lm} \tag{7-3}$$

For m=0, 1, 2… l, where $i=\sqrt{-1}$. The normalization constant K_{lm} is given by

$$K_{lm}=(-1)^{m}\,2\sqrt{(2-\delta_{m0})\pi}\,\big/(2l+1) \tag{8-3}$$

Equation (7-3) relates the physical quantity Γ_{lm} (multiple moments of the density distribution $\rho(r)$) to the geodetic parameters C_{lm} and S_{lm}.

Geoid is the equipotential surface of the Earth's gravity field which best fits, in a least squares sense, global mean sea level. The geoid surface (or its deviation from a reference ellipsoid- a mathematical shape of the Earth- the geoidal height N) can be computed globally from Global Gravity Models like GRACE models. It is usual to compute the geoidal height from a spherical harmonic representation of Earth's gravity field:

$$N(\varphi,\lambda) = a\sum_{l=0}^{\infty}\sum_{m=0}^{l}\tilde{P}_{lm}(\sin\varphi)\left(C_{lm}\cos\left(m\lambda\right)+S_{lm}\sin\left(m\lambda\right)\right) \tag{9-3}$$

where a is the radius of the Earth. The GRACE mission, and its numerical coefficients C_{lm}, S_{lm} are very useful for time-variable gravity− or geoid ΔN−studies. ΔN is a time-dependent change in the geoid. ΔN can represent either the change in N at one time to another, or as the difference between N at one time and a time average of N, or as some other representation of a changing N. This change can be represented in terms of changes, ΔC_{lm} and ΔS_{lm}, in the spherical harmonic geoid coefficients as

$$\Delta N(\varphi,\lambda) = a\sum_{l=0}^{\infty}\sum_{m=0}^{l}\tilde{P}_{lm}(\sin\varphi)\left(\Delta C_{lm}\cos\left(m\lambda\right)+\Delta S_{lm}\sin\left(m\lambda\right)\right) \tag{10-3}$$

Changes in the gravity field/geoid are caused by the redistribution of mass within the Earth and on or above its surface. Therefore, the density redistribution $\Delta\rho\left(r,\varphi,\lambda\right)$ can cause the geoid change ΔN. By combining equations (3-3), (4-3), (6-3), (7-3), and (8-3) it can be shown that (see also Wahr et al., 1998)

$$\begin{Bmatrix}\Delta C_{lm}\\ \Delta S_{lm}\end{Bmatrix} = \frac{3}{4\pi\rho_{\text{ave}}\left(2l+1\right)}\int\Delta\rho\left(r,\varphi,\lambda\right)\tilde{P}_{lm}\left(\sin\varphi\right)\times\left(\frac{r}{a}\right)^{l+2}\begin{Bmatrix}\cos\left(m\lambda\right)\\ \sin\left(m\lambda\right)\end{Bmatrix}\cos\varphi\,\mathrm{d}\varphi\,\mathrm{d}\lambda\,\mathrm{d}r \tag{11-3}$$

where ρ_{ave} is the average density of the Earth (=5517kg/m^3). $\Delta\rho$ is concentrated in a thin layer of thickness H at the Earth's surface. This layer must be thick enough to include those portions of the atmosphere, oceans, ice caps, and below-ground water storage with significant mass fluctuations. Thus H is mostly determined by the thickness of the atmosphere and is of the order of 10-15 km. We define the change in surface density (i.e., mass/area), $\Delta\sigma$ as the radial integral of $\Delta\rho$ through this layer:

$$\Delta\sigma(\varphi,\lambda)=\int\Delta\rho(r,\varphi,\lambda)\,\mathrm{d}r \tag{12-3}$$

The GRACE errors for large values of l are likely to be large enough that there is little hope of GRACE recovering useful time variable geoid coefficients for $l \succ\approx 100$. In fact, most of the recoverable time-dependent gravity signal will be concentrated at degrees well below 80 or so. Thus the sum over (l, m) in (10-3) can be truncated to degrees $l \prec l_{\max}$, where, at most, $l_{\max}\approx 100$. Considering H thin enough that $\left(H/a\right)^{(l_{\max}+2)} << 1$ then $\left(r/a\right)^{l+2}\approx 1$, and so (11-3) reduces to

$$\begin{Bmatrix}\Delta C_{lm}\\ \Delta S_{lm}\end{Bmatrix}_{\text{surface mass}}=\frac{3}{4\pi\rho_{\text{ave}}(2l+1)}\int\Delta\sigma(\varphi,\lambda)\tilde{P}_{lm}(\sin\varphi)\begin{Bmatrix}\cos(m\lambda)\\ \sin(m\lambda)\end{Bmatrix}\cos\varphi\,\mathrm{d}\varphi\,\mathrm{d}\lambda \tag{13-3}$$

Equation (13-3) describes the contribution to the geoid from the direct gravitational attraction of the surface mass. That surface mass also loads and deforms the underlying solid Earth, which causes an additional geoid contribution:

$$\begin{Bmatrix}\Delta C_{lm}\\ \Delta S_{lm}\end{Bmatrix}_{\text{solid Earth}}=\frac{3k_l}{4\pi a\rho_{\text{ave}}(2l+1)}\int\Delta\sigma(\varphi,\lambda)\tilde{P}_{lm}(\sin\varphi)\begin{Bmatrix}\cos(m\lambda)\\ \sin(m\lambda)\end{Bmatrix}\cos\varphi\,\mathrm{d}\varphi\,\mathrm{d}\lambda \tag{14-3}$$

where k_l is the load Love number of degree l. The total geoid change is the sum of (13-3) and (14-3):

$$\begin{Bmatrix}\Delta C_{lm}\\ \Delta S_{lm}\end{Bmatrix}=\begin{Bmatrix}\Delta C_{lm}\\ \Delta S_{lm}\end{Bmatrix}_{\text{surface mass}}+\begin{Bmatrix}\Delta C_{lm}\\ \Delta S_{lm}\end{Bmatrix}_{\text{solid Earth}} \tag{15-3}$$

To summarize these results for ΔC_{lm} and ΔS_{lm} in a more compact form, we expand $\Delta\sigma$ as

$$\Delta\sigma(\varphi,\lambda)=a\rho_{\text{w}}\sum_{l=0}^{\infty}\sum_{m=0}^{l}\tilde{P}_{lm}(\sin\varphi)\left(\Delta\hat{C}_{lm}\cos(m\lambda)+\Delta\hat{S}_{lm}\sin(m\lambda)\right) \tag{16-3}$$

where ρ_{w} is the density of water (assumed to be 1000 kg/m^3), and is included here so that $\Delta\hat{C}_{lm}$ and $\Delta\hat{S}_{lm}$ are dimensionless. Note that $\Delta\sigma/\rho_{\text{w}}$ is the change in surface mass

expressed in equivalent water thickness. By noting that the $\tilde{P}_{lm}$ variables are normalized so that

$$\int_0^{\pi} \overline{P}_{lm}^2(\sin\varphi)\cos\varphi \mathrm{d}\varphi = 2\left(2-\delta_{m,0}\right) \tag{17-3}$$

We conclude from (16-3) that

$$\begin{Bmatrix} \Delta\hat{C}_{lm} \\ \Delta\hat{S}_{lm} \end{Bmatrix} = \frac{1}{4\pi a\rho_{\mathrm{w}}} \int_0^{2\pi} \mathrm{d}\lambda \int_0^{\pi} \cos\varphi \mathrm{d}\varphi \times \Delta\sigma(\varphi,\lambda)\tilde{P}_{lm}(\sin\varphi) \begin{Bmatrix} \cos(m\lambda) \\ \sin(m\lambda) \end{Bmatrix} \tag{18-3}$$

Using (13-3) and (14-3) in (15-3), and using (18-3), we find a simple relation between $\Delta\hat{C}_{lm}$, $\Delta\hat{S}_{lm}$ and ΔC_{lm}, ΔS_{lm}:

$$\begin{Bmatrix} \Delta\hat{C}_{lm} \\ \Delta\hat{S}_{lm} \end{Bmatrix} = \frac{\rho_{\mathrm{ave}}}{3\rho_{\mathrm{w}}} \frac{2l+1}{1+k_l} \begin{Bmatrix} \Delta C_{lm} \\ \Delta S_{lm} \end{Bmatrix} \tag{19-3}$$

Now, using (19-3) in (16-3) one can find the change in surface mass density from changes ΔC_{lm} and ΔS_{lm} in the geoid coefficients.

$$\Delta\sigma(\varphi,\lambda) = \frac{a\rho_{\mathrm{ave}}}{3} \sum_{l=0}^{\infty} \sum_{m=0}^{l} \frac{2l+1}{1+k_l} \tilde{P}_{lm}(\sin\varphi)\left[\Delta C_{lm}\cos(m\lambda) + \Delta S_{lm}\sin(m\lambda)\right] \tag{20-3}$$

where ΔC_{lm} and ΔS_{lm} are time-variable components of the e.g. GRACE observed Stokes coefficients for some month of degree and order (l, m) or it can be defined as changes relative to the mean of the monthly solutions.

Equation (20-3) is the starting point for using the GRACE level-2 data to recover changes in surface mass density. Figures 3.1 - 3.3 show the 2002-2011 secular trend maps of mass changes over the world which have been plotted using monthly GRACE level 2 release 4.0 data sets from three different processing centers; CSR, GFZ, and JPL. The data obtained from the University of Colorado GRACE Data Analysis Website - http://geoid.colorado.edu/grace/grace.php. As shown in the Figures, the larger degree in the coefficients, the larger errors in the GRACE level-2 data and the larger contributions

to the sum in Equation (20-3). Therefore the use of Equation (20-3) as written can lead to highly inaccurate results.

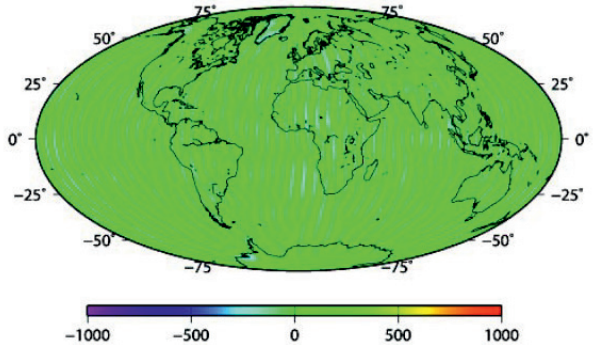

Figure 3.1. The 2002-2011 secular trend map (mm/year) over the world using CSR GRACE level 2 data release 4.0

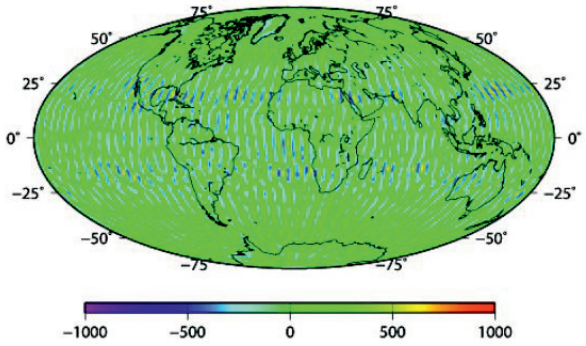

Figure 3.2. The 2002-2011 secular trend map (mm/year) over the world using GFZ GRACE level 2 data release 4.0

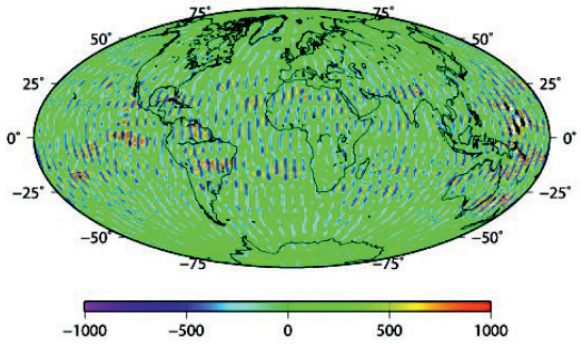

Figure 3.3. The 2002-2011 secular trend map (mm/year) over the world using JPL GRACE level 2 data release 4.0

3.2. Spatial averaging function

Using spatial averages of the surface mass density, GRACE can deliver useful results. Spatial averages of the surface mass density can be formulated as:

$$\overline{\Delta\sigma}(\varphi,\lambda)=\int\cos\varphi' d\varphi' d\lambda' \Delta\sigma(\varphi',\lambda') W(\varphi,\lambda,\varphi',\lambda') \tag{21-3}$$

where $W(\varphi,\lambda,\varphi',\lambda')$ is an averaging function. Using (20-3) in (21-3) gives, after some manipulation:

$$\begin{aligned}\overline{\Delta\sigma}(\varphi,\lambda)=\frac{a\rho_{\text{ave}}}{12\pi}\sum_{l,m}\tilde{P}_{lm}(\sin\varphi)\sum_{l',m'}\frac{2l'+1}{1+k_{l'}}\Big[&\left(\Delta C_{l'm'}W_{lmc}^{l'm'c}+\Delta S_{l'm'}W_{lmc}^{l'm's}\right)\cos(m\lambda)\\ &+\left(\Delta C_{l'm'}W_{lms}^{l'm'c}+\Delta S_{l'm'}W_{lms}^{l'm's}\right)\sin(m\lambda)\Big]\end{aligned} \tag{22-3}$$

where

$$\begin{aligned}\begin{Bmatrix}W_{lmc}^{l'm'c}\\ W_{lms}^{l'm'c}\\ W_{lmc}^{l'm's}\\ W_{lms}^{l'm's}\end{Bmatrix}=\int\cos\varphi d\varphi d\lambda\int\cos\varphi' d\varphi' d\lambda'\begin{Bmatrix}\cos(m'\lambda')\cos(m\lambda)\\ \cos(m'\lambda')\sin(m\lambda)\\ \sin(m'\lambda')\cos(m\lambda)\\ \sin(m'\lambda')\sin(m\lambda)\end{Bmatrix}\\ \times W(\varphi,\lambda,\varphi',\lambda')\tilde{P}_{lm}(\sin\varphi)\tilde{P}_{l'm'}(\sin\varphi')\end{aligned} \tag{23-3}$$

For averaging over large regions, the $W_{lmc}^{l'm'c}$, $W_{lms}^{l'm'c}$, etc., are small for large l, m, l′, m′, so that the contributions to $\overline{\Delta\sigma}$ from the poorly known $\Delta C_{l'm'}$ and $\Delta S_{l'm'}$ at large values of l′, m′, tend to be small. The averaging function $W(\varphi,\lambda,\varphi',\lambda')$ can be defined as an isotropic or non-isotropic function.

3.2.1. Isotropic averaging function

Assuming $W(\varphi,\lambda,\varphi',\lambda')$ depends only on the angle α between the points (φ,λ) and (φ',λ') (i.e. $W(\varphi,\lambda,\varphi',\lambda')=W(\alpha)$, where $\cos\alpha=\cos\varphi\cos\varphi'+\sin\varphi\sin\varphi'\cos(\lambda-\lambda')$), Equations (22-3) and (23-3) are reduced to

$$\Delta\sigma(\varphi,\lambda)=\frac{2a\rho_{\text{ave}}\pi}{3}\sum_{l=0}^{\infty}\sum_{m=0}^{l}\frac{2l+1}{1+k_l}W_l\tilde{P}_{lm}(\sin\varphi)\left[\Delta C_{lm}\cos(m\lambda)+\Delta S_{lm}\sin(m\lambda)\right] \quad (24\text{-}3)$$

where

$$W_l = \int_0^{\pi} W(\alpha)P_l(\cos\alpha)\sin\alpha\, d\alpha \quad (25\text{-}3)$$

and where $P_l = \frac{\tilde{P}_{lm=0}}{\sqrt{2l+1}}$ are the Legendre polynomials.

The most common isotropic averaging function is a Gaussian kernel which was developed by Jekeli (1981) to compensate for poorly known, short-wavelength spherical harmonic coefficients to improve estimates of the Earth's gravity field. Jekeli's Gaussian averaging function is:

$$W(\alpha)=\frac{b}{2\pi}\frac{\exp\left[-b(1-\cos\alpha)\right]}{1-e^{-2b}} \quad (26\text{-}3)$$

with

$$b=\frac{\ln(2)}{\left(1-\cos(r/R_{\text{E}})\right)} \quad (27\text{-}3)$$

where R_E is the Earth's radius and r is the distance on the Earth's surface, where the kernel drops to ½ its value at $\alpha=0$, which is commonly used to indicate the degree of smoothing. The coefficients W_l can be computed with recursion formulae:

$$W_0=1 \quad (28\text{-}3)$$

$$W_1=\frac{1+e^{-2b}}{1-e^{-2b}}-\frac{1}{b} \quad (29\text{-}3)$$

$$W_{l+1}=-\frac{2l+1}{b}W_l+W_{l-1} \quad (30\text{-}3)$$

Figures 3.4 – 3.6 show the 2002-2011 secular trend maps of mass changes over the world using the GRACE level 2 release 4.0 data sets from three different data centers;

CSR, GFZ, and JPL which have been smoothed with 340 km of Gaussian radius. The data obtained from the University of Colorado GRACE Data Analysis Website http://geoid.colorado.edu/grace/grace.php.

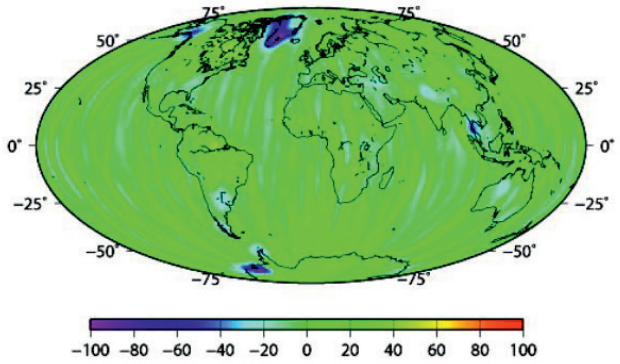

Figure 3.4. The 2002-2011 secular trend map (mm/year) over the world using CSR GRACE level 2 data release 4.0 smoothed with 340 km of Gaussian radius

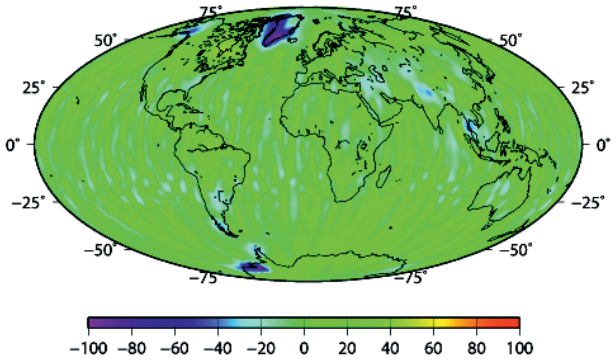

Figure 3.5. The 2002-2011 secular trend map (mm/year) over the world using GFZ GRACE level 2 data release 4.0 smoothed with 340 km of Gaussian radius

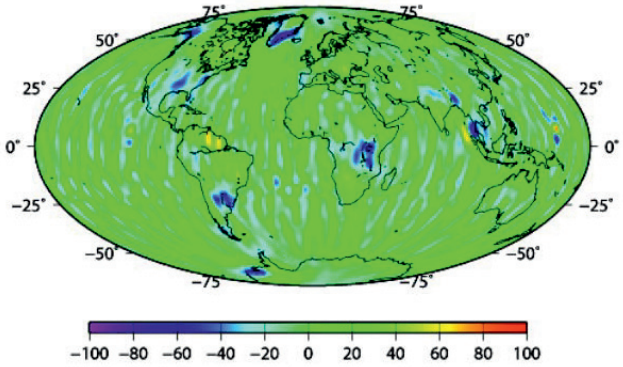

Figure 3.6. The 2002-2011 secular trend map (mm/year) over the world using JPL GRACE level 2 data release 4.0 smoothed with 340 km of Gaussian radius

3.2.2. Non-isotropic averaging function

Assuming the averaging function $W(\varphi,\lambda,\varphi',\lambda')$ depends on both spherical harmonic degree and order, $W(\varphi,\lambda,\varphi',\lambda')$ is written as

$$W(\varphi,\lambda,\varphi',\lambda')=\frac{1}{4\pi}\sum_{l=0}^{\infty}\sum_{m=0}^{l}\tilde{P}_{lm}(\sin\varphi)\left[G_{lm}^{c}(\varphi',\lambda')\cos(m\lambda)+G_{lm}^{s}(\varphi',\lambda')\sin(m\lambda)\right] \quad (31\text{-}3)$$

where

$$G_{lm}^{c}(\varphi',\lambda')=W_{lm}\tilde{P}_{lm}(\sin\varphi')\cos(m\lambda') \quad (32\text{-}3)$$

$$G_{lm}^{s}(\varphi',\lambda')=W_{lm}\tilde{P}_{lm}(\sin\varphi')\sin(m\lambda') \quad (33\text{-}3)$$

W_{lm} is a non-isotropic kernel which should be defined. The $W(\varphi,\lambda,\varphi',\lambda')$ can be characterized into symmetric (or diagonal) and non-symmetric kernels with respect to the points φ,λ and φ',λ' (Klees et al., 2008). The DDK filters (Kusche et al., 2009) are non-isotropic kernels which have been used in this thesis. The DDK kernel is non-symmetric and is derived by regularization of a characteristic normal equation system that involves a priori information on the GRACE signal covariance and the GRACE

error covariance. The DDK kernel ($W_{(\alpha)}$) is a matrix with a damping parameter α that controls the degree of smoothness.

$$W_{(\alpha)} = L_{\alpha} N = \left(N + \alpha M\right)^{-1} N \tag{34-3}$$

with M being an approximation to the GRACE signal covariance and N being an approximation to the GRACE error covariance (Kusche et al., 2009). Figures 3.7-3.8 show the 2002-2011 secular trend maps of mass changes over the world using the GRACE level 2 release 4.0 from two different data centers; CSR and GFZ which have been de-striped by the DDK filter with a smoothing parameter of $\alpha = 10^{13}$ which corresponds to 340 km of Gaussian radius.

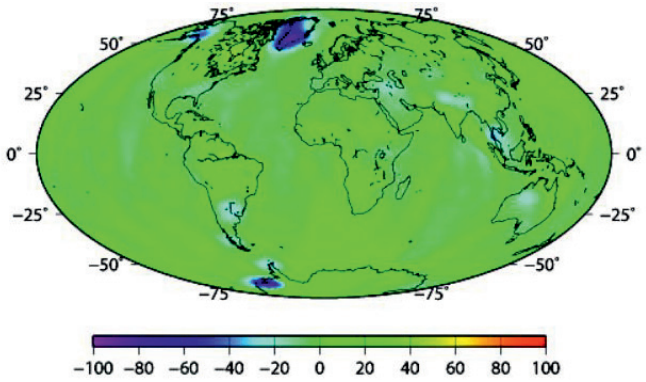

Figure 3.7. The 2002-2011 secular trend map (mm/year) over the world using CSR GRACE level 2 data release 4.0 de-striped by the DDK filter with a smoothing parameter of $\alpha = 10^{13}$ which corresponds to 340 km of Gaussian radius.

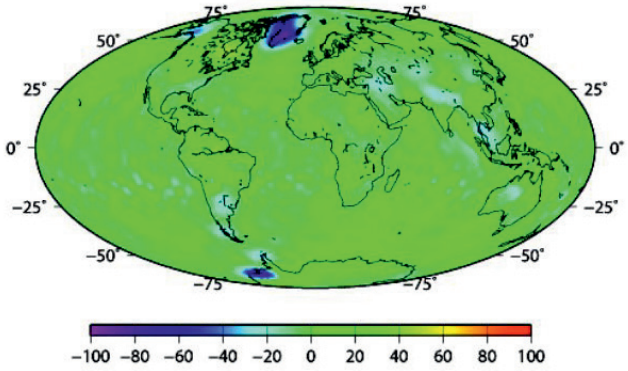

Figure 3.8. The 2002-2011 secular trend map (mm/year) over the world using GFZ GRACE level 2 data release 4.0 de-striped the DDK filter with a smoothing parameter of $\alpha = 10^{13}$ which corresponds to 340 km of Gaussian radius.

3.3. Accuracy of GRACE measurements: formal, omission and leakage errors

3.3.1. Formal error

The degree amplitude of the GRACE error is defined as:

$$\sigma_N(l) = a\sqrt{\sum_{m=0}^{l}\left(\sigma^2_{C_{lm}} + \sigma^2_{S_{lm}}\right)} \tag{35-3}$$

where $\sigma^2_{C_{lm}}$ and $\sigma^2_{S_{lm}}$ are the errors on the gravity potential coefficients and a is the radius of the Earth.

It can be seen as the square-root of the total variance from all terms of a given spatial scale, as the degree l is the measure of the spatial scale of a spherical harmonics (i.e., a half wave- length of 20,000/l km). These errors increase at degrees 20 to 30 and become dominant at degrees 40 to 50. As a consequence, GRACE monthly solutions are low-pass filtered at degree 50 or 60 to remove the noise contained in the high frequency domain.

3.3.2 Omission or cut-off frequency error

Error in cut-off frequency represents the loss of energy in the short spatial wavelength due to the low-pass harmonic decomposition of the signals that is stopped at the

maximum degree N_1. For the GRACE land water solutions; N_1=60, thus the spatial resolution is limited and stopped at ~330 km by construction. This error is simply evaluated by considering the difference of reconstructing the remaining spectrum between two cutting harmonic degrees N_1 and N_2, where $N_2 > N_1$ and N_2 should be large enough compared to N_1 (e.g., N_2=300):

$$\sigma_{truncation} = \sum_{n=0}^{N_2} \xi_n - \sum_{n=0}^{N_1} \xi_n = \sum_{n=N_1}^{N_2} \xi_n \tag{36-3}$$

using the scalar product:

$$\xi_n = \sum_{m=0}^{n} \left(\Delta C_{nm}(\Delta t) A_{nm} + \Delta S_{nm}(\Delta t) B_{nm} \right) \tag{37-3}$$

These errors are generally lower than 1% of the amplitude of the signal.

3.3.3. Leakage effects

Because of the averaging function is nonzero for all values of α (Eq. 26-3 and Eq. 34-3), the hydrological and atmospheric pressure signals over continents will leak into the oceanic estimates, and oceanic effects will contaminate the hydrological estimates. The oceanic signals are smaller than the hydrology and atmospheric pressure signals. The leakage can be reduced by employing an iterative estimation technique. For example, the effects of surface mass over land from the oceanic estimates can be reduced by using the GRACE geoid data to first solve for continental mass distribution, removing the effects of that mass distribution from the GRACE geoid and then using the residual geoid to solve for the oceanic estimates. To estimate the continental signal using Eq. (22-3), the averaging radius should be small; otherwise it should be large enough to provide reasonably accurate GRACE averages. To indicate that a smoothed continental surface mass is nonzero only over land, Equation. (22-3) is multiplied by a land function $C(\varphi,\lambda)$, where

$$\begin{aligned} C(\varphi,\lambda) &= 1 \quad \text{over land} \\ C(\varphi,\lambda) &= 0 \quad \text{over ocean} \end{aligned} \tag{38-3}$$

The spherical harmonic coefficients for the smoothed continental surface mass are given by Eq. (18-3) and those coefficients can then be used in Eq. (19-3) to estimate the geoid coefficients caused by the continental surface mass. Subtracting those coefficients from the original GRACE geoid coefficients, the geoid coefficients caused by the oceanic contributions are obtained. Using the oceanic geoid coefficients to find the averaged surface mass at the original oceanic location, the results are relatively free of the effects of surface mass over land. A similar approach can be used to remove the contaminating effects of the ocean from estimates of continental water storage. By the way, the continental signals can also be obtained by the hydrological models such as the NOAH version of NASA's Global Land Data Assimilation System (GLDAS) model (Rodell et al., 2004), forced with NCEP/NCAR Reanalysis 1 atmospheric data (Qian et al, 2006), and version 4.0 of the Community Land Model (CLM4), maintained by the National Center for Atmospheric Research and forced with CRUNCEP atmospheric data (Oleson et al., 2010). These models provide values for soil moisture, snow cover, and canopy storage. The CLM4 model includes groundwater component, but GLDAS/NOAH does not. None of the models include surface storage in lakes or rivers or marshes, and none of them include anthropogenic contributions.

3.4. Glacial Isostatic Adjustment (GIA)

Extraction of the mass signals from GRACE and interpret them as changes in the water content of hydrologic basins, or ocean bottom pressure, or ice sheet mass, is complicated by the need to remove the effect of Glacial Isostatic Adjustment (GIA) of the lithosphere and mantle since the Last Glacial Maximum. GRACE detects not only present-day mass loss but also changes in the gravity filed caused by ongoing GIA (Wahr et al., 2000; Velicogna and Wahr, 2006; Ramilien et al., 2006) and it is not possible to separate these two signals from GRACE observations. Traditionally, separating mass change signals from GIA relies upon modeled estimates. Despite of the divergence in spatial distribution and in the magnitudes of the modeled GIA signals, the size of the errors in GIA models constitutes a significant proportion of the signal. The reason for this is that these models involve reconstructions of the past ice load since the Last Glacial Maximum (LGM) and require parameterizations of the Earth's rheology (elastic and viscous properties, density), which are generally poorly constrained and

uncertain. In fact, there are three general sources of error in the GIA estimates: the ice (deglaciation) history, the viscosity profile of the mantle, and physical and numerical approximations in the model. Comparing 14 GIA models from different authors, Guo et. al. (2012) showed that the accuracy and consistency of GIA models need to be substantially improved to full exploit GRACE data, to enhance the constraints on ice-sheet mass balance and the mass component of global sea level change. Figure 3.9 shows the effects of GIA of the lithosphere and mantle using by A et al (2013) model. This model has a compressible Earth, and uses the ICE-5G deglaciation history and VM2 viscosity profile, and the same PREM-based elastic structure as Peltier (2004). The model includes polar wander feedback (computed as described in Mitrovica et al, 2005), uses the self-consistent sea level equation to distribute meltwater into the ocean, and includes degree-one terms when computing the uplift rate. The uncertainty of this model is about +/- 20%. This uncertainty comes from looking at results for various viscosity values and alternative deglaciation models for Antarctica and Greenland. This value probably over-estimates the uncertainty in northern Canada, where the deglaciation history is reasonably well-known; and it probably underestimates the uncertainty in Antarctica and Greenland, where the ice history is not as well-known.

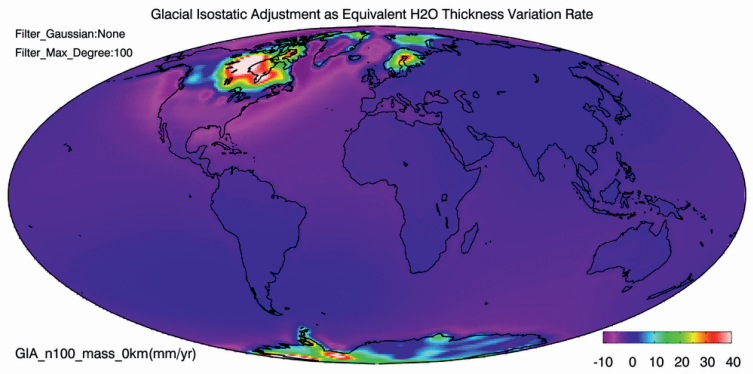

Figure 3.9. Effects of GIA of the lithosphere and mantle. (Courtesy to GRACE Tellus, A et al., 2013)

Chapter 4

Numerical Investigations

4.1. Introduction

Regarding to the main goal of this Ph.D. study, its numerical investigations are done in three areas: ice sheets, ocean, and continental areas. In fact, this thesis focuses on the following research questions in three different case studies; Greenland, Nordic Seas, and Middle East.

1. Is Greenland losing or gaining ice?
2. How fast ice is changing across Greenland?
3. How is the present-day of Greenland ice sheet thinning?
4. How is present-day of water mass change across the Nordic Seas?
5. How is present-day of sea height change due to variations in temperature and salinity across the Nordic Seas?
6. How is present-day of total groundwater storage change across from the Middle East?
7. How much changes in the total groundwater storage across the Middle East are due to human activities?

Numerical investigations will find answers of these questions using the GRACE monthly gravity filed solutions.

4.2. Greenland

The Polar Regions are among the areas in the world, where global temperature changes are most noticeable. After the Antarctic Ice Sheet, the Greenland ice sheet is the second largest ice body in the World. Almost 80% of its area has been covered by ice. The distance from north to south of Greenlandic ice sheet is almost 2,670 kilometers, and its greatest width is 1,050 kilometers at latitude of 77°N, near its northern margin. The Greenland ice sheet is very thick, generally more than 2 km and over 3 km at its thickest point. In addition to the ice mass of Greenland, isolated glaciers and small ice caps cover between 76,000 and 100,000 square kilometers around the periphery. Greenland has arctic climate and permafrost. Its temperature normally varies between 10 degrees in the warmest months of the year and minus 10 to minus 20 degrees on an average during winter. During the past decades there has been an increasing focus on the consequences of global warming in Greenland such as raising the average temperature in South Greenland from 0.6 to almost 2 degrees over the past three decades. This means that the Greenlandic ice sheet is melting much faster than previously, and this increases the chances of flooding globally. In July 2012, a very unusual weather event occurred on the Greenlandic ice sheet. For a few days, 97 per cent of the entire ice cap indicated surface melting. Roughly the total ice on the Greenland ice sheet is estimated 2.85 million km^3. If it was to melt, it would tend to a global sea level rise of 7.2 m. This would inundate most coastal cities in the World and remove several small island countries with a maximum altitude below or just above this number. Because of the potential for an increasing contribution of Greenland ice loss to rising sea level and its sensitivity to climate change, mass changes in the Greenland ice sheet are of considerable interest. Accurate estimates of the Greenland ice mass variability, accompanied by realistic error bars, would greatly improve uncertainties in projected sea level change, with obvious societal and economic impacts. There are several estimates of the Greenland mass variability which have been obtained using a variety of techniques such as airborne laser altimeter measurements (Krabill et al., 2004), comparing modeled accumulation minus melt with an estimate of mass discharge based on steady state conditions (Box et al., 2004), and comparing measured ice flux with observed accumulation minus modeled melt estimates (Rignot, 2005). A common

problem to all these techniques is the difficulty of monitoring the entire ice sheet and they can provide estimates for only a portion of ice sheet or critical regions. This problem could be overcome by using satellite remote sensing techniques. GRACE satellite mission has large effective footprint and sensitivity to mass. It offers the best available method for measuring the total mass balance of the polar ice sheets. Time series of ice mass changes over the Greenland using GRACE level 2 data were studied in papers A, B, and C. The results are summarized and discussed in this section.

Three different GRACE level 2 RL04 data from CSR, GFZ, and JPL during the period April 2002 to February 2010 have been used to compute the time series of ice mass changes across the Greenland (data available at http://icgem.gfz-potsdam.de/ICGEM/). All of data have been de-striped by non-isotropic smoothing procedure developed by Kusche et al., (2009) with smoothing parameters of $a = 10^{14}, 10^{13}$, and 10^{12} corresponding to Gaussian radii: 530 km, 340 km, and 240 km. Because of the degree-0 Stokes coefficient is proportional to the total mass of the Earth and atmosphere, it is assumed constant and it is not used in the computations of the time series of ice mass changes. The geocenter motion is showed by the changes in degree-1 Stokes coefficients which cannot be derived from GRACE data. In these three papers, the changes in degree-1 coefficients are ignored, but it should be noted that the absence of the geocenter motion might introduce an error in the mass balance estimates (Chambers et al., 2004; Chen et al., 2005). The lowest-degree zonal harmonics, C_{20} Stoke coefficient is related to the Earth's oblateness. Because of the relative short separation length between the two GRACE Spacecrafts, the C_{20} coefficient cannot be well determined by GRACE. The C_{20} values provided in the level-2 data also show anomalous variability (e.g. Chen et al., (2005)). Therefore, the monthly Satellite Laser Ranging (SLR) values for C_{20} coefficients derived from five SLR satellites (LAGEOS-1 and 2, Starlette, Stella and Ajisai) (Cheng and Tapley, 2004) are used to replace the estimates from GRACE in these three papers. This method is a well-established technique for determining independent degree-2 coefficients. The SLR C_{20} coefficients and their associated standard deviations are continuously provided in the GRACE project Technical Note 05 (ftp://podaac.jpl.nasa.gov/pub/grace/doc/TN-05_C20_SLR.txt).

Extending the averaging kernel beyond the boundaries of Greenland causes geophysical signals outside Greenland leak into our estimates. For a reliable estimate of ice mass changes over Greenland one needs to correct for leakage effects. The contaminations from continental hydrology outside Greenland and the ocean can be estimated through two methods; 1) using global hydrological models such as Global Land Data Assimilation System (GLDAS) models and ocean models such as Estimation the Circulation and Climate of the Ocean (ECCO) models, and 2) GRACE level 2 data alone. In this study, the second method has been used to remove the leakage effects. The leaking signals follow the Newton's law of gravitation and its impact reduces with increasing distances. As shown in Figure 4.1 the strongest signals on Greenland can be caused by Alaska, Fennoscandia and the Canadian Shield.

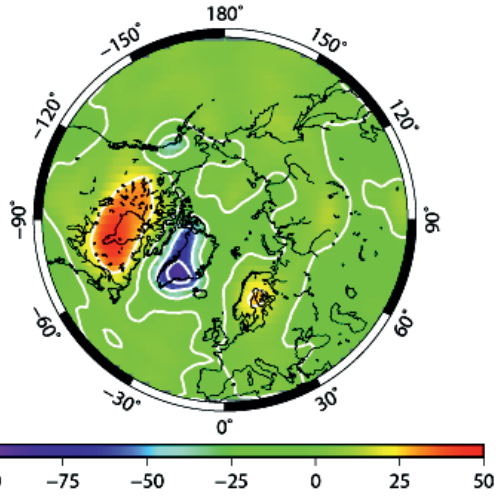

Figure 4.1. The 2002-2011 secular trend map (mm/year) using GFZ GRACE level 2 data release 4.0 de-striped by the DDK filter with a smoothing parameter of $\alpha = 10^{13}$ which corresponds to 340 km of Gaussian radius.

The effects of leakage out are estimated based on the Stokes coefficients which have been computed by the mass anomaly only inside of Greenland. Using the Stokes coefficients which have been calculated by the mass anomaly outside of Greenland, the effects of leakage in are computed. After removing the leakage effects, the GIA effects on the ice mass changes should be removed. The ice mass changes computed by the

GRACE data have no vertical resolution because GRACE cannot distinguish between secular gravity signals caused by present-day ice mass changes and those caused by GIA induced mass redistribution, or other causes. Therefore, if not corrected, GIA signals will manifest as an apparent ice mass change. However, it is well known that GIA models available to the GRACE community differ significantly from one another (e.g. Tamisiea, 2011). Basically, the GIA models depend on assumptions of the ice load history and mantle viscosity, leading to considerably large error bounds (Chen et al., 2006; Velicogna and Wahr, 2006). Considering the total uncertainty in the GIA modeling, the ice mass change estimates given in these three papers are not corrected for GIA effects. Nevertheless, to show the order of magnitude of the GIA effect for the whole of the Greenland area, it has been introduced to -7.4 ± 19 Gt/yr according to Velicogna and Wahr, (2006).

To estimate the secular trend of ice mass changes over Greenland, a 8-parameter trend analysis including bias, trend, annual, semiannual, and seasonal is used by un-weighted least squares method. In paper A, using the Akaike's Information Criterion (AIC) (Akaike, 1973), the periodic variations of the model such as annual, semiannual, and seasonal has been explored. This exploration shows that the 8-parameter model is a proper model. Figure 4.2 Shows the ice mass results which have been averaged over scale of 340 km and do not include the error estimates. It seems that the trends of ice mass changes derived from CSR, and GFZ data have a very good agreement, but the JPL solutions show a very low trend compared to them. The small trend in the JPL solutions in the Greenland has been also observed by others (e.g. Sørensen et al. (2010), Baur et al. (2009), and Sasgen (2009)). Table 4.1 shows the mass balance estimates based on the different GRACE data sets. The results in this table are based on the full time periods of the different GRACE level-2 data Figure 4.2.

Table 4.1. Greenland mass balance estimated from GRACE monthly gravity field solutions provided by CSR, GFZ, and JPL.

GRACE Level 2 Data	Mass Balance [Gt/yr]
CSR	-163±20
GFZ	-161±21
JPL	-84±26

The uncertainties listed in Table 4.1 take into account the errors of the least squares adjustments of mathematical model which is used to detect the secular trend and periodic variations in the monthly mass anomalies, the leakage effects and the calibrated GRACE errors. In estimation of these uncertainties, the GIA effects are not applied.

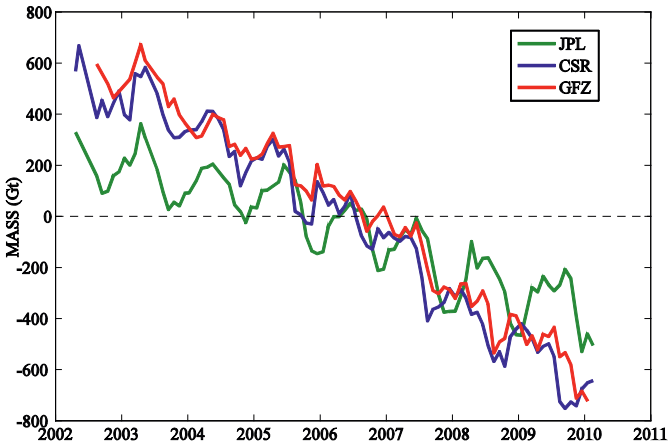

Figure 4.2. The 2002-2010 ice mass changes over Greenland using CSR, GFZ, and JPL GRACE level 2 data release 4.0 de-striped by the DDK filter with a smoothing parameter of $\alpha = 10^{13}$.

The spatial distribution of the ice mass changes (cm equivalent water thickness per year) for all three level-2 data sets during the period April 2002 to February 2010 are shown in Fig. 4.3. It is seen that very similar pattern are derived from CSR, and GFZ data which reveals large coastal mass losses, with largest values found along the south-east and north-west coasts. A small mass increase is observed in the central, northern part of the ice sheet. A somewhat different picture is revealed by the JPL solutions, which shows a larger central mass increase than the other results, and which also predicts a mass increase in south-west Greenland.

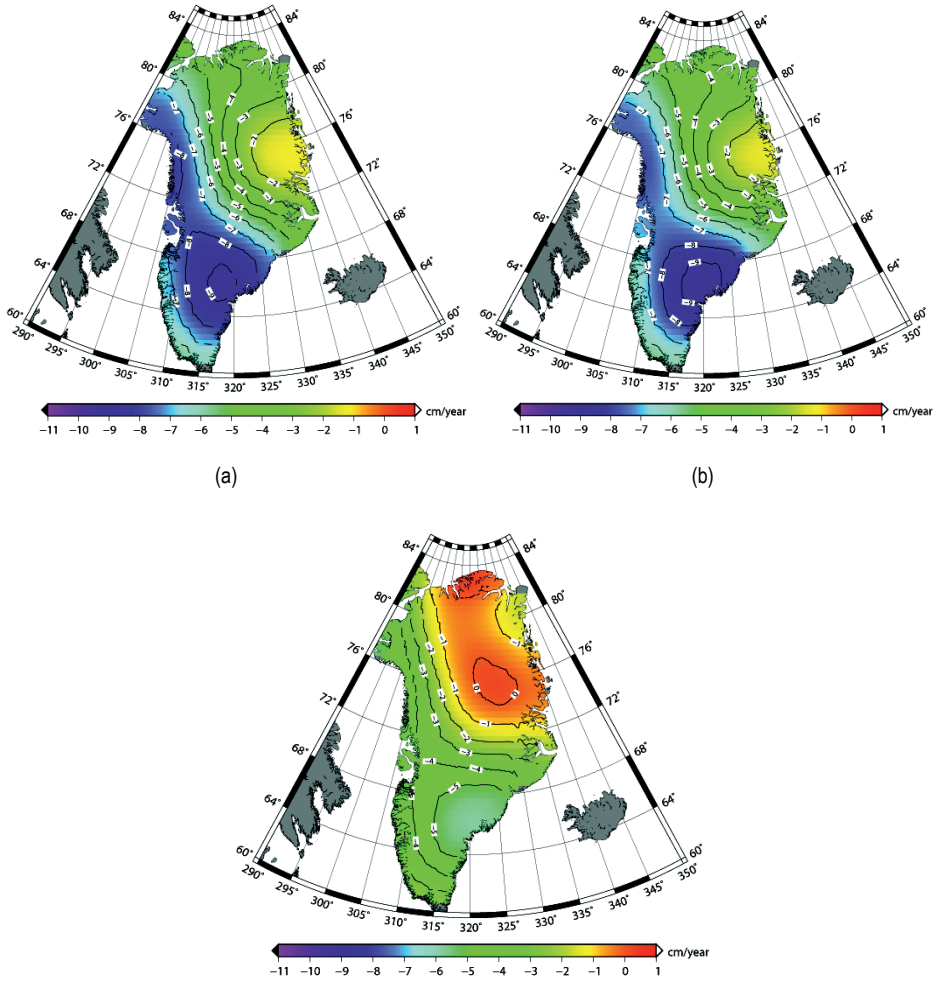

Figure 4.3. The 2002-2010 spatial distribution of the ice mass changes across the Greenland for the three different GRACE level-2 Release 04 data sets; (a) CSR data de-striped by the DDK filter with a smoothing parameter of $\alpha = 10^{13}$ which corresponds to 340 km of Gaussian radius, (b) same as (a) but for GFZ data, (c) same as (a) but for JPL data.

Khan et al., (2010) found that GRACE and GPS measurements reveal that the pattern of the Greenland mass loss is changing in time. In the paper A, it has been shown that the summer ice loss values are different during the period April 2002 to February 2010. The maximum summer ice loss was on 2007 (see also Wouters et al., 2008). The summers of 2003, 2005 and 2007 have been recorded as the three warmest years since 1961 (Hanna et al., 2009). Figure 4.4 shows that the ice loss, which has been well-documented over southern portions of Greenland (Figure 4.4 (left)), has been started to spread up along the northwest coast since 2007 (Figure 4.4 (right)).

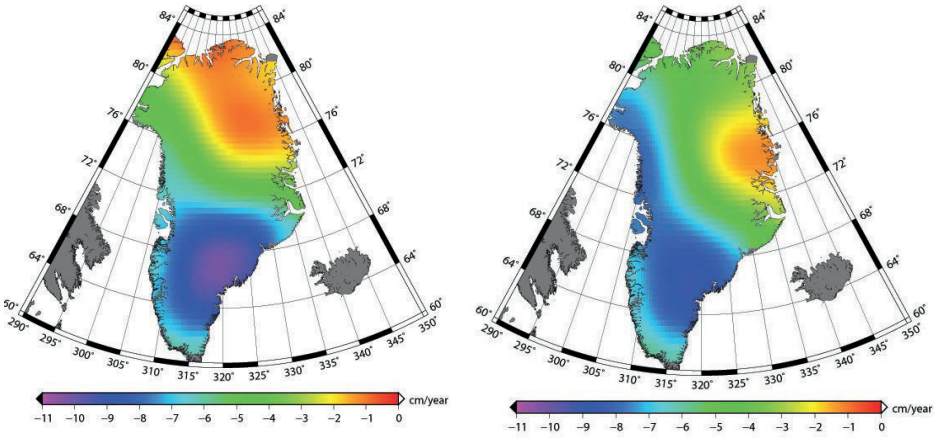

Figure 4.4. GRACE Model estimation of the Greenland ice mass balance (cm equivalent water thickness per year). (left) It is from April 2002 to December 2007 and (right) it is during the period April 2002 to December 2010.

In comparison between Figures 4.4 (right) and (left), it is seen that after 2007, a large area experienced losses of 6 to 10 centimeter per year. It is also seen that the interior parts of Greenland shows less negative trend and the northern and northeastern parts show the least negative trends.

In the previous sections, it had been assumed linear trends in gravity in time and the ice mass change results were presented. Velicogna (2009) found increasing rates of ice mass loss across the Greenland based on GRACE data. The secular trends of ice mass changes over Greenland derived from two year intervals are listed in Table 4.2. These estimates indicate that the rate of Greenland ice mass loss was indeed increasing

from 2002 to 2007, but also that it decreased in the period 2008-2009 and again increased in the period 2010-2011. It should be noted, that the secular trend estimates listed in Table 4.2 are associated with large uncertainties, due to the short time span of data.

Table 4.2. Secular trends estimates from two year intervals of CSR GRACE level 2 data release 04 de-striped by the DDK filter with a smoothing parameter of $\alpha = 10^{13}$.

Time period (both years included)	Secular Trend (Gt/yr)
2002-2003	-121
2004-2005	-167
2006-2007	-210
2008-2009	-189
2010-2011	-271

By linear least squares fitting to the values listed in Table 4.2, we find that the acceleration in Greenland ice sheet mass loss is –32±6 Gt/yr^2 in 2002–2011. The uncertainty in the acceleration is calculated by errors in the least squares adjustment of the mathematical model which is used to detect the linear secular trend. Afterwards, by fitting a quadratic trend to the 2002–2011 time series of ice mass changes over the Greenland, we compute a trend of –111±21 Gt/yr for Greenland ice sheet. The uncertainty in our estimate is calculated by taking the root sum squares of the errors in the least squares adjustment of the mathematical model which is used to detect the secular trend and periodic variations in time series of ice mass changes, the leakage effects and the gravity field error. To investigate whether a curved line will better fit to the GRACE time series of ice mass loss of Greenland than a linear regression, we also fit a linear trend to the same time series of ice mass changes which have been fitted by a quadratic form. By fitting linear trend model to the 2002-2011 GRACE ice mass changes over the Greenland, we find a trend of –166±20 Gt/y for it. The uncertainty in our estimate for the linear trend is calculated the same as in the quadratic trend model. Figure 4.5 shows the GRACE ice mass changes across the Greenland compared with its fitting trends, linear and quadratic form. By using a goodness of fit statistic, we conclude that the time series of Greenland ice mass changes better modeled by an increasing rate of ice mass loss, i.e. including acceleration term, than with a constant ice mass loss.

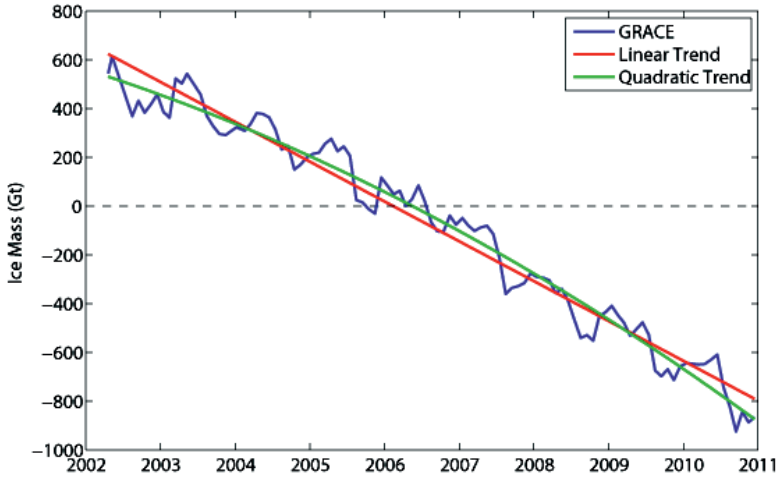

Figure 4.5. The 2002-2011 GRACE time series of Greenland ice mass changes, compared with the best fitting linear trend and the best fitting quadratic trend.

4.3. Nordic Seas

The Nordic Seas including the Norwegian, Iceland and Greenland Seas are a region of special significance in the world ocean. This region is bounded by the Arctic Ocean to the north, the deep North Atlantic Ocean to the south, and the shallow North Sea to the southeast. It covers about 2.5×10^6 km^2 or about 0.75%, of the area of the world. The Nordic Seas are usually characterized by strong east to west hydrographic gradients, seasonal and spatial variations in surface waters, major oceanographic boundaries, seasonally variable sea-ice distribution, and deep-water formation (Fig. 4.6).

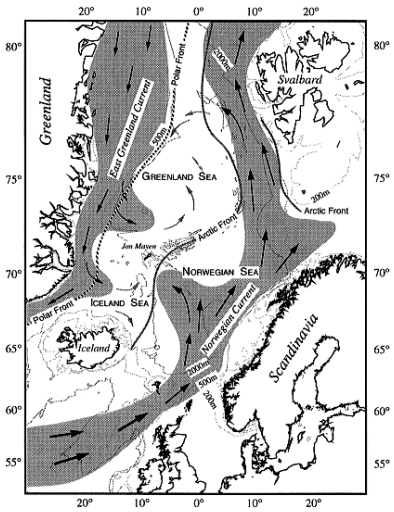

Figure 4.6. Map of the Nordic Seas including generalized surface current pattern, and oceanographic fronts (from various sources) (Baumann et al., 2000).

The present surface-current system in the eastern Nordic Seas is characterized by the Norwegian Current, a relatively warm (6-10° C), saline (> 35.0 psu) branch of the North Atlantic Drift entering the Iceland and Norwegian Seas, and flowing northward into the Arctic Ocean (Swift, 1986). In the west, the East-Greenland Current carries cold (< 0° C), less saline (< 34.4 psu, in summer as low as 29 psu) polar water southward along the East Greenland coast. Between these two main water masses, the Arctic surface water (0-4° C, 34.6-34.9 psu) is formed as a mixture of them (Johannessen,

1986). The system of warm and cold currents results in distinctive oceanographic fronts. The surface water of the Norwegian Current usually is free of sea-ice throughout the year whereas the Arctic surface water is characterized by large seasonal and interannual variability in sea-ice cover. In winter, maximum sea-ice covers the whole area of mixed Arctic water up to the Arctic front, while during summer ice-free seas extent to the Polar front. The polar water usually is permanently covered by sea-ice (Swift, 1986).

The Nordic Seas plays an important role in the Earth's climate system because it is the region where deep water is formed and where the warm Atlantic water loses heat to the atmosphere, and carries the residual heat into the Arctic Ocean. This region is, despite its small extent, very dynamic and diverse. Monitoring of sea level variability as an indicator for the climate change is very important in the study of this region. Sea level variability has two major components; steric sea level and water mass change. Steric sea level shows variation in the sea level due to changes in the water temperature and salinity at all depths. The ocean mass redistribution or water mass flux causes the water mass changes, resulting in sea level changes. The wind stress and atmospheric pressure can also cause the ocean mass to redistribute (Gill and Niiler, 1973), resulting in sea level changes of the order of a cm or less. These fluctuations are much smaller than the sea level variations caused by expansion or contraction due to the steric variability (Gill and Niiler, 1973). Therefore, these variations in total sea level changes from either tide gauges or satellite altimeters which are used for estimating of steric sea level changes could be ignored (e.g. White and Tai, 1995; Chambers et al., 1997; Wang and Koblinsky, 1997).

Measuring Ocean Bottom Pressure (OBP), the pressure of the water column at the sea floor, is the only way to directly measure the mass fluctuations. Like mentioned before, the monthly GRACE gravity field solutions can be used to produce maps of OBP. Though the surface mass density is not a meaningful quantity for oceanographic applications, but it is straightforward to convert it to either anomalies of ocean bottom pressure or equivalent surface elevation. In summary, the following processing steps were performed in calculating the bottom pressure anomalies across the Nordic seas from the GFZ GRACE monthly gravity solutions during the period of October 2002 to October 2010 that its results are presented in paper E.

1. The degree 1 coefficients are estimated from the variations of the Earth's center of mass proposed by Chen et al., 1999.
2. The coefficient of degree 2 and order 0 (C_{20}) is replaced by estimates from SLR (Chen et al., 2005).
3. The time-mean of the coefficients from October 2002 to October 2010 is subtracted from the monthly fields.
4. The de-aliasing product for non-tidal ocean and atmosphere variability (GAD) is added back.
5. Correlated errors are removed following Kusche et al., 2009.
6. SH coefficients are smoothed using a parameter of $\alpha = 10^{14}$ following Kusche et al., 2009.
7. Ocean bottom pressure is synthesized on a 0.5° spatial grid over the Nordic seas.
8. Leakage errors from ice sheets and glaciers melting on Greenland, and Scandinavia are removed following Joodaki and Nahavandchi, 2012a.
9. Global mean correction for GIA (+2.0 mm/yr) is added (Peltier, 2009; Cazenave et al., 2009).

Figure 4.7 shows the OBP variations over the Nordic seas during the period October 2002 to October 2010.

By having the OBP variations and sea surface height changes over the Nordic seas, the steric sea level variations across it can be computed. Sea surface height data from the Environmental Satellite (ENVISAT) altimetry mission, cycles 10 to 93 is used to estimate the Sea Level Anomaly (SLA) across the Nordic seas during the period of October 2002 to October 2010. In summary, the following processing steps were performed in calculating the SLA over the Nordic seas from the ENVISAT altimetry data.

1. Sea surface height (SSH) data retrieval and reduction are carried out by using the Stackfiles database (Yi, 2010).
2. An inverted barometer correction (IB) is subtracted from the altimetry data.
3. Taking average of along track SSH profiles to a regular grid (approximately 6×2 km).
4. Estimation of the mean tracks following to Ghazavi and Nahavandchi, 2011.

5. Subtracting the tracks from the mean tracks, the SLA is estimated for all the ENVISAT cycles.

6. By gridding the SLA on a $0.5^{o}\times0.5^{o}$ grid and summing it over grid elements with cosine latitude weighting, an approximate estimate of total SLA for each month is obtained (Figure 4.8).

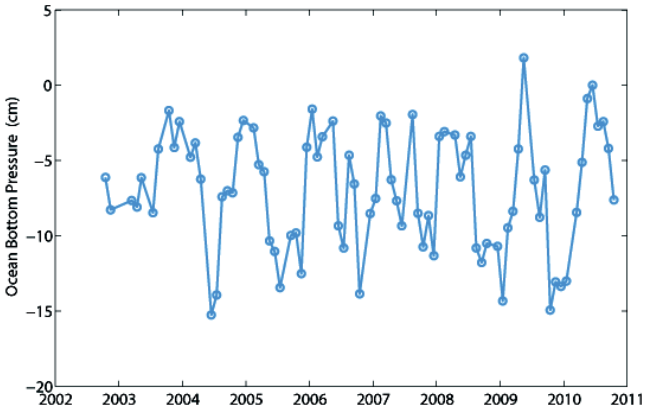

Figure 4.7. The 2002-2010 OBP variations over the Nordic seas

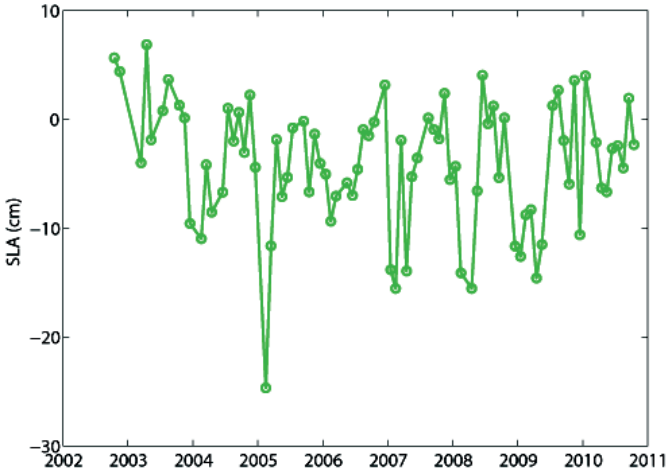

Figure 4.8. The 2002-2010 Sea level anomaly changes over the Nordic Seas

And finally, by subtracting the ocean mass variations from the SLA changes, the 2002-2010 steric sea level anomaly (SSLA) variations over the Nordic Seas are estimated (Figure 4.9).

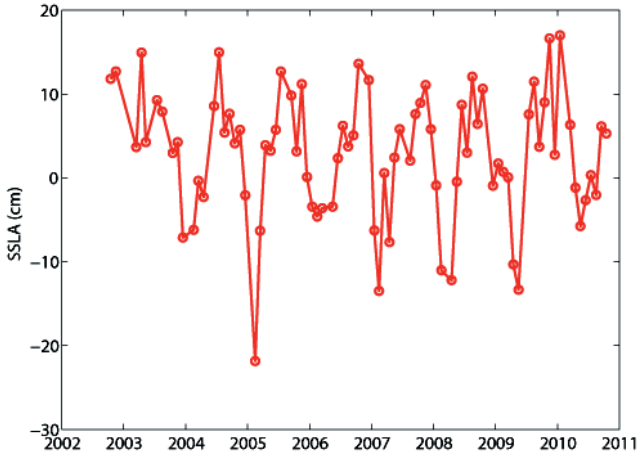

Figure 4.9. The 2002-2010 steric sea level anomaly changes over the Nordic Seas

4.4. Middle East

Water scarcity in the Middle East has been a big challenge since the onset of a drought that began in 2007. According to the World Bank report in 2007, about half of the countries in this region are consuming more water on average than they are receiving in rainfall and 85% of the water is used for irrigation. Desertification has also vast effects in the Middle East especially in countries such as Iran, Iraq, Syria, and Jordan.

Monitoring of the temporal and spatial variability of ground water storage can be useful for managing sustainable water resources in this region. Due to the paucity of hydrologic data for this region, the monitoring of the groundwater storage from traditional in situ observational methods is difficult. Satellite gravity data from GRACE is a new and invaluable tool for groundwater monitoring. GRACE is the only current satellite remote sensing mission able to monitor water below the first few centimeters of the land surface.

The main application of GRACE is quantifying the terrestrial hydrological cycle through measurements of vertically-integrated water mass changes inside aquifers, soil, surface reservoirs and snow pack, with a precision of a few millimeters in terms of water height and a spatial resolution of ~ 400 km (Wahr et al., 1998; Rodell & Famiglietti, 1999). A comparison of a large a number of modeled outputs of Terrestrial Water Storage (TWS) and the expected GRACE measurements accuracy showed that water storage changes would be detectable at spatial scales greater than 200,000 km^2, at monthly and longer timescales, and with monthly accuracies of roughly 1.5 cm (Rodell & Famiglietti, 1999). Similar conclusions were obtained using a network of hydrological observations of snow, surface water, soil moisture (SM) and groundwater (GW) in Illinois (Rodell & Famiglietti, 2001). At basin-scale, the accuracy of GRACE measurements is expected to be 0.7 cm equivalent water height (EWH) for a basin with an area of 0.4×10^6 km^2, and about 0.3 cm EWT for a basin with an area of 3.9×10^6 km^2 (Swenson et al., 2003).

In summary, the following processing steps were performed in calculating the total water storage across the Middle East from the CSR GRACE level 2 release 5 data during February 2003 to December 2013 that its results are presented in paper F.

1. The computed degree 1 coefficients are included as described by Swenson et al., 2008.
2. The coefficient of degree 2 and order 0 (C_{20}) is replaced by estimates from SLR (Cheng et al., 2013).
3. The time-mean of the coefficients from February 2003 to December 2013 is subtracted from the monthly fields.
4. The effects of Glacial Isostatic Adjustment (GIA) are removed by subtracting the GIA Stokes coefficients computed by A et al., 2013.
5. SH coefficients are smoothed using a Gaussian smoothing function with a 350 km radius.
7. Total water storage is synthesized on a 0.5° spatial grid over the Middle East.
8. The Caspian Sea signal is removed following Swenson and Wahr, 2007.
9. Lake storage contributions such as Tharthar Lake in Iraq and Urmiah Lake in Iran are removed using altimeter lake level observations following Swenson and Wahr, 2007.
10. The de-aliasing product for non-tidal ocean and atmosphere variability (GAD) is added back.

Figure 4.10 shows the total water storage trends map over the Middle East using the CSR GRACE Level 2 release 5 data during February 2003 to December 2013. The most prominent feature in Figure 4.9 is the negative trend centered over eastern Iraq and western Iran that is a clear indication of net water loss in that region.

The monthly groundwater storage variations across the Middle East are estimated as the residual of the water storage balance, after subtracting the variations in snow water equivalent, surface water and soil moisture storage from those of total water storage observed by GRACE. Using monthly output from a global, gridded land surface model, the changes in snow water equivalent, surface water and soil moisture storage are estimated. In this study, version 4.5 of the Community Land Model (CLM4.5) is used (Oleson et al., 2013). CLM4.5 includes groundwater component therefore to

isolate the changes in groundwater, CLM4.5 modeled soil moisture + snow + canopy + river storage (SSCR) is subtracted from the GRACE total water storage results.

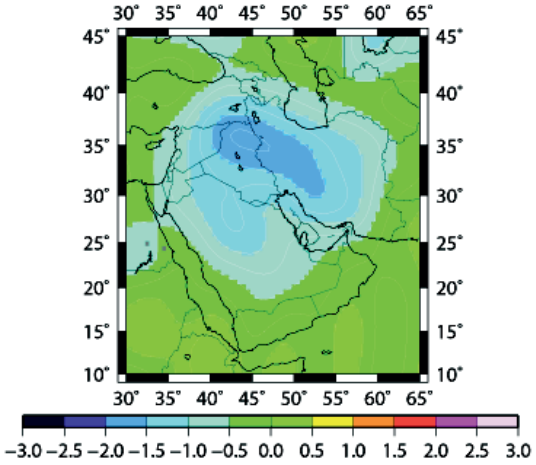

Figure 4.10. The 2003-2012 secular trends map (cm/year) in total water storage over the Middle East

Figure 4.11 shows the total groundwater storage changes over the Middle East during February 2003 to December 2013 using the same GRACE data which has been used for the Figure 4.10.

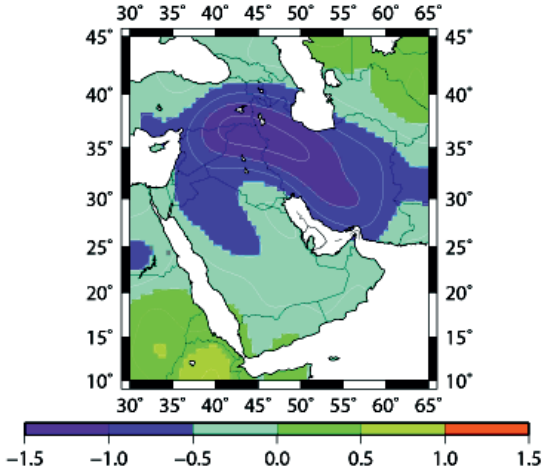

Figure 4.11. The 2003-2012 secular trends map in total groundwater storage (cm/year) over the Middle East

Groundwater levels change for many reasons. Some changes are due to natural phenomena such as drought, and others are caused by man's activities such as anthropogenic activities. To separate the groundwater changes into naturally occurring and anthropogenic components, the CLM4.5 2003-2012 groundwater trend which does not explicitly model anthropogenic contributions is subtracted from the 2003-2012 secular trends in total groundwater storage shown in Figure 4.11. The results are shown in Figure 4.12.

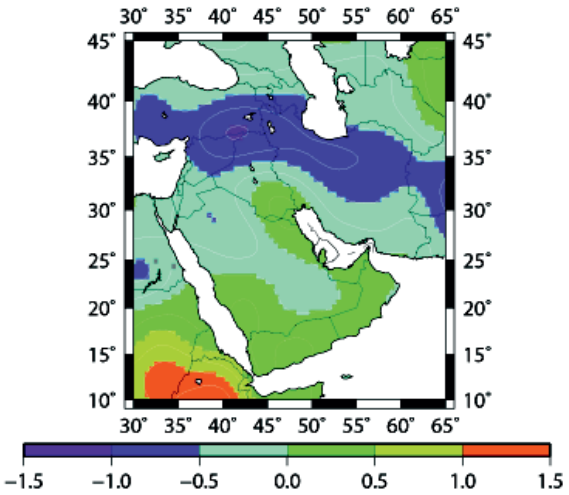

Figure 4.12. The 2003-2013 secular trends map (cm/year) in anthropogenic groundwater over the Middle East.

This map shows a notable negative trend over Iran. It seems true that the negative trend in the total groundwater storage map would be accompanied by a negative anthropogenic trend, because when drought occurs in an already dry region, increased groundwater extraction can supply the precipitation deficit required to maintain agriculture productivity.

A mascon analysis of the GRACE data as described by Jacob et al., 2012 is used to estimate time series of the total water storage, total groundwater storage and anthropogenic groundwater storage for specific regions of the Middle East which has been chosen largely to coincide with political boundaries. The entire region is subdivided into seven mascons: Iran, Iraq, Syria, eastern Turkey (east of 35^{o} longitude),

northern and southern Saudi Arabia (north and south of 25^{o} latitude), and the region immediately west of Caspian Sea.

According to Jacob et al., 2012, mascons are user-defined regions of the Earth's surface, for example chosen here to coincide with political boundaries. For each mascon, the set of Stokes coefficients is found that it would be caused by a unit mass distributed uniformly over that mascon. Let $M_i(t)$ is the actual mass of mascon *i* at time *t,* which is unknown. By fitting the $M_i(t)$'s for all the mascons simultaneously to the GRACE monthly Stokes coefficients, the mass of each mascon at time *t* is estimated. The results are shown in Figure 4.13, and Table 4.3 lists the trends for those regions.

Table 4.3. Secular trends, in Gt/yr, of the total groundwater storage (GRACE-minus-CLM4.5 SSCR) and anthropogenic groundwater (GRACE-minus-CLM4.5) for the seven mascons in the Middle East, for 2003-2012

Region	GRACE-minus-CLM4.5 SSCR	GRACE-minus-CLM4.5
Iran	-25±6	-14±6
Iraq	-2±3	3±3
Eastern Turkey	-5±2	-6±2
Northern Saudi Arabia	-6±2	-5±5
Southern Saudi Arabia	-5±2	2±2
Syria	-4±1	-3±1
West of Caspian Sea	0±1	0±1

The uncertainties in Table 4.3 are an attempt to account both for measurement errors in the GRACE data, and for errors in the CLM4.5 model output. The results show that all of the mascons have negative trends in the total groundwater storage and anthropogenic contributions. Iran with a mass loss rate of -25±6 Gt/yr has the largest groundwater depletion in the region during February 2003- December 2012. This mass loss rate is supported by in situ well data from across Iran. The results also show that in this region the naturally occurring groundwater loss is larger than the anthropogenic loss.

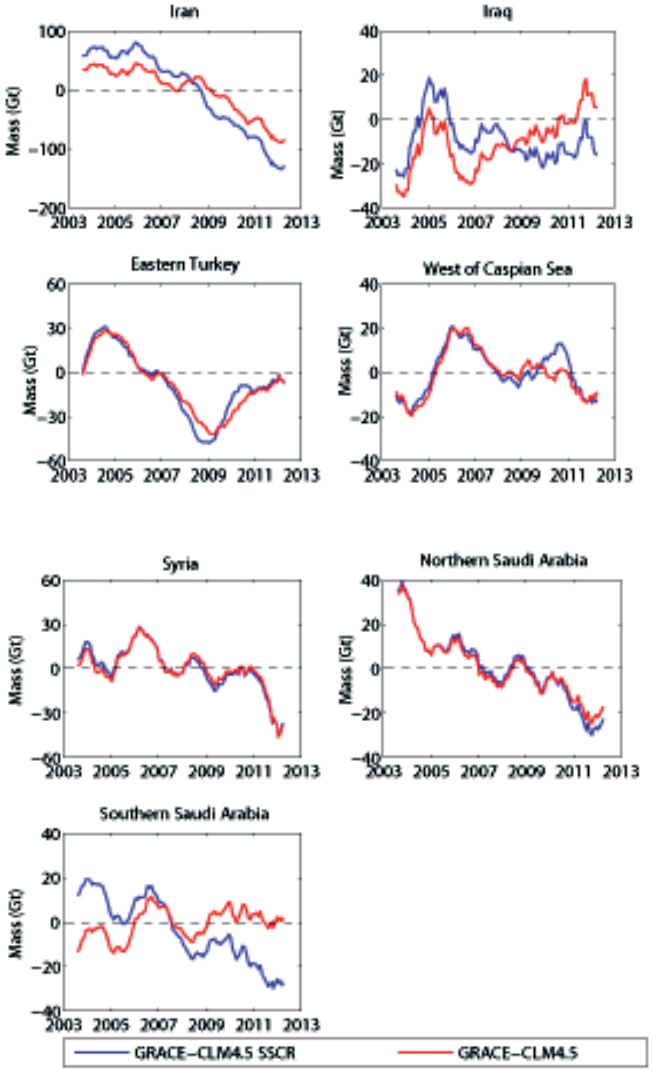

Figure 4.13. Changes in total groundwater storage, integrated across seven mascons in the Middle East including Iran, Iraq, eastern Turkey, Syria, northern and southern Saudi Arabia, and the region immediately west of Caspian Sea. Shown are smoothed monthly values of the total groundwater storage inferred from GRACE-minus-(CLM4.5 SSCR), compared with the anthropogenic groundwater component (GRACE-minus-CLM4.5).

Chapter 5
Concluding Remarks

In this PhD study, time series of Earth's mass changes in ice sheet, ocean, and continental water storage were derived by using the satellite Gravimetry data such as GRACE. This study was done across three case studies; Greenland, Nordic Seas, and Middle East.

In Greenland, three different GRACE Level 2 release 4.0 data from CSR, GFZ, and JPL were used to estimate the time series of the ice mass changes. All of these data were during April 2002 to December 2010; but some months were missing for all three data sets. All of the data were de-striped by a non-isotropic filter and were smoothed in three parameters of $a = 10^{14}, 10^{13}$, and 10^{12} according to Gaussian smoothing radii: 530 km, 340 km, and 240 km. A good agreement was found for ice mass loss models based on the CSR and GFZ solutions, while the corresponding ice mass loss model based on the JPL solutions, was significantly smaller. A disagreement between the rate based on the JPL solution and the rates from the other solutions needs further investigation. Excluding the JPL solution and taking the average over the rates based on the CSR and GFZ solutions; the net ice mass balance during April 2002 to December 2010 is estimated of -162±29 Gt/yr. The uncertainty of this estimate is RSS (Root Sum Square) of the uncertainties of the rates based on the CSR and GFZ solutions. The spatial distribution of the ice mass changes showed large coastal mass losses and a small interior mass gain. A clear mass loss was also seen spreading up along the northwest coast. This spread of ice mass loss has been started since 2007. And in the end, the

results showed that the mass loss of the Greenlandic ice sheets is not a constant, but accelerating with time. Its acceleration is estimated of –32±6 Gt/yr^2 during 2002 to 2011.

In Nordic Seas, the GFZ GRACE Level 2 release 04 data was used to estimate the time series of water mass changes. The data time spans were from October 2002 to October 2010. All of them were de-striped by a non-isotropic filter and were smoothed by a parameter of $a = 10^{14}$ according to Gaussian smoothing radius of 530 km. There are significantly limitations to estimate time series of ocean mass changes by using the GRACE data. Initial studies suggested that the usefulness of GRACE data for understanding ocean dynamics was limited to measuring mean ocean mass variations. Because gravity signals are attenuated as altitude increases, the inherent resolution of measurements from space, both spatially and in amplitude, is restricted by the altitude of the satellite. Even if there were no errors in the GRACE measurement, the smallest resolution that is theoretically possible from a satellite at GRACE's altitude is about 300 km, which means that GRACE would only be able to observe an average mass fluctuation for a disc with a radius of 300 km. However, because of filtering required to reduce correlated errors ("stripes") and random errors that increase with decreasing wavelength, the effective resolution is 1000 km. Using of de-striped GRACE data which have been filtered by a non-isotropic filter is caused to decrease the effective resolution of GRACE data. By removing hydrological signals which are leaking from land to ocean, from obtained the time series of ocean mass changes and add back oceanic signals which are leaking from ocean to land, to the time series of ocean mass changes, the GRACE data can be used to measuring regional ocean mass variations.
In Nordic Seas, water mass variations from the GRACE data and sea level anomalies from ENVISAT altimetry data, cycles 10 to 93 were used to study the steric sea height changes. This methodology can be very useful to get an estimate of the steric sea level, overcoming the problem of sparse or inexistent in situ hydrographic data.

In Middle East, the CSR GRACE Level 2 release 05 data during February 2003 to December 2012 were used to estimate the trends of total water storage (groundwater plus soil moisture plus surface water and snow), total groundwater, and anthropogenic groundwater. This methodology can be very useful to monitoring monthly changes in

total water storage in the regions where there is a lack of hydrologic data. Release 05 of the GRACE level 2 data is the latest release of the GRACE data which is more accurate to its release 04. To separate the groundwater and anthropogenic contributions from the total water storage across the Middle East, the CLM4.5 hydrological model was used. The CLM4.5 simulation gave a reasonably good match to the GRACE seasonal variability in this region, but this was not true for the other models such as GLDAS (Global Land Data Assimilation System). The results from the trend map of total water storage show a large negative trend centered over eastern Iraq and western Iran. The most of the long-term, sub-surface water loss in this region is due to a decline in groundwater storage. The rates of change of groundwater volume within each mascon inside the Middle East showed that Iran with a rate of 25±6 Gt/yr has the most groundwater loss rate during February 2003 to December 2012 in this region. An analysis of in situ well data from across Iran supported the Iran's rate of groundwater loss from the GRACE data. Because CLM4.5 also includes an unconfined aquifer store, groundwater loss caused by human's activities such as anthropogenic contributions was estimated. The results showed that in the most regions of the Middle East, groundwater loss caused by natural climate variations such as drought is larger than the anthropogenic contributions.

Although the results of this study showed that the GRACE level 2 data can be useful to monitoring the Earth's mass transport, in ice sheets, ocean, and land, especially in the regions with the paucity of direct measurements such as hydrological data. However, there are still significant limitations to the use of GRACE level 2 data for understanding the Earth's mass transport such as discrepancies in the monitoring by the different GRACE data sets (e.g. Greenland Ice mass loss), and depending on methods for the analysis that need to more investigations in the future. GRACE follow-on mission with a new high-precision laser metrology system will provide a more precise observation of the distribution of mass on the Earth. It is recommended to continue in the study of the Earth's mass transport using the GRACE follow-on data in future.

References

A, G., J. Wahr, and S. Zhong (2013), Computations of the viscoelastic response of a 3-D compressible Earth to surface loading: an application to Glacial Isostatic Adjustment in Antarctica and Canada. Geophysical Journal International, 192:557–572, doi: 10.1093/gji/ggs030.

Akaike, H. (1973), Information theory and an extension of maximum likelihood principle. In: Petrov, B.N., Csaki, F. (Eds.), Second International Symposium on Information Theory. Akademial Kaido, Budapest, pp. 267-281.

Baumann, K.H., H. Andruleit, and C. Samtleben (2000), Coccolithosphores in the Nordic Seas: Comparison of living communities with surface sediment assemblages, Deep Sea Research Part II: Topical Studies in Oceanography, 47, 1743–1772.

Baur, O., M. Kuhn, and W. E. Featherstone (2009), GRACE-derived ice-mass variations over Greenland by accounting for leakage effects. Journal of Geophysical Research, 114(B6):B06407.

Bettadpur, S. (2003), Level-2 gravity field product user handbook, The GRACE Project.

Bettadpur, S. (2007), Gravity Recovery and Climate Experiment. Product Specification Document, GRACE 327-720 (CSR-GR-03-02)

Beyerle, G., T. Schmidt, J. Wickert, S. Heise, M. Rothacher, G. Konig-Langlo, and K. B. Lauritsen (2006), Observations and simulations of receiver-induced refractivity biases in GPS radio occultation, Journal of Geophysical Research, 111, D12101, doi: 10.1029/2005JD006673

Box, J. E., D.H. Bromwich, and L. Bai (2004), Greenland ice sheet surface mass balance 1991-2000: Application of Polar MM5 mesoscale model and in situ data, Journal of Geophysical Research, 109, D16105, doi: 10.1029/2003JD004451.

Buis, A. (2012), At 10, GRACE Continues Defying, and Defining, Gravity, NASA, URL: http://www.nasa.gov/mission_pages/Grace/news/grace20120316.html

Chambers D.P., B.D. Tapley and R.H. Stewart (1997), Long-period heat storage rates and basin scale heat fluxes from TOPEX, Journal of Geophysical Research, 102, 10525-10533, doi: 10.1016/j.jog.2011.04.004.

Chambers, D. P., J. Wahr, and R.S. Nerem (2004), Preliminary observations of global ocean mass variations with GRACE, Geophysical Research Letter, 31, L13310, doi: 10.1029/2004GL020461.

Chambers, D. P., J. Schroter (2011), Measuring ocean mass variability from satellite Gravimetry, Journal of Geodynamics, 52, 333-343.

Chen, J.L., C.R. Wilson, B.D. Tapley, J.S. Famiglietti, and Matt Rodell (2005), Seasonal global mean sea level change from satellite altimeter, GRACE, and geophysical models, Journal of Geodesy, 79(9), 532, doi: 10.1007/s00190-005-0005-9.

Chen, J.L., C.R Wilson, J.S. Famiglietti, and M. Rodell (2005), Spatial sensitivity of the Gravity Recovery and Climate Experiment (GRACE) time-variable gravity observations, Journal of Geophysical Research, 110, B08408, doi: 10.1029/2004JB003536.

Chen, J.L., C.R. Wilson, and B.D. Tapley (2006), Satellite gravity measurements confirm accelerated melting of Greenland ice sheet, Science, 313, doi: 10.1029/science.1129007.

Cheng, M.K., and B.D. Tapley (2004), Variations in the Earth's oblateness during the past 28 years. Journal of Geophysical Research, 109(B09402)

Cheng, M.K., B.D. Tapley, and J.C. Ries (2013), Deceleration in the Earth's oblateness, Journal of Geophysical Research, V118, 1-8, doi:10.1002/jgrb.50058.

Dobslaw H., P. Schwintzer, F. Barthelmes, F. Flechtner, Ch. Reigber, R. Schmidt, T. Schone and M. Wiehl (2004), Geostrophic ocean surface velocities from TOPEX altimetry, and CHAMP and GRACE satellite gravity models. Scientific Technical Report STR04/07, GFZ Potsdam, pp. 22.

Dunn, C, W. Bertiger, Y. Bar-Sever, S. Desai, B. Haines, D. Kuang, G. Franklin, I. Harris, G. Kruizinga, T. Meehan, S. Nandi, D. Nguyen, T. Rogstad, J. Thomas, J. Tien, L. Romans, M. Watkins, S. Wu, S. Bettadpur, and J. Kim (2003), Instrument of GRACE: GPS augments gravity measurements, GPS World, Vol. 14, No. 2, pp 16-28.

Famiglietti, J.S., M. Lo, S.L. Ho, J. Bethune, K. J. Anderson, T. H. Syed, S.C. Swenson, C.R. de Linage, and M. Rodell (2011), Satellites measure recent rates of groundwater depletion in California's Central Valley, Geophysical Research Letters, 38, doi: 10.1029/2010GL046442.

Ghazavi K. and H. Nahavandchi (2011), Mean Sea Surface and ocean circulation in North Atlantic and the Arctic Sea. Journal of Geodetic Science, Vol. 1, No 2, pp. 181-190, DOI 10.2478/v10156-010-0021-4.

Gill, A.E., and P.P. Niiler (1973), The theory of the seasonal variability in the ocean, Deep Sea Research, 20, 141– 177.

Guo, J.Y., Z.W. Huang, C.K. Shum, and W. van der Wal (2012), Comparisons among contemporary glacial isostatic adjustment models. Journal of Geodynamics, 61, 129–137.

Hanna, E., J. Cappelen, X. Fettweis, P. Huybrechts, A. Luckman, and M. Ribergaard (2009), Hydrologic response of the Greenland ice sheet: the role of oceanographic warming. Hydrological Processes, 23(1):7{30}.

Ilk, K.H., J. Flury, R. Rummel, P. Schwintzer, W. Bosch, C. Haas, J. Schroter, D. Stammer, W. Zahel, H. Miller, R. Dietrich, P. Huybrechts, H. Schmeling, D. Wolf, H.J. Gotze, J. Riegger, A. Bardossy, A. Gunter, and T. Gruber (2005), Mass transport and mass distribution in the Earth system. Technical report, GOCE Projectburo Deutschland, Technische Universitat Munchen, GFZ Potsdam.

Jacob, T., J. Wahr, W. Tad Pfeffer, and S. Swenson (2012), Recent contributions of glaciers and ice caps to sea level rise, Nature, 482, 514–518 doi: 10.1038/nature10847.

Jayne, S.R., J.M. Wahr, and F.O. Bryan (2003), Observing ocean heat content using satellite gravity and altimetry, Journal of Geophysical Research, 108, 3031, doi: 10.1029/2002JC001619, C2.

Jekeli, C. (1981), The downward continuation to the earth's surface of truncated spherical and ellipsoidal harmonic series of the gravity and height anomalies, Technical Report 323, Ohio State University.

Johannessen, O.M. (1986), Brief overview of the physical oceanography. In B. G. Hurdle (ed.): Nordic seas. Pp. 103‑127. New York: Springer.

Joodaki G. and H. Nahavandchi (2012a), Mass loss of the Greenland ice sheet from GRACE time-variable gravity measurements. Studia Geophysica et Geodaetica, DOI 10.1007/s11200-010-0091-x.

Joodaki G. and H. Nahavandchi (2012b), Mass balance and mass loss acceleration of the Greenland ice sheet (2002– 2011) from GRACE gravity data, Journal of Geodetic Science, 2(2), 156-161 DOI: 0.2478/v10156-011-0032-9.

Joodaki G., H. Nahavandchi, and K. Ghazavi (2013), Steric sea level changes from ENVISAT and GRACE in the Nordic Seas, 20 years of Progress in Radar Altimetry symposium, ESA publication SP-710.

Khan, S.A., J. Wahr, M. Bevis, I. Velicogna, and E. Kendrick (2010), Spread of ice mass loss into northwest Greenland observed by GRACE and GPS. Geophysical Research Letter, 37:L06501.

Klees, R., E. Revtova, B. Gunter, P. Ditmar, E. Oudman, H. Winsemius, and H. Savenije (2008), The design of an optimal filter for monthly GRACE gravity models, Geophysical Journal International, 175, 417–432.

Krabil, W., E. Hanna, P. Huybrechts, W. Abdalati, J. Cappelen, B. Csatho, E. Frederick, S. Manizade, C. Martin, J. Sonntag, R. Swift, R. Thomas, and J. Yungel (2004), Greenland Ice Sheet: Increased coastal thinning, Geophysical Research Letter, 31, L24402, doi: 10.1029/2004GL021533.

Kusche J., R. Schmidt, S. Petrovic, R. Rietbroek (2009), Decorrelated GRACE Time-Variable Gravity Solutions by GFZ, and their Validation using a Hydrological Model, Journal of Geodesy, Volume 83, Number 10, 903-913, DOI: 10.1007/s00190-009-0308-3.

Mitrovica J.X., J. Wahr, I. Matsuyama, A. Paulson (2005), The rotational stability of an ice-age Earth. Geophysical Journal International, 161:491‐506.

Morison, J., J. Wahr, R. Kwok, C. Peralta-Ferriz (2007), Recent trends in Arctic Ocean mass redistribution revealed by GRACE. Geophysical Research Letter 34, L07602, doi: 10.1029/2006GL029016.

Nahavandchi H. and G. Joodaki, (2012), Greenland ice-melt spread into Northwest revealed by GRACE, Kart og Plan, Volume 72, Annual 105, 234-240.

Oleson, K.W., D.M. Lawrence, G.B. Bonan, M.G. Flanner, E. Kluzek, P.J. Lawrence, S. Levis, S.C. Swenson, P.E. Thornton, A. Dai, M. Decker, R. DIckinson, J. Feddema, C.L. Heald, F. Hoffman, J.F. Lamarque, N. Mahowald, G.Y. Niu, T. Qian, J. Randerson, S. Running, K. Sakaguchi, A. Slater, R. Stockli, A. Wang, Z.L. Yang, X. Zeng, and X. Zeng (2010), Technical description of version 4.0 of the Community Land Model, NCAR Technical Note NCAR/TN-478+STR, 257.

Oleson, K.W., D.M. Lawrence, G.B. Bonan, B. Drewniak, M. Huang, C.D. Koven, S. Levis, F. Li, W.J. Riley, Z.M. Subin, S.C. Swenson, P.E. Thornton, A. Bozbiyik, R. Fisher, C.L. Heald, E. Kluzek, J.-F. Lamarque, P.J. Lawrence, L.R. Leung, W. Lipscomb, S. Muszala, D.M. Ricciuto, W. Sacks, Y. Sun, J. Tang, and Z.-L. Yang (2013), Technical description of version 4.5 of the Community Land Model (CLM), NCAR Technical Note NCAR/TN-503+STR, 434 pp.

Peltier, W.R. (2004), Global glacial isostasy and the surface of the ice-age Earth: the ICE-5G (VM2) model and GRACE. Annual Review of Earth and Planetary Sciences, Vol 32, 111-149.

Qian, T., A. Dai, K.E. Trenberth, and K.W. Oleson (2006), Simulation of global land surface conditions from 1948 to 2004: Part I: Forcing data and evaluations, Journal of Hydrometeorology, 7, 953–975, doi:10.1175/JHM540.1.

Ramillien, G., A. Lombard, A. Cazenave, E. R. Ivins, M. Llubes, and R. Biancale (2006), Interannual variations of the mass balance of the Antarctica and Greenland ice sheets from GRACE, Global Planetary Change, 53, 198–208.

Ramillien, G., F. Frappart, A. Güntner, T. Ngo-Duc, A. Cazenave, and K. Laval (2006), Time variations of the regional evapotranspiration rate from Gravity Recovery and Climate Experiment (GRACE) satellite gravimetry, Water Resources Research, 42, W10403, doi: 10.1029/2005WR004331.

Rignot, E. (2005), Mass budget of the Greenland Ice Sheet in 2000 from Radarsat-1 interferometry, abstract EGU05-A-10435, Eur. Geophys. Union, Vienna.

Rodell, M., and J. S. Famiglietti (1999), Detectability of variations in continental water storage from satellite observations of the time dependent gravity field, Water Resources Research, 35, 2705– 2723.

Rodell, M., and J. S. Famiglietti (2001), An analysis of terrestrial water storage variations in Illinois with implications for the Gravity Recovery and Climate Experiment (GRACE), Water Resources Research, 37, 1327– 1340.

Rodell M, P. R. Houser, U. Jambor, J. Gottschalck, K. Mitchell, C.-J. Meng, K. Arsenault, B. Cosgrove, J. Radakovich, M. Bosilovich, J. K. Entin, J. P. Walker, D. Lohmann, and D. Toll (2004), The Global Land Data Assimilation System. Bulletin of the American Meteorological Society, vol 85 (3), pp 381-394.

Rodell, M., I. Velicogna, and J.S. Famiglietti (2009), Satellite-based estimates of groundwater depletion in India, Nature, 460, 999-1002, doi: 10.1038/460789a.

Sasgen, I. (2009), Present-day ice-mass change and glacial-isostatic adjustment in the polar regions from satellite gravimetry and geophysical modelling. PhD thesis, Freien Universitat Berlin.

Solomon, S., D. Qin, M. Manning, Z. Chen, M. Marquis, K. Averyt, M. Tignor, and H. Miller (2007), Climate change 2007: the physical science basis. Cambridge University Press.

Song, Y.T., and F. Colberg (2011), Deep Ocean warming assessed from altimeters, Gravity Recovery and Climate Experiment, in situ measurements, and a non-Boussinesq ocean general circulation model, Journal Geophysical Research, 116, C02020, doi: 10.1029/2010JC006601.

Sørensen, L.S. and R. Forsberg (2010), Greenland Ice Sheet Mass Loss from GRACE Monthly Models. In Mertikas, S. P., editor, Gravity, Geoid and Earth Observation, pages 527-532. Proceedings of International Association of Geodesy Symposia 135.

Swenson, S., and J. Wahr (2002), Methods for inferring regional surface-mass anomalies from Gravity Recovery and Climate Experiment (GRACE) measurements of time-variable gravity, Journal Geophysical Research, 107(B9), 2193, doi: 10.1029/2001JB000576.

Swenson, S., J. Wahr, and P.C.D. Milly (2003), Estimated accuracies of regional water storage variations inferred from the Gravity Recovery and Climate Experiment (GRACE), Water Resources Research, 39(8), 1223, doi: 10.1029/2002WR001808.

Swenson, S., and J. Wahr (2007), Multi-sensor analysis of water storage variations of the Caspian Sea, Geophysical Research Letter, 34, L16401, doi: 10.1029/2007GL030733.

Swenson, S., J. Famiglietti, J. Basara, and J. Wahr (2008), Estimating profile soil moisture and groundwater variations using GRACE and Oklahoma Mesonet soil moisture data, Water Resources Research, 44, W01413, doi: 10.1029/2007WR006057.

Swenson, S and J Wahr (2009), Monitoring the water balance of Lake Victoria, East Africa, from space. Journal of Hydrology, 370 (4-Jan) 163-176, issn: 0022-1694, ids: 453WY, doi: 10.1016/j.jhydrol.2009.03.008.

Swift, J.H. (1986), The Arctic waters. Nordic Seas, B. G. Hurdle, Ed., Springer-Verlag, 129–153.

Tamisiea, M.E. (2011), Ongoing glacial isostatic contributions to observations of sea level change. Geophysical Journal International, 186: 1036–1044, doi: 10.1111/j.1365-246X.2011.05116.x

Tapley, B.D., S. Bettadpur, M. Watkins, and C. Reigber (2004), The gravity recovery and climate experiment: Mission overview and early results, Geophysical Research Letter, 31, L09607, doi:10.1029/2004GL019920.

Tiwari, V.M., J. Wahr, S. Swenson (2009), Dwindling groundwater resources in northern India, from satellite gravity observations. Geophysical Research Letters 36 - L18401, doi: 10.1029/2009GL039401.

Velicogna, I. and J. Wahr (2002), Postglacial rebound and Earth's Viscosity Structure from GRACE. Journal of Geophysical Research, doi: 10.1029/2001JB001735

Velicogna, I., & Wahr, J. (2005), Greenland mass balance from GRACE, Geophysical Research Letters, 32(18), doi: 10.1029/2005gl023955

Velicogna, I., and J. Wahr (2006), Measurements of time variable gravity show mass loss in Antarctica, Science, 311, 1754–1756.

Velicogna, I. (2009). Increasing rates of ice mass loss from the Greenland and Antarctic ice sheets revealed by GRACE. Geophysical Research Letter, 36(19):L19503.

Wahr, J., M. Molenaar, and F Bryan (1998), Time variability of the Earth’s gravity field: Hydrological and oceanic effects and their possible detection using GRACE, Journal of Geophysical Research, 103, 30205--30,230

Wahr, J., D. Wingham, and C. Bentley (2000), A method of combining ICESat and GRACE satellite data to constrain Antarctic mass balance, Journal of Geophysical Research, 105, 16,279–16,294.

Wahr, J. M., S.R. Jayne, and F.O. Bryan (2002), A method of inferring changes in deep ocean currents from satellite measurements of time-variable gravity, Journal of Geophysical Research, 107(C12), 3218, doi:10.1029/2001JC001274.

Wang, L., and C. Koblinsky (1997), Can the Topex/Poseidon altimetry data be used to estimate air-sea heat flux in the North Atlantic?, Geophysical Research Letter, 24(2), 139-142.

Wang, X., C. de Linage, J. Famiglietti, and C. Zender (2011), Gravity Recovery and Climate Experiment (GRACE) detection of water storage changes in the Three Gorges Reservoir of China and comparison with in situ measurements, Water Resources Research, 47, W12502, doi: 10.1029/2011WR010534

Watkins, M, F. Flechtner, P. Morton, and F. Webb (2013), Status of the GRACE Follow-On Mission, Geophysical Research Abstracts, Vol. 15, EGU2013-6024.

White, W., and C.K. Tai (1995), Inferring interannual changes in global upper ocean heat storage from TOPEX altimetry, Journal of Geophysical Research, 100, 24943-24954.

Wouters, B., D. Chambers, and , E.J.O., Schrama (2008), GRACE observes small-scale mass loss in Greenland. Geophysical Research Letter, 35(20):L20501.

Yi Y. (2010), The Ohio State University Stackfiles for Satellite Radar Altimeter data, Report No. 495, The Ohio State University, USA.

Paper A

Gholamreza Joodaki and Hossein Nahavandchi, (2010), **Greenland mass balance estimation from satellite gravity measurements**, ESA Living Planet Conference, ESA Special Publication SP-686.

GREENLAND MASS BALANCE ESTIMATION FROM SATELLITE GRAVITY MEASUREMENTS

Gholamreza Joodaki, Hossein Nahavandchi

Norwegian University of Science and Technology, Division of Geomatics, N-7491, Trondheim, Norway, Email: gholamreza.joodaki@ntnu.no, Email: hossein.nahavandchi@ntnu.no

ABSTRACT

The Gravity Recovery and Climate Experiment (GRACE) data is used to estimate the secular trend and periodic variations of ice mass variability over Greenland. To do this, we use 92 monthly GRACE level 2 Release-04 (RL04) data from the Center for Space Research at the University of Texas (UTCSR) during the period April 2002 to February 2010. The high frequency noise of data has been filtered out with three smoothing cap radius as in [3]. For separation of leakage effects, the appropriate reduction model is used. Taking the average over all smoothing radius after the leakage effects correction, the annual ice-mass loss becomes -155±3 Gt/year. Note that these values are free of any GIA correction.

1. Introduction

The GRACE satellites have been providing the scientific community with valuable information regarding Earth's gravity field. Due to its global coverage, GRACE provides an excellent tool for mapping the gravity field over large areas. GRACE not only maps the Earth's static gravity field but it also provides temporal variations of Earth's gravity field to a scale of several hundred kilometers and with a period of around one month. Changes in the gravity field are caused by the redistribution of mass within the Earth and on or above the Earth's surface. The majority of the change is related to water mass transport [8]. The GRACE data have been used by numerous authors to study changes in land water storage, ocean mass and changes in land-locked ice, including glaciers, the Greenland and the Antarctic ice sheets. Several authors have used GRACE data to estimate the rate of mass loss over Greenland. There are also several estimates of the Greenland mass variability which have been obtained using a variety of other techniques than GRACE. A problem common to all these techniques is the difficulty of monitoring the entire ice body and they can provide estimates for only a portion of ice sheet or critical regions. This problem can be overcome using GRACE satellite time variable gravity measurements. The main advantages of satellite time variable gravity measurements are that they are sensitive to the entire ice body, and that they provide mass estimates with only minimal use of supporting physical assumptions or ancillary data. Due to the limited spatial resolution and the presence of non-random noise, obtaining ice-volume loss estimates from GRACE data is not straightforward and results vary widely between 111 km³/yr and 250 km³/yr ([1], [4], [5], [6], [7] and [9]). In this paper, we estimate the secular trend in Greenland mass based on almost all available monthly GRACE data until now (June 2002, July 2002 and June 2003 data are missing). We also use the latest release (UTCSR RL04) with improved geophysical signal models and data processing techniques resulting to smallest error among other releases. The issues of high frequency noise of GRACE data and the leakage effects of the mass loss signal of the Greenland ice sheet to adjacent regions as well as signals from other regions leaking into the domain of the Greenland ice sheet are also addressed.

2. Surface mass change from GRACE

The change in surface mass density can be computed as [8]:

$$\Delta\sigma(\varphi,\lambda)=\frac{a\rho_{\text{ave}}}{3}\sum_{l=0}^{\infty}\sum_{m=0}^{l}\frac{2l+1}{1+k_l}\bar{P}_{lm}(\sin\varphi)\times\left[\Delta C_{lm}\cos m\lambda+\Delta S_{lm}\sin m\lambda\right] \quad (1)$$

where ρ_{ave} is the average mass density of the Earth (=5517 kg/m^3), $\bar{P}_{lm}$ is the normalized associated Legendre function, (φ, λ) denote latitude and longitude of point of the interest, k_l is the load Love number of degree l, a is the major semi axis of a reference ellipsoid and ΔC_{lm} and ΔS_{lm} are time-variable components of the GRACE observed Stokes coefficients for some month of degree and order (l, m) or the changes relative to the mean of the monthly solutions. Values of the Love numbers used in this study are given in [8]. Many applications require estimates of mass variability for specific regions; for example in this investigation, estimating total changes in mass of the Greenland ice sheet. For these sorts of problems, we can use specific averaging functions which are optimized

Proc. 'ESA Living Planet Symposium', Bergen, Norway
28 June – 2 July 2010 (ESA SP-686, December 2010)

for those regions. An exact regional average would take the form:

$$\Delta\sigma_{\text{region}} = \frac{1}{A_{\text{region}}} \int \Delta\sigma(\varphi,\lambda)\tau(\varphi,\lambda) \times \cos\varphi \mathrm{d}\varphi \mathrm{d}\lambda \quad (2)$$

where A_{region} is the area of the region of interest, and

$$\tau(\theta,\lambda) = \begin{cases} 0 & \text{outside the basin} \\ 1 & \text{inside the basin} \end{cases} \quad (3)$$

3. Numerical investigating

We estimate the secular trend and periodic variations of ice mass variability over Greenland using about 8 years of GRACE level 2 RL04 data from the Centre for Space Research at the University of Texas (UTSR) during the period April 2002 to February 2010. We have also used monthly Satellite Laser Ranging (SLR) estimates for C_{20} coefficient to be used to replace the estimates from GRACE (J. Ries, personal communication, 2010). In the first step, the high frequency noise in the GRACE observed Stokes coefficients has to be filtered out by appropriate smoothing techniques, as these errors manifest themselves in maps of surface mass variability as elongated, linear features, generally oriented north to south. Kusche et al (2007) developed a method in which they designed a regional spatial filter so as to minimize the satellite measurement error. Kusche et al (2009) revised the method with three smoothing cap radius of 240 km, 340 km and 530 km. In this study, we use these three decorrelation filters to account for the correlated noise contained in GRACE data (see also [3]). Because the regional filter is optimized by the trade-off between the satellite measurement error and the leakage error, it is impossible to reduce these errors simultaneously. The leakage errors were estimated as follows. We first calculated the Stokes coefficients associated with the leakage effects using Eq. 4 by integrating only outside the area concerned:

$$\begin{Bmatrix} \Delta C_{lm} \\ \Delta S_{lm} \end{Bmatrix} = \frac{3(k_l+1)}{4\pi a \rho_{\text{ave}}(2l+1)} \times \iint \Delta\sigma(\varphi,\lambda)\bar{P}_{lm}(\sin\varphi) \begin{Bmatrix} \cos m\lambda \\ \sin m\lambda \end{Bmatrix} \cos\varphi \mathrm{d}\varphi \mathrm{d}\lambda \quad (4)$$

The leakage effects were then estimated by using Eq. 1 in to the derived Stokes coefficients. Finally, the effects were subtracted from the GRACE gravity solutions.

There may be two candidates for the input data of $\Delta\sigma(\varphi,\lambda)$ in Eq. 4: one is calculated from model values and the other from GRACE data. In this study, we chose to use the GRACE data. The next step is to form an approximate estimate of total mass change for each month, by taking Eq. 2 over grid elements. To calculate secular and periodic variations, a general expression of the form

$$f(\varphi,\lambda,t) = A + Bt + \sum C_i \cos(\omega_i t) + D_i \sin(\omega_i t) \quad (5)$$

is used. Here, the value of the considered functional f is the mass anomaly at a selected location (φ, λ) and time t is approximated by a static value A, and its secular (B) and periodic (amplitudes C_i and D_i of typical angular frequencies ω_i) variations. Fig. 1 shows monthly estimates of total Greenland mass change in Gigatonne. The results show a clear trend (long term variability), supper-imposed on short-period variability. Our objective is to estimate the long term trend in ice mass change. To recover the trend, using un-weighted least squares method, a four-parameter fit for bias, secular trends and yearly seasonal variations is used. It is evident from Fig. 1 that the procedure used in this study reduces the contamination by the seasonal variability. Fig. 1 shows a clear decrease in ice mass during the investigation (about 8 years) period. Interpreting the trend as due entirely to a change in ice, we obtain a mass decrease of 155±3 Gt/yr. This estimate is an average of the results derived from three smoothing cap radius.This value of mass decrease is equivalent to a global sea level rise of 0.43±0.01 mm/yr.

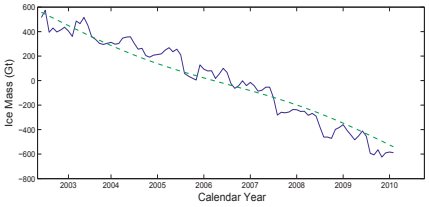

Figure1. Time series of ice mass changes for the Greenland estimated from UTCSR monthly mass solutions using non-isotropic decorrelation filter during the period April 2002 to February 2010 (continuous blue line) . The best-fitting four-parameter profile is shown in dashed green line.

In this estimation, the contaminating factors like the effects of variations in atmospheric mass and the solid Earth contribution from high-latitude Post Glacial Rebound (PGR) are not applied. The atmospheric effect is negligible for Greenland on the long term trend ([6], [7]). We also chose not to apply the correction for the

PGR signal in this study, considering the total uncertainty in the PGR estimations ([6], [7]).

4. Conclusions

Greenland is a major contributor to recent global sea level rise. Given the size and shape and complexity of the Greenland ice body, it makes it difficult to measure ice mass change in the Greenland. A variety of techniques are used to estimate Greenland ice mass balance each of which with limitations and uncertainties. The spherical harmonics coefficients of GRACE twin satellites allow regional estimation of Greenland ice mass balance. In contrast to most other techniques, GRACE measures Greenland mass variability over the entire ice sheet. Furthermore, to obtain this mass variability, the process is less ambiguous for GRACE as the relationship between gravity and mass variability follows directly from Newton's law. The main disadvantage of GRACE models for obtaining the Greenland mass change is errors caused from mismodeled postglacial rebound. GRACE is unable to separate gravitational effects of the Greenland ice sheet from those of the underlying solid Earth. Our GRACE estimate of the total Greenland mass loss using about 8 years of GRACE level 2 RL04 data from UTCSR during the period April 2002 to February 2010 is 155±3 Gt/yr. This result is in agreement with previous studies and shows an acceleration of the ice mass loss over Greenland. Time periods of higher losses and also longer periods are observed during April 2002 to February 2010. It should be stated here that mass balance estimates from GRACE measurements are not straightforward and results vary widely. This could be due to the different observation periods, and different methods used. Our GRACE estimate shows that the ice mass loss is not constant and trends are increasingly negative.

5. References

1. Chen, J.L., Wilson, C.R. & Tapley, B.D. (2006). *Satellite gravity measurements confirm accelerated melting of Greenland ice sheet.* Science 313. doi:10.1029/science.1129007.

2. Kusche, J. (2007). *Approximate decorrelation and non-isotropic smoothing of time-variable GRACE-type gravity fields*, Journal of Geodesy, 81, 11, 733-749.

3. Kusche, J., Schmidt, R., Petrovic, S. & Rietbroek, R. (2009). *Decorrelated GRACE time-variable gravity solutions by GFZ, and their validation using a hydrological model*, Journal of Geodesy, 83, 10, 903-913.

4. Luthcke, S.B., Zwally, H.J., Abdalati, W., Rowlands, D.D., Ray, R.D., Nerem, R.S., Lemoine, F.G., McCarthy, J.J. & Chinn, D.S. (2006). *Recent Greenland ice mass loss by drainage system from satellite gravity observations*. Science 314:1286–1289. Doi:10.1126/Science.1130776.

5. Ramillien, G., Lombard, A., Cazenave, A., Ivins, E.R., Llubes, M., Remy, F. & Biancale, R. (2006). *Interannual variations of the mass balance of the Antarctica and Greenland ice sheets from GRACE.* Global and Planetary Change 53:198–208. doi:10.1016/j.

6. Velicogna, I. & Wahr, J. (2006a). *Acceleration of Greenland ice mass loss in spring 2004.* Nature 443:329-331.

7. Velicogna, I. & Wahr, J. (2006b). *Measurements of Time-Variable Gravity Show Mass Loss in Antarctica*. Science 311:1754-1756. doi:10.1126/science. 1123785.

8. Wahr J., Molenaar, M. & Bryan, F. (1998). *Time variability of the Earth's gravity field*: *Hyrological and oceanic effects and their possible detection using GRACE*. J Geophys Res 103(B12): 30205-30229.

9. Wouters, B., Chambers, D.P. & Schrama, E.J.O. (2008). *GRACE observes small-scale mass loss in Greenland*. Geophys Res Lett 35:L20501. doi:10.1029/2008GL034816.

Paper B

Gholamreza Joodaki and Hossein Nahavandchi, (2012), **Mass loss of the Greenland ice sheet from GRACE time-variable gravity measurements**, Studia Geophysica et Geodetica, 56, 197-214, DOI: 10.1007/s11200-010-0091-x.

Is not included due to copyright

Paper C

Gholamreza Joodaki and Hossein Nahavandchi, (2012), **Mass balance and mass loss acceleration of the Greenland ice sheet (2002– 2011) from GRACE gravity data**, Journal of Geodetic Science, 2(2), 156-161 DOI: 0.2478/v10156-011-0032-9.

Journal of Geodetic Science

• 2(2) • 2012 • 156-161 DOI: 10.2478/v10156-011-0032-9 •

Mass balance and mass loss acceleration of the Greenland ice sheet (2002 – 2011) from GRACE gravity data

Research article

G. Joodaki*, H. Nahavandchi

Norwegian University of Science and Technology, Division of Geomatics, N-7491 Trondheim, Norway

Abstract:

We examine the magnitude and acceleration of the Greenland ice sheet mass loss between 2002 and 2011. We use monthly observations of time-variable gravity from the Gravity Recovery and Climate Experiment (GRACE) satellite gravity mission. The Greenland mass loss during this time period is not a constant, but accelerating with time. We have used a quadratic trend in addition to a linear trend, which is usually applied to the GRACE monthly time series of ice mass changes, to show that it better represents GRACE observations. Results of computations provide a mass decrease of -166±20 Gigatonne per year (Gt/yr) by using a linear trend and -111±21 Gt/yr by fitting a quadratic trend to the monthly time series. Quadratic fitting shows that the mass loss increases from -121 Gt/yr in 2002 – 2003 to -210 Gt/yr in 2006 – 2007 and -271 Gt/yr in 2010 – 2011 with an acceleration of -32±6 Gt/yr^2 in 2002 – 2011. This implies that the Greenland ice sheet contribution to sea level rise becomes larger with time. Contrary to recent studies, we use a non-isotropic filter whose degree of smoothing corresponds to a Gaussian filter with a radius of 340 km. Stripping effects in the GRACE data, C_{20} effect, and leakage effects are applied.

Keywords:

Greenland • GRACE gravity satellites • Mass loss • Acceleration • non-isotropic filter

Received 04-05-2012; accepted 21-06-2012

1. Introduction

Earth's gravity field has been explored from the GRACE satellite gravity mission. GRACE is a satellite mission jointly implemented by the US National Aeronautics and Space Administration (NASA) and German Aerospace Center (DLR) (Tapley et al. 2004a). In addition to the mapping of the Earth's static gravity field, GRACE also provides temporal variations of Earth's gravity field. GRACE can resolve temporal variations in gravity at length scales of a few hundred kilometers and with a period of around one month. Changes in the gravity field caused by the redistribution of mass within the Earth and on or above the Earth's surface can be detected by GRACE and its global coverage enables us to map the gravity field over large areas, like Greenland (see e.g. Wahr et al. 1998). Several research groups have focused their studies to use GRACE data for estimating Greenland rate of ice mass variability, such as Luthcke et al. (2006) that used raw GRACE KBRR (K-Band Range and Range rate) data; Chen et al. (2006) used the CSR monthly solutions Release 01 (RL01) during 2002 – 2005; Ramillien et al. (2006) used the same period as Chen et al. (2006) but with the GRGS/CNES GRACE solutions; Velicogna and Wahr (2006a) used the CSR monthly solutions RL01 during 2002 to 2006; Wouters et al. (2008) used the CSR RL04 monthly solutions from 2003 to 2008; Baur et al. (2009) used monthly GRACE solutions RL04 provided by GRACE processing centers of CSR, GFZ (German Research Center for Geosciences) and JPL (Jet Propulsion Laboratories) for the period 2002 to 2008, and Velicogna (2009) used the CSR RL04 monthly solutions between 2002 and 2009. Note that all of the results reported above are based on isotropic filters. Joodaki and Nahavandchi (2012) ap-

*E-mail: gholamreza.joodaki@ntnu.no; Tel.: +47-7359-4715; Fax: 47-7359-7021

plied a non-isotropic filter to CSR, GFZ and JPL monthly solutions RL04.

Velicogna (2009) estimated an increase in mass loss from Greenland ice sheet, i.e. it was shown that mass loss is accelerating. However, filtering procedure and removal of periodic variations are different from our study. The observation period is also different. Decorrelating kernels in the filtering approach used in this study are not axisymmetric (isotropic) and they tend to exhibit negative sidelobes in north-south direction with a shape depending on the geographical positions. The GRACE noise also manifests itself as near north-south "stripes" and it has a non-isotropic nature.

Other satellite based sensors are also used to study Greenland ice mass variability. Some examples are Abdalati et al. (2001), Rignot et al. (2004), Rignot and Kanagaratnam (2006) and Joughin et al. (2010) that used Synthetic Aperture Radar (SAR) imaging to reveal an acceleration of a large number of outlet glaciers in Greenland, Slobbe et al. (2008), Howat et al. (2008), Pritchard et al. (2009) and Sørensen et al. (2011) that used laser altimetry and Sørensen et al. (2010) that used satellite laser, radar and gravity measurements to study the Greenland ice mass variability.

In this paper, we present an analysis of trend in Greenland ice mass variability and its rate of change based on monthly GRACE solutions provided by CSR during April 2002 to April 2011. The CSR RL05 Level-2 data products have been recently available for the data span January 2004 through December 2010 which did not cover the study period therefore the latest release RL04 (at the time of this study) is used with improved geophysical signal models and data processing techniques. This release has smallest error among other releases (Bettadpur 2007). Unlike other studies, a filtering technique based on non-isotropic filter is applied (see also Joodaki and Nahavandchi 2012). We examine different ways of fitting a regression through the monthly time series of ice mass change data. Regression of linear and quadratic forms are compared and concluded on the best statistical representation of the ice mass data.

1.1. Data and Methodology

The GRACE twin satellites launched in March 2002 measures Earth gravity changes with unprecedented accuracy. GRACE tracks the changes in the distance between its twin satellites and combines these measurements with data from on-board Global Positioning System (GPS) receivers and accelerometers. Monthly GRACE gravity field solutions are then determined from these data. Solutions consist of monthly spherical harmonic coefficients of the Earth's gravity field. Each monthly field consists of fully normalized (Stokes) coefficients, C_{lm} and S_{lm}, up to degree and order (l, m). We use monthly GRACE gravity coefficients up to degree and order 60 generated at the CSR at the University of Texas (Tapley et al. 2004b). This study is based on 105 monthly models between April 2002 and April 2011. Wahr et al. (1998) introduces a method to estimate monthly local changes in surface mass, using the static monthly spherical harmonic coefficients. The mass changes in this method (ibid) are assumed in a very thin layer of water concentrated at the surface with a variable thickness. This assumption is not far from reality as changes in water storage in hydrologic reservoirs, by moving ocean, atmospheric and cryospheric masses, and by exchange among these reservoirs causes monthly changes in gravity signals (Chambers 2007). The vertical extent of the water is much smaller than the horizontal scales of the changes. It is called equivalent water thickness. Mass variations are modeled as surface density variations $\Delta\sigma$(the unit of $\Delta\sigma$ is mass/surface area) in a spherical layer. One then can estimate monthly local changes in surface mass density using monthly spherical harmonic coefficients of the Earth's gravity field (Wahr et al. 1998):

$$\Delta\sigma(\phi,\lambda) = \frac{a\rho_{\text{ave}}}{3}\sum_{l=0}^{\infty}\sum_{m=0}^{l}\frac{2l+1}{1+k_l}\bar{P}_{lm}(\sin\phi)[\Delta C_{lm}\cos m\lambda + \Delta S_{lm}\sin m\lambda] \quad (1)$$

where ϕ and λ are the spherical latitude and longitude of the point of interest, a is the radius of the Earth (a = 6377 km in this study), ρ_{ave} is the average mass-density of the solid Earth (assumed throughout this paper to be 5517 kg/m^3), k_l is the Love number of degree l which is given in Wahr et al. (1998), $\bar{P}_{lm}$ is the normalized associated Legendre function of the first kind, andΔC_{lm} and ΔS_{lm} are time-variable components of the GRACE observed Stokes coefficients for some month of degree and order (l, m) or as changes relative to the mean of the monthly solutions. It should be stated here that $\Delta\sigma/\rho_w$ transforms surface mass-densities to equivalent water thickness values, where ρ_w is the mass-density of freshwater. There are several correction terms and contaminating factors which must be applied before the ice mass loss estimates can be interpreted.

Due to the orbital geometry of GRACE, and nature of the measurement technique, the monthly Stokes coefficients are contaminated with short-wavelength noise. The noise is significant when one is interested in signals of geographical extension of a few hundreds km and/or using the higher degree coefficients. The GRACE noise structure mainly manifests itself as near north-south "stripes" and it has a non-isotropic nature. Convolving against an isotropic Gaussian smoothing kernel, and recently probabilistic decorrelation methods in GRACE solutions in conjunction with an additional smoothing are among the methods used to identify and remove error correlation (noises) in the GRACE monthly spherical harmonic coefficients. The latter methods result in decorrelation kernels that are not isotropic. We used Kusche et al. (2009) non-isotropic decorrelation and smoothing technique to de-stripe monthly GRACE RL04 gravity models. The non-isotropic filter was also used by Joodaki and Nahavandchi (2012).

Due to the GRACE orbit geometry and the separation length between its twin satellites, the monthly GRACE C_{20} coefficients cannot be well determined (Tapley et al. 2004b). The GRACE C_{20} estimates also are well-known to be affected by significant long-period tidal aliases. An alternative which improves the estimation of mass

variations from GRACE is to replace the monthly GRACE C_{20} coefficient by their estimates from Satellite Laser Ranging (SLR) (Chen et al. 2005). The SLR time series are also more precise, with about a third of the noise of the GRACE time series. In this study, we replace GRACE C_{20} coefficient with monthly SLR estimates which are obtained from the analysis of SLR data to five geodetic satellites: LAGEOS-1 and 2, Starlette, Stella and Ajisai. These estimates are provided from the CSR GRACE Science Data System (TN05) (Cheng and Tapley, 2004).

Leakages from other geophysical signals besides the ice mass loss are an error source which should be accounted for a reliable estimate of secular mass changes over Greenland. Leakages are divided into leakage in and leakage out effects. On the one hand, mass change at a place outside Greenland propagates into a signal spreading over Greenland and has an impact on the Greenland mass-change estimates. On the other hand, mass change over Greenland propagates into a signal spreading over outside the Greenland area. The leakage out signal has to be restored back into the region of interest. The leakage in signal has to be reduced from the region of interest. We used the model as described by Joodaki and Nahavandchi (2012) to estimate the leakage effects. In this model, only GRACE data is used to delineate the leakage effects. The model calculates spherical harmonic coefficients, associated with leakage effects, from the surface mass densities on the areas concerned. The GRACE data alone is used to calculate the surface mass densities. The sources generating leakage in signals could be from all over the world, however the impact reduces with increasing distances following the Newton's law of gravitation. The strongest signals on Greenland are caused by Alaska, Fennoscandia and the Canadian Shield. These three sources are used in this study to determine the leakage effects which were also used in Baur et al. (2009) investigations.

The degree-0 Stokes coefficient in Equation (1) is assumed constant and is not used in this investigation. It is proportional to the total mass of the Earth and atmosphere. The geocenter motion represented by variations in the degree-1 Stokes coefficients cannot be derived from the GRACE data. We have not applied these variations in our monthly models, but it is recognized that neglecting the geocenter motion might introduce an error in the rate of Greenland ice mass variability (Chambers et al. 2004 and Chen et al. 2005).

We have not applied, in our estimation of ice mass change rates, contaminating factors caused by the effects of variations in atmospheric mass, and the solid Earth contribution from high-latitude Post Glacial Rebound (PGR). The atmospheric effects are negligible for Greenland on the long term trend (Velicogna and Wahr 2006a, b). We also chose not to apply the correction for the PGR signal, considering the total uncertainty in the PGR estimations (Velicogna and Wahr 2006a, b). It is left to others to choose their preferred PGR model. Nevertheless, it should be noted that the PGR signal for the entire Greenland is estimated to -7.4 Gigaton per year (Gt/yr) with a standard deviation of $\pm$19 Gt/yr (Velicogna and Wahr 2006b) and this value or other preferred PGR model can easily be applied to the ice-mass estimates by readers. When comparing to the ice-mass estimates, the PGR signal is more than one order of magnitude smaller.

2. Numerical investigations

We obtain the time series for Greenland ice mass change and the secular trend in ice mass rate, calculated from GRACE level 2 RL04 monthly solutions generated at CSR processing centers from April 2002 to April 2011. The maximum degree of the expansion for the CSR spherical harmonic coefficients is 60. This spatial resolution may not be enough fine to isolate the source of the ice mass variability but it is the maximum resolution available by CSR model and enough to show the Greenland ice sheet mass loss. Unphysical striping error pattern (noises) in monthly solutions of the GRACE is decorrelated/filtered in the corresponding Gaussian radius of 340 km (see Kusche et al. 2009, Joodaki and Nahavandchi 2012). We calculated potential leakage effects and applied them in monthly total mass change estimations. The average leakage in and leakage out effects for CSR monthly gravity solutions and smoothing degree of corresponding Gaussian radius of 340 km is estimated to 7.7 Gt and 17 Gt, respectively. Finally, GRACE C_{20} coefficients were replaced by the monthly SLR estimates for C_{20} to complete the data correction step.

The time-mean of the GRACE Stokes coefficients from April 2002 to April 2011 is calculated and the monthly gravity field residuals ΔC_{lm} and ΔS_{lm} are determined by removing the time-mean average of the coefficients from monthly Stokes spherical harmonics. The gravity field residuals obtained by the GRACE are then converted into surface mass variations using Equation 1. This process is performed on a $1^\circ \times 1^\circ$ grid, where we estimate monthly mass variability over Greenland (see Chen et al. 2006; Joodaki and Nahavandchi 2012). Then we form an estimate of total mass change for each month by summing over grid elements with cosine latitude weighting. Figure 1 shows the time series for Greenland ice mass changes.

As it can be seen from Figure 1, the ice mass change shows seasonal changes superimposed on long-period variability. The objective of this study is to estimate the long term trend in Greenland ice mass variability; therefore, we examine a process to remove from time series of ice mass changes, the periodic variations. This is to reduce as much as possible the contamination of the long term trend by periodic variations. To detect the secular trend and periodic variations in the monthly mass anomalies, a general expression of the following form is used:

$$f(\phi, \lambda, t) = A + Bt + \sum_i C_i \cos(\omega_i t) + D_i \sin(\omega_i t) + \varepsilon \quad (2)$$

where f is the value of the ice mass anomaly at a selected location (φ, λ) and time t, that is approximated by a static value A, and its secular (B) and periodic (with amplitude C_i and D_i of typical angular frequencies ωi) variations. The variable ε characterizes noise

and un-modeled effects. In our estimation of the secular trend, we simultaneously fit periodic and secular terms to the time series of ice mass changes. A bias term, trend and four annual and semi-annual terms as well as seasonal variations are considered. The periodic variations terms of the ice mass change have then been removed so that the long term variations would be more evident. As it is obvious from Equation 2, we fit a linear trend, as done in most prior studies. The average value of -166±20 Gt/yr between 2002 and 2011 is obtained for the Greenland ice sheet. This corresponds to a 0.46±0.06 mm/yr sea level rise. The uncertainty in our estimate is calculated by taking the root sum squares of the errors in the least squares adjustment of the mathematical model which is used to detect the secular trend and periodic variations in time series of ice mass changes, the leakage effects and the gravity field error. In estimation of these errors, the PGR effects are not applied.

One objective of this study was to consider higher order regression models instead of a linear trend. This is to investigate whether a curved line will better fit to the GRACE time series of ice mass loss of Greenland than a linear regression. We therefore fit a quadratic trend to the time series of ice mass changes. The computation process is the same as for the linear trend. In Equation 2, we replace the linear trend term by a quadratic form. The least squares estimate for the acceleration in Greenland ice sheet mass loss is -32±6 Gt/yr^2 in 2002 – 2011. This corresponds to 0.09±0.02 mm/yr^2 of sea level rise from Greenland ice mass loss acceleration. For the period 2002-2011, we obtain a trend of -111±21 Gt/yr for Greenland ice sheet using a quadratic form. The uncertainties in the quadratic regression are calculated the same as in the linear trend model.

To investigate which of the two linear or quadratic models best fits the time series of ice mass changes, we used a goodness of fit statistic. Statistically speaking, it is more appropriate to compare two fit results rather than testing whether a particular fit result is good. There are statistics that can be used to compare the fit results to a dataset. R-square (R^2) and adjusted R-square (R^2_{Adj}) are two of the statistics. These are indicators of how successful the fit is in explaining the variation of the data. R^2 can be calculated from $R^2 = 1 - SSE/SST$ where SSE is summed square of residuals and SST is the sum, over all observations, of the squared difference of each observation from the mean. R-square can take on any value between 0 and 1, with a value closer to 1 indicating that a greater proportion of variance is accounted for by the model. For example, an R-square value of 0 indicates that the proposed model does not improve prediction over the mean and a value of 0.90 means that the fit explains 90% of the total variation in the data about the mean. There are situations that the number of model parameters is increased, and then R-square will increase although the fit is not improved in practice. To avoid these situations we use degree of freedom adjusted R-square. Adjusted R^2 (R^2_{Adj}) is used to compensate for the addition of parameters to the model. We use R^2_{Adj} to determine which of the two models best fits the data. Unlike R-square, the R^2_{Adj} increases only if the new term improves the model more than would be expected by chance. R^2_{Adj} is defined as $R^2_{Adj} = 1 - \left[\left(1 - R^2\right)(N-1)/(N-M-1)\right]$, where N is the number of observations and M is the number of unknowns in the model. R^2_{Adj} can take any value less than or equal to 1, with a value closer to 1 indicating a better fit.

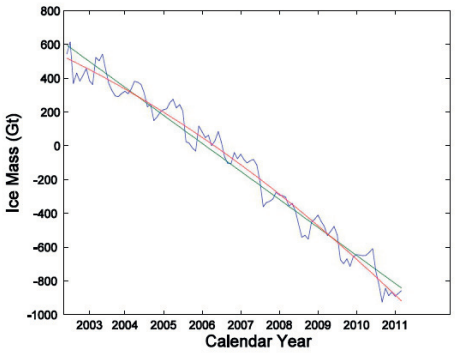

Figure 1. GRACE estimation of time series of Greenland ice mass changes in Gigatone for the period from April 2002 to April 2011(blue line). The best fitting linear trend is shown as green line, and the best fitting quadratic trend is depicted as red line.

For Greenland we find that R^2_{Adj} is larger when quadratic form is used. This means that the time series of ice mass changes are better modeled by an increasing rate of ice mass loss, i.e. including acceleration term, than with a constant ice mass loss. R^2_{Adj} is calculated to 0.975 for quadratic trend. This value is 3% larger than for the linear trend.

3. Discussions and conclusions

The GRACE twin satellites have been providing comprehensive survey of the Earth's gravity field over more than 10 years. It offers an excellent tool to study the entire Greenland ice sheet. The monthly GRACE gravity field solutions allow regional estimation of Greenland ice mass balance free from the issue of incomplete sampling and other limitations that are present in competing techniques. Furthermore, to obtain the mass variability, the process is less ambiguous using GRACE data as the relationship between gravity and mass variability follows directly from Newton's law.

Our monthly GRACE model of time variable gravity measurements for 105 months during the period April 2002 – April 2011 shows an acceleration of the Greenland ice sheet mass loss. Several other studies also pointed out that the Greenland ice sheet mass loses is accelerating. However, the ice mass estimates and acceleration are not all in agreement and differ significantly (see Table 1).

Joodaki and Nahavandchi (2012) obtained an ice mass decrease of -163 ±20 Gt/yr. Baur et al. (2009a) estimated an average value of -162±11 Gt/yr, Velicogna (2009) estimated a decrease of the Greenland ice mass of -230±33 Gt/yr, another estimate by the same

Table 1. Ice mass change and mass loss acceleration of the Greenland ice sheet using different GRACE data time span and methods. Where applicable, the ice mass change unit is converted from km^3/yr to Gt/yr, by multiplying an ice density of 917 kg/m^3.

Authors	Time span	Ice Mass change	Mass loss acceleration
Ramillien et al. (2006)	2002-2005	-109±9 Gt/yr	–
Chen et al. (2006)	2002-2005	-219 ± 21 Gt/yr	–
Lutchke et al. (2006)	2003-2005	-101 ± 16 Gt/yr	–
Velicogna and Wahr (2006)	2002-2006	-227±33 Gt/yr	–
Wouters et al. (2008)	2003-2008	-179±25 Gt/yr	–
Baur et al. (2009)	2002-2008	-162±11 Gt/yr	–
Velicogna (2009)	2002-2009	-230±33 Gt/yr	-30 ± 11 Gt/yr^2
Joodaki and Nahavandchi (2012)	2002-2010	– 163 ±20 Gt/yr	–
Current study	2002-2011	-166±20 Gt/yr	-32±6 Gt/yr^2

author amounts to -227±33 Gt/yr (Velicogna and Wahr, 2006a), Wouters et al. (2008) estimated a value of -179±25 Gt/yr, Luthcke et al. (2006 estimate was -101±16 Gt/yr, Chen et al. (2006) computed a decrease of ice mass of -219±21 Gt/yr for the Greenland, Ramillien et al. (2006) estimated a value of -109±9 Gt/yr mass loss for the Greenland ice sheet. The large differences in the estimates can partly be attributed to the different observation periods used, combined with the large variability in Greenland's mass balance, but they are mainly due to the different methods used and corrections applied. Besides differences introduced by the different groups processing the raw data, they can be caused by truncating GRACE monthly coefficients differently, using different filters and different smoothing radii, and from failing to restore power lost by smoothing. The results presented in this study might help to settle and resolve doubts in these different GRACE estimates of the Greenland ice mass loss. In the estimates mentioned above, a linear trend fit was used. The acceleration term used in this study shows that different GRACE observation periods give different mass loss estimates. The longer the period of study is the more mass-loss estimate might be resulted. During the 9-year period of this study, we obtained ice mass loss estimates of -121 Gt/yr in 2002 – 2003, -167 Gt/yr in 2004 – 2005, -210 Gt/yr in 2006 – 2007, -189 Gt/yr in 2008 – 2009, and -271 Gt/yr in 2010 – 2011. As mentioned above, there are other parameters which affect the mass loss estimates in addition to the observation period. The acceleration estimated here is tested statistically with a significance of around 98%.

Important features in our computations are: 1) GRACE level 2 release 4 datasets from CSR is used to compute the Greenland mass changes, 2) non-isotropic filter in 340 km corresponding radius is used to decorrelate high frequency GRACE measurements provided by high degree terms and order of the Stokes's coefficients, 3) leakage effects are estimated and applied, 4) un-weighted least squares method is used to estimate secular trends and periodic variations for the Greenland mass changes, and 5) A linear trend and a quadratic form are used to fit to the GRACE time series of ice mass changes. Note that our estimated values are free of any PGR corrections. PGR signals are more than one order of magnitude smaller than ice mass loss signals.

The secular trend error estimates for both linear and quadratic forms take into account the residuals between the recovered mass-variation time series and the least-squares fit to this series, the leakage effects and the gravity field solution error.

The acceleration term estimated in this study emphasizes the need for continuous observation of Greenland ice sheet and extending observation time in order to extract time series of ice mass changes by GRACE and future gravity missions.

Acknowledgements.

This study was supported by the Norwegian University of Science and Technology (NTNU).

References

Abdalati W., Krabill W., Frederick E., Manizade S., Martin C., Sonntag J., Swift R., Thomas R., Wright W. and Yungel J., 2001, Outlet glacier and margin elevation changes: near-coastal thinning of the Greenland ice sheet, J Geophys. Res., 106, 33729–33741, DOI:10.1029/2001JD900192.

Baur O., Kuhn M. and Featherstone W.E., 2009, GRACE-derived ice-mass variations over Greenland by accounting for leakage effects, J Geophys. Res., 114, B06407, DOI:10.1029/2008JB006239.

Bettadpur S., 2007, CSR Level-2 processing standards document for product release 04. Report GRACE 327-742, Center for Space Research, University of Texas at Austin, Austin.

Chambers D.P., 2007, Effects of ice melting on GRACE observations of ocean mass trends, Geophys. Res. Lett., 34, L05610, DOI:10.1029/2006GL029171.

Chambers D.P., Wahr J., Nerem R.S., 2004, Preliminary observations of global ocean mass variations with GRACE, Geophys. Res. Lett., 31, L13310, DOI:10.1029/2004GL020461.

Chen J.L., Wilson C.R., Famiglietti J.S., Rodell M., 2005, Spatial sensitivity of the Gravity Recovery and Climate Experiment

(GRACE) time-variable gravity observations, J Geophys. Res., 110, B08408, DOI:10.1029/2004JB003536

Chen J.L., Wilson C.R. and Tapley B.D., 2006, Satellite gravity measurements confirm accelerated melting of Greenland ice sheet, Science, 313, DOI:10.1029/science.1129007.

Cheng M. and Tapley B.D., 2004, Variations in the Earth's oblateness during the past 28 years, J Geophys. Res., v109, B9.

Howat I.M., Smith B.E., Joughin I. and Scambos T.A., 2008, Rates of Southeast Greenland ice volume loss from combined ICESat and ASTER observations, Geophys. Res. Lett., 35, L17505, DOI:10.1029/2008GL034496.

Joodaki G. and Nahavandchi H., 2012, Mass loss of the Greenland ice sheet from GRACE time-variable gravity measurements, Stud. Geophys. Geod., 56, 197-214, DOI:10.1007/s11200-010-0091-x.

Joughin I., Smith B.E., Howat I.M., Scambos T. and Moon T., 2010, Greenland flow variability from ice-sheet wide velocity mapping, Journal of Glaciology, 56, 16, 415–430, DOI:10.3189/002214310792447734.

Kusche J., Schmidt R., Petrovic S. and Rietbroek R., 2009, Decorrelated GRACE time-variable gravity solutions by GFZ, and their validation using a hydrological model, J Geod., 83, 10, 903-913.

Luthcke S.B., Zwally H.J., Abdalati W., Rowlands D.D., Ray R.D., Nerem R.S., Lemoine F.G., McCarthy J.J. and Chinn D.S., 2006, Recent Greenland ice mass loss by drainage system from satellite gravity observations, Science, 314, 1286–1289, DOI:10.1126/Science.1130776.

Pritchard H.D., Arthern R.J., Vaughan D.G. and Edwards L.A., 2009, Extensive dynamic thinning on the margins of the Greenland and Antarctic ice sheets, Nature, 461, 971–975, doi:10.1038/nature08471.

Ramillien G., Lombard A., Cazenave A., Ivins E.R., Llubes M., Remy F. and Biancale R., 2006, Interannual variations of the mass balance of the Antarctica and Greenland ice sheets from GRACE, Glob. Planet. Chan., 53, 198–208, DOI:10.1016/j.gloplacha.

Rignot E. and Kanagaratnam P., 2006, Changes in the velocity structure of the Greenland ice sheet, Science, 311, 986–990, DOI:10.1126/science.1121381.

Rignot E., Braaten D., Gogineni S.P., Krabill W.B. and Mc-Connell J.R., 2004, Rapid ice discharge from Southeast Greenland glaciers, Geophys. Res. Lett., , 31, L10401, DOI:10.1029/2004GL019474.

Slobbe D., Lindenbergh R. and Ditmar P., 2008, Estimation of volume change rates of Greenland's ice sheet from ICESat data using overlapping footprints, Rem. Sens. Environ., 112, 4204–4213, DOI:10.1016/j.rse.2008.07.004.

Sørensen L.S., Stenseng L., Simonsen S.B., Forsberg R., Poulsen S.K. and Helm V., 2010, Greenland Ice Sheet changes from space using laser, radar and gravity, In Proceedings of the ESA Living Planet Symposium, 28 June – 2 July, SP-686. ESA Publication Division, Nordwijk, The Netherlands.

Sørensen L.S., Simonsen S.B., Nielsen K., Lucas-Picher P., Spada G., Adalgeirsdottir G., Forsberg R. and Hvidberg C.S., 2011, Mass balance of the Greenland ice sheet (2003–2008) from ICESat data – the impact of interpolation, sampling and firn density, The Cryosphere, 5, 173-186, DOI:10.5194/tc-5-173-2011.

Tapley B.D., Bettadpur S., Watkins M.M. and Reigber C., 2004, The Gravity Recovery and Climate Experiment: Mission overview and early results, Geophys. Res. Lett., , 31, L09607, DOI:10.1029/2004GL019920.

Tapley B.D., Bettadpur S. and Ries J.C., 2004, Thompson P.F., Watkins M.M., GRACE measurements of mass variability in the Earth system, Science, 305, 503-505.

Velicogna I., 2009, Increasing rates of ice mass loss from the Greenland and Antarctic ice sheets revealed by GRACE, Geophys. Res. Lett., , 36, L 19503, DOI:10.1029/2009GL040222.

Velicogna I. and Wahr J., 2006, Acceleration of Greenland ice mass loss in spring 2004, Nature, 443, 329-331.

Velicogna I. and Wahr J., 2006, Measurements of Time-Variable Gravity Show Mass Loss in Antarctica, Science, 311, 1754-1756, DOI:10.1126/science. 1123785.

Wahr J., Molenaar M. and Bryan F., 1998, Time variability of the Earth's gravity field: Hyrological and oceanic effects and their possible detection using GRACE, J Geophys. Res., 1998, 103, B12, 30205-30229.

Wouters B., Chambers D.P. and Schrama E.J.O., 2008, GRACE observes small-scale mass loss in Greenland, Geophys. Res. Lett., 35, L20501, DOI:10.1029/2008GL034816.

Paper D

Hossein Nahavandchi and Gholamreza Joodaki, (2012), **Greenland ice-melt spread into Northwest revealed by GRACE**, Kart og Plan, Volume 72, Annual 105, 234-240.

GRACE data viser at issmeltingen på Grønland sprer seg til nordvestkysten

Hossein Nahavandchi og Gholamreza Joodaki

Vitenskapelig bedømt (refereed) artikkel

Hossein Nahavandchi and Gholamreza Joodaki: Greenland ice-melt spread into Northwest Coast revealed by GRACE

KART OG PLAN, Vol. 72, pp. 234–240, P.O.B. 5003, NO-1432 Ås, ISSN 0047-3278

We examine the extent and magnitude of Greenland ice sheet surface melting between 2002 and 2010. We show that the well documented Greenland ice mass loss in the southern region spread to northwest Greenland in the period from 2007 to 2010. We use Gravity Recovery and Climate Experiment (GRACE) satellite data to estimate ice mass variability over time in Greenland. Monthly GRACE level 2 Release-04 (RL04) data from Center for Space Research (CSR) are used for the period April 2002 to December 2010. In contrast to other recent studies, our method employs a non-isotropic filter whose degree of smoothing corresponds to a Gaussian filter with a radius of 340 km. Stripping effects in the GRACE data, C_{20} effect, and leakage effects are taken into consideration in the computations.

Key words: Greenland, Ice mass loss, Ice-melt spread, GRACE gravity satellites

Hossein Nahavandchi, Professor, Norwegian University of Science and Technology, Division of Geomatics, NO-7491 Trondheim. E-mail: hossein.nahavandchi@ntnu.no

Gholamreza Joodaki, PhD student, Norwegian University of Science and Technology, Division of Geomatics, NO-7491 Trondheim. E-mail: gholamreza.joodaki@ntnu.no

1. Introduction

The GRACE satellite gravity mission has been providing valuable information regarding Earth's gravity field. GRACE not only maps the Earth's static gravity field but it also measures temporal variation in the Earth's gravity field to a scale of several hundred kilometers and with a period of around one month. GRACE detects changes in the gravity field caused by redistribution of mass within the Earth and on or above the Earth's surface. Due to its global coverage, GRACE provides an excellent tool for mapping the gravity field over large areas such as Greenland. In recent years, several research groups have used GRACE data to estimate the rate of ice mass change over Greenland.

Several studies indicate that the Greenland ice sheet has been losing mass at a significant rate over the last decade. Ice mass loss estimates from GRACE are reported by Luthcke et al. (2006) using raw GRACE KBRR (K-Band Range and Range rate) data; Chen et al. (2006) using the CSR monthly solutions RL01 from 2002-2005; Ramillien et al. (2006) using the same period as Chen et al. (2006) but using the GRGS/CNES GRACE solutions; Velicogna and Wahr (2006a) using the CSR monthly solutions Release 01 (RL01) from 2002 to 2006; Wouters et al. (2008) using the CSR RL04 monthly solutions from 2003 to 2008; Baur et al. (2009) using monthly GRACE solutions RL04 provided by GRACE processing centers of CSR, GFZ (German Research Center for Geosciences) and JPL (Jet Propulsion Laboratories) for 2002 to 2008, and Velicogna (2009) using the CSR RL04 monthly solutions from 2002 to 2009. Note that all of the results reported above are based on isotropic filters.

Other satellite based sensors can also be used to study Greenland ice mass changes. Abdalati et al. (2001), Rignot et al. (2004), Rignot and Kanagaratnam (2006) and Joughin et al. (2010) used Synthetic Aperture Radar (SAR) imaging to reveal accelerated mass change in a large number of outlet glaciers in Greenland. Slobbe et al. (2008), Howat et al. (2008), Pritchard et al. (2009) and Sørensen et al. (2011) used laser altimetry to

study the mass balance of Greenland. Sørensen et al. (2010) used satellite laser, radar and gravity measurements to study Greenland ice mass change.

In this study we estimate Greenland ice mass change and ice-melt spread based on monthly GRACE solutions provided by CSR from April 2002 to December 2010. The latest release RL04 is used along with improved geophysical signal models and data processing techniques. This release has the smallest error compared to other releases (Bettadpur 2007). Due to the presence of noise in the provided spherical harmonic coefficients of the GRACE data, a filtering technique based on non-isotropic filter is applied (See Joodaki and Nahavandchi 2012).

2. Surface mass change estimation from GRACE

The GRACE twin satellites were launched in March 2002 and are jointly implemented by the US National Aeronautics and Space Administration (NASA) and the German Aerospace Center (DLR) (Tapley et al. 2004a). GRACE measures Earth gravity changes with unprecedented accuracy by tracking changes in the distance between the two satellites and combining these measurements with data from on-board accelerometers and Global Positioning System (GPS) receivers. GRACE data are used to determine monthly spherical harmonic coefficients of the Earth's gravity field. Each field consists of gravity field normalized (Stokes) coefficients, C_{lm} and S_{lm}, up to degree and order (l, m) 60 in CSR products (Tapley et al. 2004b). Using the static 30-day fully normalized spherical harmonic coefficients, one can estimate monthly local changes in surface mass (Wahr et al. 1998). The mass changes can be assumed to be located in a very thin layer of water concentrated at the surface and with variable thickness. This assumption is not far from reality. Changes in water storage in hydrologic reservoirs, by moving ocean, atmospheric and cryospheric masses, and by exchange among these reservoirs has been shown to cause monthly changes in gravity signals (Chambers 2007). The vertical extent of the water is much smaller than the horizontal scale of the changes and is called equivalent water thickness. Mass variations are modeled as surface density variations $\Delta\sigma$ (the unit of $\Delta\sigma$ is mass/surface area) in a spherical layer.

Having obtained monthly spherical harmonic coefficients of the Earth's gravity field, one can estimate monthly local changes in surface mass density (Wahr et al. 1998):

$$\Delta\sigma(\varphi,\lambda) = \frac{a\rho_{\text{ave}}}{3}\sum_{l=0}^{\infty}\sum_{m=0}^{l}\frac{2l+1}{1+k_l}\bar{P}_{lm}(\sin\varphi)\left[\Delta C_{lm}\cos m\lambda + \Delta S_{lm}\sin m\lambda\right] \quad (1)$$

where φ and λ are the spherical latitude and longitude of the point of interest, a is the major semi axis of a reference ellipsoid and $\bar{P}_{lm}$ is the normalized associated Legendre function of the first kind. ρ_{ave} is the average mass-density of the solid Earth (assumed throughout this paper to be 5517 kg/m^3), ΔC_{lm} and ΔS_{lm} are time-variable components of the GRACE observed Stokes coefficients for some month of degree and order (l, m) or as changes relative to the mean of the monthly solutions, and k_l is the Love number of degree l which is given in Wahr et al. (1998). It should be stated here that $\Delta\sigma/\rho_{\text{w}}$ transforms surface mass-densities to equivalent water thickness values, where ρ_{w} is the mass-density of freshwater (=1000 kg/m^3 in this study).

Crucial for a reliable estimate of secular mass changes from GRACE monthly solutions is the ability to correct for systematic errors in the surface mass density computation as discussed below.

Due to the nature of the measurement technique in GRACE and mission geometry, the monthly spherical harmonic coefficients are contaminated by short-wavelength noise. The noise is significant when one is interested in signals extending geographically a few hundred km or when using higher degree co-

efficients (short-wavelengths). Non-isotropic filters are used in this study since the GRACE noise structure mainly manifests itself as near north-south "stripes" and has a non-isotropic nature. We use the Kusche et al. (2009) decorrelation and smoothing method to correct monthly GRACE RL04 gravity models, as did Joodaki and Nahavandchi (2012).

Due to the GRACE orbit geometry and the separation length between its satellites, the lowest-degree zonal harmonics, C_{20} (or in another format as J_2) cannot be satisfactorily determined from the GRACE data (Tapley et al. 2004b). The C_{20} estimates from GRACE also are well-known to be affected by significant long-period tidal aliases. Replacement of the GRACE C_{20} coefficient by its estimate from Satellite Laser Ranging (SLR) improves the estimation of mass variations from GRACE (Chen et al. 2005). The SLR time series are also more precise, with about a third of the noise of the GRACE time series. Therefore, the monthly SLR estimates for C_{20} coefficient are used to replace the estimates from GRACE in this study. The SLR time series for C_{20} coefficient are taken from J. Ries (personal communication, 2010).

For a reliable estimate of secular mass changes over Greenland one needs to correct for leakage effects. On the one hand, mass change located outside Greenland propagates into a signal spreading over Greenland and has an impact on the Greenland mass-change estimates. On the other hand, mass change over Greenland propagates into a signal spreading over areas outside Greenland. These are called leakage in and leakage out effects, respectively. The leakage out signal has to be restored back into the region of interest. The leakage in signal has to be reduced from the region of interest. We use results from Joodaki and Nahavandchi (2012) to estimate leakage effects. In this approach, we use only GRACE results to delineate the leakage effects rather than additional information from sources such as remote sensing or global hydrological models. The procedure is to calculate the spherical harmonic coefficients associated with leakage effects, on the areas concerned, from the surface mass density derived from GRACE data alone. The sources generating leakage in signals could be from all over the world; however, the impact declines with increasing distance. This is because leaking signals follow Newton's law of gravitation. The strongest signals on Greenland are caused by Alaska, Fennoscandia and the Canadian Shield. These three sources are also used in investigations by Baur et al. (2009).

In the estimation for ice mass change rates in this study, contaminating factors like the effects of variation in atmospheric mass and the solid Earth contribution from high-latitude Post Glacial Rebound (PGR) are not applied. Atmospheric effects are negligible for Greenland on the long term trend (Velicogna and Wahr 2006a, b). We also chose not to apply the correction for the PGR signal, considering the total uncertainty in the PGR estimations (Velicogna and Wahr 2006a, b). It is left to others to choose their preferred PGR model. Nevertheless, it should be stated here that the PGR signal for the entire Greenland is computed to about –7.4 Gigaton per year (Gt/yr) with standard deviation of ±19 Gt/yr (Velicogna and Wahr 2006b). When compared to the ice-mass estimates, the PGR signal is more than one order of magnitude smaller.

3. Numerical investigations

We estimate the secular trend in Greenland ice mass rate using more than 8 years of GRACE level 2 RL04 data. Monthly GRACE solutions by CSR processing centers are used for the period April 2002 to December 2010. The maximum degree of expansion for the CSR in this study is 60. This spatial resolution may not be enough fine to isolate the source of the ice mass variability, but it is the maximum resolution available by the CSR model and enough to show the Greenland ice sheet mass loss. As mentioned in section 2, monthly solutions of GRACE when computing ice mass rates include a non-physical striping error pattern which can be considered noise and must be decorrelated/filtered. It has been filtered in the corresponding Gaussian radius of 340 km (see Joodaki and Nahavandchi 2012). The monthly SLR estimates for the C_{20} coefficient are used to replace the estimates from GRACE to complete

the data edition step. Leakage effects are corrected for in the estimation of total mass change for each month. The average leakage in and leakage out effects for CSR monthly gravity solutions and smoothing degree of corresponding Gaussian radius of 340 km are estimated at 7.7 Gt and 17 Gt, respectively.

We convert the gravity field residuals observed by GRACE into surface mass using Equation (1).To do this, the time-mean of the GRACE Stokes coefficients from April 2002 to December 2010 is calculated and the monthly coefficients anomalies ΔC_{lm} and ΔS_{lm} are determined by removing the mean from monthly Stokes spherical coefficients. On a 1° x 1° grid, we estimate monthly mass variability over Greenland using Eq. (1) (see Chen et al. 2006; Joodaki and Nahavandchi 2012). To detect the secular trend and periodic variations in the monthly mass anomalies, a general expression of the following form can be used:

$$f(\varphi,\lambda,\ t) = A + Bt + \sum_i C_i \cos(\omega_i t) + D_i \sin(\omega_i t) + \varepsilon \qquad (2)$$

The value of the considered functional f (the ice mass anomaly, here) at a selected location (φ, λ) and time t is approximated by a static value A, and its secular (B) and periodic (with amplitude C_i and D_i of typical angular frequencies ω_i) variations. The variable ε characterizes noise and unmodeled effects. To detect the secular trend, we have simultaneously fit periodic and secular terms to the results (a bias, trend and four annual and semiannual terms as well as seasonal variations). These terms are applied to a time series of grids from which Figure 1 is derived. The seasonal terms of the ice mass loss variations have been removed to make the long term variations more evident. The average value of –162±20 Gt/yr between 2002 and 2010 is estimated for the Greenland ice-mass change using CSR monthly solutions. This estimate is –151±20 Gt/yr between 2002 and 2007. These results are reached by application of a non-isotropic filter whose degree of smoothing corresponds to a Gaussian filter with a radius of 340 km. These annual mass loss estimates of the Greenland ice sheet agree well with several other studies of the Greenland ice sheet mass balance using different remote-sensing techniques. However, it should be noted that each study is characterized by its observation period, individual analysis method and monthly gravity solutions. Therefore, it would be very difficult to compare different GRACE studies objectively. Previously published estimates of the Greenland ice mass loss range from -101 Gt/yr to –240 Gt/yr (see e.g. Velicogna 2009 and Sørensen et al. 2011). The secular trend error estimates for both periods above take into account errors of the least squares adjustments of the mathematical model used to detect the secular trend and periodic variations in the monthly mass anomalies, the leakage effects and the gravity field error. Table 1 shows the bias, trend and annual terms for the period 2002-2010. The error estimates in Table 1 are only derived from residuals between the recovered mass-variation time series and the least-squares fit to this series; they do not account for the uncertainties of leakage effects and GRACE gravity field errors.

Table 1. Summary statistics for the model estimation of the Greenland secular trend.

	Bias (Gt)	Trend(Gt/yr)	Annual Cos-term (Gt)	Annual Sin-term (Gt)
2002-2010	601±13	–162±3	35±7	-57±9

We decided to calculate the resulting secular trends in Greenland ice mass in two different periods to see whether the extent and magnitude of ice mass melting is constant, accelerating or decelerating. Figure 1 shows the secular trends in the Greenland ice mass vari-

ability represented as equivalent water thickness change averaged between April 2002 and December 2007, and between April 2002 and December 2010. These two figures illustrate areas in which Greenland lost mass at different rates during the study period. It is obvious that the ice mass loss has been significant along the northwest coast of Greenland. A large area experienced losses of 6 to 10 centimeters per year (blue). Losses were highest over southeastern Greenland. The interior parts of Greenland shows less negative trend and the northern and northeastern parts show the least negative trends.

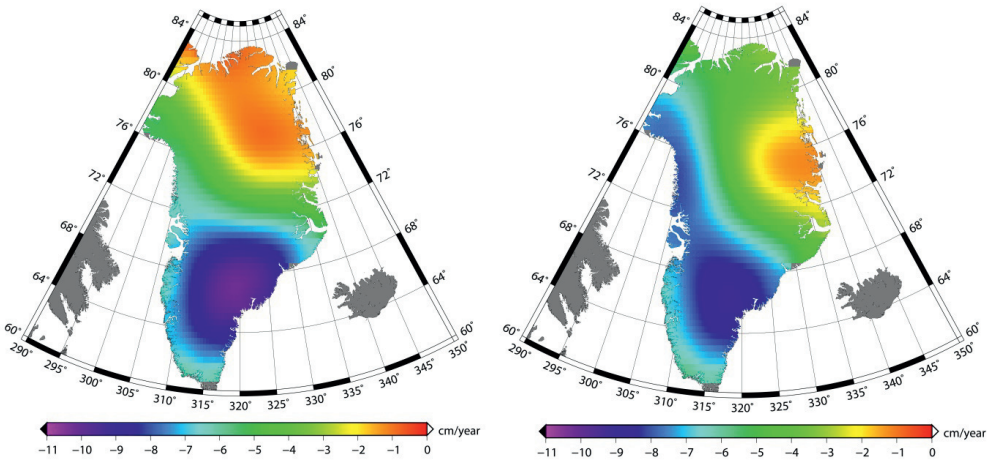

Figure 1. GRACE model estimation of the Greenland Ice mass loss rate in units of equivalent water height change per year, cm / year. The left figure is the averaged rate from April 2002 to December 2007 and the right figure is the averaged rate from April 2002 to December 2010.

4. Discussions and conclusions

The GRACE twin satellites have been providing a continuous record of the Earth's gravity field for more than 9 years, offering an excellent tool to study mass changes over large areas. The Earth's gravity field is a product of its mass distribution. The mass distribution is constantly changing. GRACE tracks changes in Earth's gravity field due to changes in Earth's mass distribution. This includes changes in ice of the Greenland ice sheet. Mass loss over Greenland is reported in several studies consistent with increased global warming in recent years, and indicates that Greenland is a major contributor to recent global sea level rise.

The monthly GRACE gravity field solutions allow regional estimation of Greenland ice mass balance. In contrast to some other techniques, GRACE measures Greenland mass variability over the entire ice sheet. Furthermore, the process to obtain this mass variability is less ambiguous for GRACE because the relationship between gravity and mass variability follows directly from Newton's law.

Our model shows that rapid mass loss of the Greenland icecap spread from southern portions to northwest Greenland coast in 2007-2010. From 2002 to 2010, the ice loss rate doubled (see also Velicogna 2009). The summers of 2003, 2005, 2007 and 2008 are observed to be among the warmest years since 1961. Our model reveals large mass loss in these years, indicating strong correlation between summer temperature and the ice loss observed by GRACE.

Important elements in our computations are that: 1) GRACE level 2 release 4 datasets from CSR are used to compute the Greenland mass changes, 2) non- isotropic filter in 340 km corresponding radius is used to decorrelate high frequency GRACE measurements provided by high degree terms and order of the Stokes's coefficients, 3) leakage effects are estimated and applied and 4) unweighted least squares method is used to estimate secular trends and periodic variations for the Greenland mass changes. Note that our estimated values are free of any PGR corrections. PGR signals are more than one order of magnitude smaller than ice mass loss signals.

Accelerations and decelerations of ice mass loss are apparent from the GRACE data. As mentioned, the results of this study shows a northward movement of ice mass loss along the west side of the Greenland ice sheet while at the same time we observe rapid ice melting in southeast Greenland in 2005 and 2007, followed by a moderate deceleration in 2006 and 2008 (see also Joodaki and Nahavandchi 2012). However, the deceleration is weak. Southeast Greenland is still losing mass at a high rate and continuing to contribute to global sea level rise.

The low resolution of GRACE, 250 kilometers, is not enough fine to isolate the source of ice mass variability. However, the results of this study show that the Greenland ice sheet is losing mass nearer to the ice sheet margins than in the interior portions. The ice mass loss has been very dramatic along the northwest coast of Greenland. The long term assessment of the Greenland ice mass sheet variability and its contribution to sea level rise is important for future forecasting of global sea level rise.

Acknowledgements. The authors are greatly indebted to the two reviewers of this paper for patiently reading the paper and for valuable comments. This study was supported by the Norwegian University of Science and Technology.

References

Abdalati W, Krabill W, Frederick E, Manizade S, Martin C, Sonntag J, Swift R, Thomas R, Wright W, Yungel J (2001) Outlet glacier and margin elevation changes: near-coastal thinning of the Greenland ice sheet. Journal of Geophysical Research 106: 33729–33741. doi:10.1029/2001JD900192.

Baur O, Kuhn M, Featherstone WE (2009) GRACE-derived ice-mass variations over Greenland by accounting for leakage effects. Journal of Geophysical Research 114:B06407. doi: 10.1029/2008JB006239.

Bettadpur S (2007) CSR Level-2 processing standards document for product release 04. Report GRACE 327-742, Center for Space Research, University of Texas at Austin, Austin.

Chambers DP (2007) Effects of ice melting on GRACE observations of ocean mass trends. Geophysical Research Letter 34:L05610. doi:10.1029/2006GL029171.

Chen JL, Wilson CR, Famiglietti JS, Rodell M (2005) Spatial sensitivity of the Gravity Recovery and Climate Experiment (GRACE) time-variable gravity observations. Journal of Geophysical Research 110:B08408. doi:10.1029/2004JB003536.

Chen JL, Wilson CR, Tapley BD (2006) Satellite gravity measurements confirm accelerated melting of Greenland ice sheet. Science 313. doi:10.1029/science.1129007.

Howat IM, Smith BE, Joughin I, Scambos T A (2008) Rates of Southeast Greenland ice volume loss from combined ICESat and ASTER observations. Geophysical Research Letter 35: L17505. doi:10.1029/2008GL034496.

Joodaki G, Nahavandchi H (2012) Mass loss of the Greenland ice sheet from GRACE time-variable gravity measurements. Studia Geophysica et Geodaetica 56: 197-214. doi:10.1007/s11200-010-0091-x.

Joughin I, Smith B E, Howat IM, Scambos T, Moon T (2010) Greenland flow variability from ice-sheetwide velocity mapping. Journal of Glaciology 56(16):415–430. doi:10.3189/002214310792447734.

Kusche J, Schmidt R, Petrovic S, Rietbroek R. (2009) Decorrelated GRACE time-variable gravity solutions by GFZ, and their validation using a hydrological model. Journal of Geodesy, 83, 10, 903-913.

Luthcke SB, Zwally HJ, Abdalati W, Rowlands DD, Ray RD, Nerem RS, Lemoine FG, McCarthy JJ,

Chinn DS (2006) Recent Greenland ice mass loss by drainage system from satellite gravity observations. Science 314:1286–1289. doi:10.1126/Science.1130776.

Pritchard HD, Arthern RJ, Vaughan DG, Edwards LA (2009) Extensive dynamic thinning on the margins of the Greenland and Antarctic ice sheets. Nature 461:971–975. doi:10.1038/nature 08471.

Ramillien G, Lombard A, Cazenave A, Ivins ER, Llubes M, Remy F, Biancale R (2006) Interannual variations of the mass balance of the Antarctica and Greenland ice sheets from GRACE. Global and Planetary Change 53:198–208. doi:10.1016/j.gloplacha.

Rignot E, Kanagaratnam P (2006) Changes in the velocity structure of the Greenland ice sheet. Science 311:986–990. doi:10.1126/science.1121 381.

Rignot E, Braaten D, Gogineni SP, Krabill WB, McConnell JR (2004) Rapid ice discharge from Southeast Greenland glaciers. Geophysical Research Letter 31: L10401. doi:10.1029/2004GL019474.

Slobbe D, Lindenbergh R, Ditmar P (2008) Estimation of volume change rates of Greenland's ice sheet from ICESat data using overlapping footprints. Remote Sensing Environment 112: 4204–4213. doi:10.1016/j.rse.2008.07.004.

Sørensen LS, Stenseng L, Simonsen SB, Forsberg R, Poulsen SK, Helm V (2010) Greenland Ice Sheet changes from space using laser, radar and gravity. In Proceedings of the ESA Living Planet Symposium, 28 June - 2 July, SP-686. ESA Publication Division, Nordwijk, The Netherlands.

Sørensen LS, Simonsen SB, Nielsen K, Lucas-Picher P, Spada G, Adalgeirsdottir G, Forsberg R, Hvidberg CS (2011) Mass balance of the Greenland ice sheet (2003–2008) from ICESat data – the impact of interpolation, sampling and firn density. The Cryosphere 5:173-186. doi:10.5194/tc-5-173-2011.

Tapley BD, Bettadpur S, Watkins MM, Reigber C (2004a) The Gravity Recovery and Climate Experiment: Mission overview and early results. Geophysical Research Letter 31:L09607. doi: 10.1029/2004GL019920.

Tapley BD, Bettadpur S, Ries JC, Thompson PF, Watkins MM (2004b) GRACE measurements of mass variability in the Earth system. Science 305:503-505.

Velicogna I (2009) Increasing rates of ice mass loss from the Greenland and Antarctic ice sheets revealed by GRACE. Geophysical Research Letter 36: L 19503. doi:10.1029/2009GL040222.

Velicogna I, Wahr J (2006a) Acceleration of Greenland ice mass loss in spring 2004. Nature 443:329-331.

Velicogna I, Wahr J (2006b) Measurements of Time-Variable Gravity Show Mass Loss in Antarctica. Science 311:1754-1756. doi:10.1126/science. 1123785.

Wahr J, Molenaar M, Bryan F (1998) Time variability of the Earth's gravity field: Hyrological and oceanic effects and their possible detection using GRACE. Journal of Geophysical Research 103(B12):30205-30229.

Wouters B, Chambers DP, Schrama EJO (2008) GRACE observes small-scale mass loss in Greenland. Geophysical Research Letter 35:L20501. doi:10.1029/2008GL034816.

Paper E

Gholamreza Joodaki, Hossein Nahavandchi, and Kourosh Ghazavi (2013), **Steric sea level changes from ENVISAT and GRACE in the Nordic Seas**, 20 years of Progress in Radar Altimetry symposium, ESA publication SP-710.

STERIC SEA LEVEL CHANGES FROM ENVISAT AND GRACE IN THE NORDIC SEAS

Gholamreza Joodaki[(1)], Hossein Nahavandchi[(1)], and Kourosh Ghazavi[(1)]

[(1)] Division of Geomatics, Department of Civil and Transport Engineering, Norwegian University of Science and Technology (NTNU), N-7491 Trondheim, Norway. E-Mail: gholamreza.joodaki@ntnu.no, Hossein.nahavandchi@ntnu.no, Kourosh.ghazavi@alumni.ntnu.no

Abstract:

Steric sea level changes are estimated over the Nordic Seas using ENVISAT (Environmental Satellite) altimetry and GRACE (Gravity Recovery and Climate Experiment) gravity data. We have used altimetry data from the ENVISAT during October 2002 to October 2010, cycles 10 to 93 , and the GRACE level 2 R L04 data released by GFZ (German Research Center for Geosciences) processing center during October 2002 to October 2010. It should be noted that some months are missing for the GRACE data set. Correction terms are applied to properly combine the altimetry and GRACE data, including the inverted barometer term, dynamic ocean and atmospheric terms and GRACE coefficients with degrees 0, 1, and 2 (with order 0). Finally, the steric sea level changes are derived over the Nordic Seas for October 2002 to October 2010.

Keywords: ENVISAT altimetry data; GRACE gravity data; steric sea level; Nordic Seas.

1. Introduction:

Steric sea level and water mass change are two major components of sea level variability. The steric sea level is due to variations in the sea water temperature and salinity at all depths and the other component, water mass change, is due to the ocean mass redistribution or water mass flux. Because of variations in density, the sea water temperature and salinity variations cause the dilatation/ contraction in the ocean column which has been observed as basin-wide fluctuations in sea level as large as ±10 cm in some areas of the world.

Using oceanic in situ temperature and salinity data, the steric sea level variation can be estimated alone (see for example [1], [2], [3], [4]), but generally, there is no sufficient spatial and temporal coverage for the in situ data archives which have been provided in high levels of smoothing, and they cannot adequately resolve eddies, frontal regions and boundary currents (e.g. [5], [6]). In addition, most of the existing data archives have been provided by averaging data from several periods meanwhile they represent the oceanic condition within a set period ([5], [7], [8]). Due to such procedures, there might be an unrealistic representation of boundary currents and other small scale features in the in situ data archives. [9]

Satellite altimetry measures the combined effect of the steric and mass variations precisely. Although the altimeters have the high accuracy, they cannot distinguish between steric and non-steric effects. Therefore the steric height estimation is downgraded in accuracy by the non-steric effects. Satellite gravity observations, on the other hand, can be used to estimate the non-steric effects. The water mass variations cause the temporal variations of the gravity field [10]. In the ocean, sea level variations and ocean density changes cause the local water mass changes ([11], [12]). The steric component of the sea level variation is just due to the dilatation/contraction in the sea water, i.e. no change in the density, a fact that we will use in this study for the separation of the steric component from the mass change and the other phenomena such as Rossby waves, Kelvin wave and gravity waves.

The twin satellites of the GRACE were launched in March 2002 as a joint partnership between the US National Aeronautics and Space Administration (NASA) and German Aerospace Center (DLR) [13]. GRACE measures Earth gravity changes in high level of accuracy by high-precision tracking of the satellites and changing distance between them which is being combined with the data of the on-board accelerometers and the Global Positioning System (GPS) receivers. Several research groups have used satellite altimetry and GRACE data to estimate the steric sea level change. Chambers used actual observations from Jason-1 and Release-02 GRACE data to determine monthly steric sea level variations [14]. It was found that using GRACE improves the ability to recover the dominant mode of steric sea level variability over using altimetry data alone (ibid.). Lombard et al. estimated the mean steric sea level variations over the $60°S - 60°N$ oceanic domain during August 2002 to April 2006, by combining sea level data from Jason-1 altimetry with two different sets of GRACE geoid solutions (GRGS-EIGEN-GL04 and GFZ EIGEN-GRACE04S). They found satisfactory agreement between their estimate of the annual steric sea level and one deduced from in situ ocean temperature data [15]. Kuo et al. conducted a comparison of the GRACE observations of global and Southern Ocean mass variations during April/May 2002 to June 2006 with the steric-corrected JASON-1 and ENVISAT altimetry, using the steric sea levels from WOA01 climatology and Ishii06 models [4], and with the ocean bottom pressure estimates of the ECCO ocean data assimilation model. Their study indicated that GRACE and ENVISAT observations are viable to supply an improved constraint of oceanic mass variations in the Southern Ocean [16].

Proc. '20 Years of Progress in Radar Altimetry'
24-29 September 2012, Venice, Italy (ESA SP-710, February 2013)

In this study, we investigate the steric height variability over Nordic Seas based on ENVISAT altimetry and monthly GRACE solution during October 2002 to October 2010. The Nordic Seas is the common name for the Greenland, Iceland and Norwegian Seas ([17], [18], [19]). The region is bounded by the Arctic Ocean to the north, the deep North Atlantic Ocean to the south, and the shallow North Sea to the southeast (Figure 1). The ocean mass changes, the sea level anomaly changes and the variability of steric sea level anomaly over the Nordic Seas during October 2002 to October 2010 are derived. To the best our knowledge this is the first analysis of this kind for the Nordic Seas, using ENVISAT and GRACE satellite data.

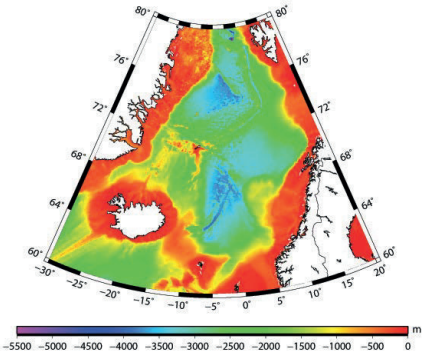

Figure 1. Bottom topography for the Nordic Seas

2. Steric sea level change from satellite altimetry and GRACE

Chambers demonstrated a method for calculating the ocean's steric height change from combination of satellite altimetry and GRACE data [14]. It included two steps: i) ocean mass variations computed from GRACE gravity coefficients and ii) sea level anomaly estimation from satellite altimetry data. In this way, the altimeter variations have to be smoothed to be comparable to the GRACE maps. In addition, several important corrections must be made in order to reconcile the GRACE data with the altimetry measurements.

2.1. Ocean mass variations from GRACE

The mass redistribution in an area causes the density distribution and the geoid to change. It mainly concentrates in the thin layer of thickness of the order 10 ~ 15 km at the Earth's surface in annual cycle, which indicates the total variations including the atmosphere, oceans, ice caps and ground water storage [10]. Assuming the thickness of the layer is thin enough, according to the relationship between the changes in spherical harmonic geoid coefficients and the density redistribution [10], and taking into account the anelastic deformation of the solid Earth, the density change of ocean in terms of change of spherical harmonic coefficients can be determined by [10]:

$$\Delta\sigma(\varphi,\lambda)=\frac{a\rho_{ave}}{3}\sum_{l=0}^{\infty}\sum_{m=0}^{l}\frac{2l+1}{1+k_l}\overline{P}_{lm}(\sin\varphi)[\Delta C_{lm}\cos m\lambda+\Delta S_{lm}\sin m\lambda] \quad (1)$$

where a is the mean Earth's radius, ρ_{ave} is the mean Earth's density (=5517kg/m^3), φ and λ are the latitude and longitude of the point of interest and (l, m) are the degree and order of the spherical harmonic coefficients. $\overline{P}_{lm}$ is the normalized associated Legendre function of the first kind. ΔC_{lm} and ΔS_{lm} are time variations of the GRACE observed Stokes coefficients which are computed as changes relative to the mean of the monthly solutions. The load Love number coefficients k_l are also given in [10]. Because of the nature of the measurement technique in GRACE and mission geometry, the GRACE observed Stokes coefficients are polluted with short-wavelength noises [20]. The non-white correlated and resolution dependent noise in the coefficients is manifested as unrealistic North-South striping. Based on the Tikhonov-type regularization, Kusche devised a non-isotropic filter algorithm which reduces the impact of the noise at increasing degree [21]. Kusche et al. have analyzed GRACE RL04 monthly gravity solutions in the three non-isotropic filters corresponds to Gaussian filter lengths of 240, 340 and 530 km [20]. In this study, the corresponding Gaussian filter length has been inferred based on comparing the 'isotropic part' of the non-isotropic decorrelation filter with the Gaussian filter in terms of matching the particular spectral degree where the filter weight drops to 0.5 (see also [22]).

Due to the smoothing on global spherical harmonics, the average over the ocean within the smoothing radius will be affected by any large change over land. To mitigate this problem, all the grids on land will be masked and their effects are not included in the computations on the Nordic seas (see [22]). The ocean mass change derived from GRACE data reflects the sum of all geophysical process associated with mass transport in the study area, including postglacial rebound signal. The model of Paulson et al. is used to correct the obtained estimates for the postglacial rebound signal [23]. Further description of the mass change estimation using GRACE gravity models can be found in [22].

2.2. Sea level anomaly from satellite altimetry

A Sea Level Anomaly (SLA) is a Sea Surface Height (SSH) minus a Mean Sea Surface Height (MSSH) along the ground track of the satellite. Having the height of the satellite above some reference ellipsoid, the SSH

can be calculated by subtracting the instantaneous range measured by the altimeter from the satellite orbit height. There are separations about 1 or 2 km for the ground tracks of altimetric satellites with repeated orbit missions. The unexpected temporal variations of SSH, caused by some significant oceanographic phenomena during particular seasons or years, will be reduced by the time-averaged altimetric SSH data with repeated orbits for all available cycles. The selected reference tracks and the related collinear tracks are used to derive the mean track (see e.g. [24]). After determining the reference tracks, two methods are used to compute the SSH of each point of the collinear tracks, which corresponds to the point of the reference. One method is collinear analyses, and the other is to make geoid gradients corrections. In this study, the time-averaging of SSH is computed by the collinear analysis. In this method, along track SSH profiles are averaged to a regular grid (the cell size (called 'bin') is approximately 6×2 km) and the mean tracks or geoid is subtracted from each individual SSH. Further description of the SLA estimation using satellite altimetry data can be found in [24].

2.3. Reconciling GRACE and altimetry data

The GRACE and satellite altimetry data processing techniques are different and non-consistent. The important issues that affect consistency of the GRACE and satellite altimetry data are discussed below.

2.3.1. GRACE coefficients with degrees 0 and 1

GRACE data do not include degrees 0 and 1 spherical harmonic coefficients. The degree 0 coefficient represents the total mass of the Earth, and the position of the Earth's center of mass in a terrestrial reference frame is represented by the degree 1 terms. Regarding the degree 0 and 1 terms, the data reconciliation is important in the combination of satellite altimetry with the GRACE data. Because of the degree 0 coefficient (C_{00}) represents the total mass of the Earth, ΔC_{00} from GRACE can be assumed to be zero at all times [10], and the degree 1 coefficients are estimated from the variations of the Earth's center of mass proposed by [25]. Following Equation (2) below, we can convert geocenter variations $(\Delta x(t), \Delta y(t), \Delta z(t))$ to degree 1 gravity coefficient anomalies.

$$\begin{aligned} \Delta C_{10}(t) &= \frac{\Delta z(t)}{a\sqrt{3}} \\ \Delta C_{11}(t) &= \frac{\Delta x(t)}{a\sqrt{3}} \\ \Delta S_{11}(t) &= \frac{\Delta y(t)}{a\sqrt{3}} \end{aligned} \qquad (2)$$

where a is the mean Earth's radius.

2.3.2. GRACE coefficient with degree 2 and order 0

The Earth's oblateness which is represented by the degree 2 and order 0 coefficient (C_{20}) [26], has not been well observed by GRACE [13]. Because of Satellite Laser Ranging (SLR) time series are less noisy than the GRACE time series, Chen et al. have shown that the estimation of mass variations from GRACE is improved by using C_{20} coefficient estimation from the monthly SLR time series [27]. In this study, the monthly SLR estimates are used to replace the estimates from GRACE. The SLR time series for C_{20} coefficient are taken from J. Ries (personal communication, 2010).

2.3.3. Background barotropic model and ocean and atmospheric mass terms

The atmospheric mass and ocean barotropic variations are processed as departures from the GRACE time-variable gravity models. For oceanographic analysis, it is necessary to add back the modeled ocean and atmospheric mass variations to the GRACE data, which is also necessary for comparison with the altimetery data. This is done using models which are available in the GFZ processing center data set (see Section 3.1). Meanwhile, an inverted barometer correction (IB) is applied to altimeter data (e.g. [28]). The IB can be easily computed from the following formula:

$$IB = -9.948\ (P_0 - P_{ref}) \qquad (3)$$

where, IB is in mm and P_0 is the sea level pressure in mb. In this study, IB model is presented in which mean pressure (P_{ref}) is calculated using the local mean sea level pressure, which is adjusted for temporal variations in the global mean pressure of European Centre for Medium-Range Weather Forecasts (ECMWF), as the spatial average of the surface pressure over the global ocean [29]. To reconcile GRACE with altimetry, the IB correction is subtracted from the altimetery data.

3. Numerical Investigations

3.1. Ocean mass variation from GRACE

We estimate the ocean mass variation in the Nordic Seas using more than 8 years of GRACE level 2 RL04 data set released by GFZ processing center during the period October 2002 to October 2010, missing out the data for December 2002 and January 2003 and 2004 due to missing accelerometer data. RL04 coefficients are distributed on the level-2 data archives as GAC, GAD and GSM files (GAC, GAD and GSM are file extensions). The GSM files contain spherical harmonic coefficients representing the gravity field of the Earth.

The atmospheric and oceanic mass signals effects have been removed from these coefficients. The GAC and GAD files include the modeled atmospheric and oceanic contributions to the GSM coefficients. The GAC files include the global atmospheric and oceanic effects and the GAD files represent ocean bottom pressure variations. For comparison with the altimetry data, the modeled ocean and atmospheric mass variations should be added back to the GRACE data. Before computing the ocean mass variation, the modeled atmospheric and oceanic contributions could be restored to the GSM coefficients by adding the GAD and GAC coefficients.

Equation (1) which is used to compute the ocean mass variation is formulated to use gravity coefficients down to degree 0. As mentioned in Section 2.3.1, ΔC_{00} from GRACE can be assumed to be zero at all times and the degree 1 coefficients are estimated from the variations of the Earth's center of mass proposed by [25]. The monthly SLR estimates for C_{20} coefficient are used to replace the estimates from GRACE to complete the data reconciling step.

The monthly solutions of the GRACE when computing ocean mass variations include an unphysical striping error pattern which can be considered as noise and must be decorrelated/filtered. They have been filtered using Kusche et al. method by the corresponding Gaussian radius of 530 km [20].

Using Equation (1) and after the data reconciling, we estimate ocean mass variations in the Nordic Seas on a $0.5^{\circ} \times 0.5^{\circ}$ grid during the period October 2002 to October 2010. Next step is to form an approximate estimate of total mass change for each month, by summing over grid elements with cosine latitude weighting. Figure 2 shows the estimated ocean mass variations over the Nordic Seas using GRACE data. As mentioned above, the reconciled data have been decorrelated in the corresponding radius of 530 km. GRACE data reflects the postglacial rebound signal associated with mass transport in the study area. Using Paulson et al. model [23], the obtained estimates have also been corrected for the postglacial rebound signal.

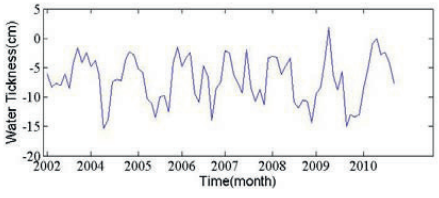

Fig 2. Ocean mass changes over the Nordic Seas during the period October 2002 to October 2010.

3.2. ENVISAT altimetry data

Using sea surface height data from the ENVISAT altimeter during October 2002 to October 2010, cycles 10 to 93, we estimate sea level anomaly over the Nordic Seas. In this study, sea surface height data retrieval and reduction are carried out using the Stackfiles database [30]. The sea surface height data in the Stackfiles database have been corrected for orbital altitude, instrument bias, sea state bias, ionospheric delay, dry and wet tropospheric corrections, solid Earth and ocean tides, ocean tide loading, pole tide, electromagnetic bias and inverse barometer correction. The corrections were done by applying specific models for each satellite altimetry missions in the Stackfiles database [30].

As mentioned in Section 2.2, we compute the mean tracks of ENVISAT altimeter, cycles 10 to 93, as shown in Figure 3. It should be noted that the presence of sea ice (such as in the East-Greenland Current, the Greenland Sea and in the Fram Strait) requires estimation of freeboard height in order to allow the mean sea surface to be determined from altimetry. The mean tracks of altimetry data in the sea ice areas have large standard deviations. In our study, we used the mean tracks with the standard deviation less than 50 cm in the sea ice area and therefore the masked areas in Figure 3 is resulted. Inverse barometer correction is subtracted from the altimetry-based sea surface height data, to be consistent with GRACE data that observe the real water mass signal. Glacial Isostatic Adjustment (GIA) causes a secular increase in the volume of the ocean basins, which reduces global mean sea level by approximately -0.3 mm/year [31]. Thus, in order to account for GIA, a l inear -0.3 mm/year correction is subtracted from the mean tracks.

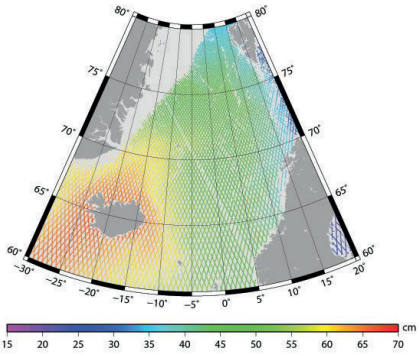

Fig 3. Mean tracks of ENVISAT altimeter over the Nordic Seas during October 2002 to October 2010

Subtracting the tracks from the mean tracks, the SLA is estimated for all the ENVISAT cycles. In addition, for

each cycle, the SLA is gridded on a $0.5^{\circ} \times 0.5^{\circ}$ grid using GEOGRID program [32].

Next step is to form an approximate estimate of total the SLA for each month, by summing over grid elements with cosine latitude weighting.

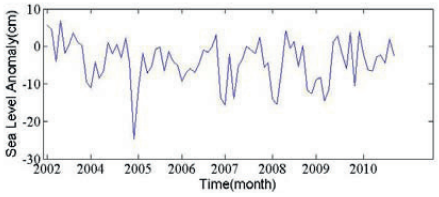

Fig 3. Sea level Anomaly changes over the Nordic Seas during October 2002 to October 2010.

3.3. Steric sea level change from ENVISAT and GRACE

Subtracting the SLA and the ocean mass variation in the Nordic Seas for each month, the Steric Sea Level Anomaly (SSLA) is estimated for each month. Figure 4 shows the variations of the SSLA over the Nordic Seas during October 2002 to October 2010.

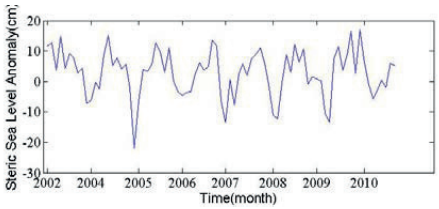

Fig 4. Steric sea level anomaly changes over the Nordic Seas during October 2002 to October 2010

4. Conclusion

Steric sea level variations over the Nordic Seas are determined from combined ENVISAT altimetry and GRACE data, at monthly interval, from October 2002 to October 2010. Note that this method provides an estimate of the total steric (thermosteric plus halosteric, for the entire water column) sea level anomaly variations. The combination of satellite altimetry with the ocean mass change observations from the GRACE mission offers a superior method for estimating the steric sea level changes over using altimetry alone, or in situ observations of temperature and salinity from the profiling floats to be used in the Argo float program. Several correction terms are applied in order to reconcile the GRACE data with ENVISAT altimetry data.

5. References

1. Fukumori I. 2002. A partitioned Kalman filter and smoother. *Monthly Weather Review* 130, 1370-1383
2. Carton J. A., Giese B. S. & Grodsky S. A. 2005. Sea level rise and the warming of the oceans in the Simple Ocean Data Assimilation (SODA) ocean reanalysis. *Journal of Geophysical Research* 110, C09006, doi:10.1029/2004JC002817
3. Levitus S., Antonov J. & Boyer T. 2005. Warming of the world ocean, 1955 – 2003. *Geophysical Research Letter* 32, L02604, doi:10.1029/2004GL021592.
4. Ishii M., Kimoto M., Sakamoto K. & Iwasaki S. I. 2006. Steric Sea Level Changes Estimated from Historical Ocean Subsurface Temperature and Salinity Analyses, *Journal of Oceanography* Vol. 62, pp. 155 to 170.
5. Conkright M. E., Antonov J. I., Baranova O. K., Boyer T. P., Garcia H E., Gelfeld R., Johnson D., Locarnini R. A., Murphy P. P., O'Brien T. D., Smolyar I. & Stephens C. 2002. *World Ocean Database 2001.* Washington, D. C.
6. Levitus S. 1982. *Climatological atlas of the world ocean.* NOAA Prof. Pap, 13, 173pp, U.S. Govt. Print. Off., Washington, D.C.
7. Lozier M., Owens W. & Curry R. 1995. The climatology of the North Atlantic. *Progress in Oceanography* 36, 1-44.
8. Ridgway K. R., Dunn J. R. & Wilkin J. L. 2002. Ocean interpolation by four-dimensional least squares - Application to the waters around Australia. *Journal of Atmospheric and Oceanic Technology* 19: 1357-1375
9. Roemmich D. & Sutton P. 1998. The mean and variability of ocean circulation past northern New Zealand: Determining the representativeness of hydrographic climatologies. *Journal of Geophysical Research* 103:13,041–13,054.
10. Wahr J, Molenaar M & Bryan F. 1998. Time variability of the Earth's gravity field: Hyrological and oceanic effects and their possible detection using GRACE. *Journal of Geophysical Research* 103(B12):30205-30229.
11. Ponte R. M. 1999. A preliminary model study of the large-scale seasonal cycle in bottom pressure over the global ocean. *Journal of Geophysical Research* 104, 1289– 1300.
12. Johnson T. J., Wilson C. R. & Chao B. F. 2001. Nontidal oceanic contributions to gravitational field changes: Predictions of the Parallel Ocean Climate Model. *Journal of Geophysical Research* 106, 11,315–11,334.
13. Tapley B. D., Bettadpur S, Watkins M. M. & Reigber C. 2004. The Gravity Recovery and Climate Experiment: Mission overview and early results. *Geophysical Research Letter* 31: L09607, doi: 10.1029/2004GL019920.
14. Chambers D. P. 2006. Observing seasonal steric sea level variations with GRACE and satellite altimetry.

Journal of Geophysical Research 111, C03010, doi:10.1029/2005JC002914.
15. Lombard A., Garcia D., Ramillien G., Cazenave A., Biancale R., Fletchner J. M., Schmidt R. & Ishii M. 2007. Estimation of steric sea level variations from combined GRACE and satellite altimetry data. *Earth and Planetary Science Letters* 254, 194–202.
16. Kuo C. Y., Shum C. K., Guo J. Y., Yi Y., Braun A., Fukumori I., Matsumoto K., Sato T. & Shibuya K. 2008. Southern Ocean Mass Variation Studies Using GRACE and Satellite Altimetry. *Earth, Planets and Space* 60,477-485.
17. Hurdle B. 1986. *The Nordic Seas*. Springer-Verlag, Berlin, Heidelberg, New. York, Tokyo.
18. Drange H., Dokken T., Furevik T., Gerdes R. & Berger W. 2005. From The Nordic Seas: An Integrated Perspective. *AGU Monograph 158*, American Geophysical Union, Washington DC, pp. 1-10.
19. Siegismund F., Johannessen J., Drange H., Mork K. A. & Korablev A. 2007, Steric height variability in the Nordic Seas. *Journal of Geophysical Research* 112, C12010, doi:10.1029/2007JC004221.
20. Kusche J., Schmidt R., Petrovic S. & Rietbroek R. 2009. Decorrelated GRACE time-variable gravity solutions by GFZ, and their validation using a hydrological model. *Journal of Geodesy* 83, 10, 903-913.
21. Kusche J, 2007. Approximate decorrelation and non-isotropic smoothing of time-variable GRACE-type gravity fields. *Journal of Geodesy* 81, 11, 733-749.
22. Joodaki G. & Nahavandchi H. 2012. Mass loss of the Greenland ice sheet from GRACE time-variable gravity measurements. *Studia Geophysica et Geodaetica*, DOI 10.1007/s11200-010-0091-x.
23. Paulson A., Zhong S. & Wahr J. 2007. Inference of mantle viscosity from GRACE and relative sea level data. *Geophysical Journal of International* 171, 497-508, doi:10.1111/j.1365-246X.2007.03556.x.
24. Ghazavi K. & Nahavandchi H. 2011. Mean Sea Surface and ocean circulation in North Atlantic and the Arctic Sea. *Journal of Geodetic Science* Vol. 1, No 2, pp. 181-190, DOI 10.2478/v10156-010-0021-4.
25. Chen J. L., Wilson C. R., Eanes R. J. & Nerem R. S. 1999. Geophysical interpretation of observed geocenter variations. *Journal of Geophysical Research* 104, 2683–2690.
26. Cox C. M. & Chao B. F. 2002. Detection of a large-scale mass redistribution in the terrestrial system since 1998, *Science* 297*,* 831.
27. Chen J. L., Wilson C. R., Famiglietti J. S. & Rodell M. 2005. Spatial sensitivity of GRACE time-variable gravity observations. *Journal of Geophysical Research* 110, B08408, doi:10.1029/2004JB003536.
28. Fu L. L. & Pihos G. 1994. Determining the response of sea level to atmospheric pressure forcing using TOPEX/POSEIDON data. *Journal of Geophysical Research* 99 (C12), pp. 24633–24642.
29. Ponte R. M., Salstein D. A. & Rosen R. D. 1991: Sea Level Response to Pressure Forcing in a Barotropic Numerical Model. *Journal of Physical Oceanography* 21, 1043–1057.
30. Yi Y. 2010. *The Ohio State University Stackfiles for Satellite Radar Altimeter data*, Report No. 495, The Ohio State University, USA.
31. Peltier W. R. 2004. Global glacial isostasy and the surface of the ice-age Earth: the ICE-5G (VM2) model and GRACE. *Annual Review of Earth and Planetary Science* 32, 111-149.
32. Forsberg R. 2003. *An Overview Manual for the GRAVSOFT Geodetic Gravity Field Modelling Programs*. Draft - 1st edition. Kort & Matrikelstyrelsen, Copenhagen.

Paper F

Gholamreza Joodaki, John Wahr, and Sean Swenson (2013), **Estimating the Human Contribution to Groundwater Depletion in the Middle East, from GRACE Data, Land Surface Models, and Well Observations**, Water Resources Research, under review.

Estimating the Human Contribution to Groundwater Depletion in the Middle East, from GRACE Data, Land Surface Models, and Well Observations

Gholamreza Joodaki[1], John Wahr[2], Sean Swenson[3]

[1] Division of Geomatics, Norwegian University of Science and Technology. N-7491 Trondheim, Norway (gholamreza.joodaki@ntnu.no)

[2] Department of Physics and Cooperative Institute for Environmental Sciences, University of Colorado, Boulder, Colorado, 80309, USA (john.wahr@gmail.com)

[3] National Center for Atmospheric Research, Boulder, Colorado, 80305, USA (swensosc@ucar.edu)

Corresponding Author:

Gholamreza Joodaki
gholamreza.joodaki@ntnu.no
(47)-735-94-715

Abstract

Data from the Gravity Recovery and Climate Experiment (GRACE) satellite mission are used to estimate monthly changes in total water storage across the Middle East during February 2003 to December 2012. The results show a large negative trend in total water storage centered over western Iran and eastern Iraq. Subtracting contributions from the Caspian Sea and two large lakes, Tharthar and Urmiah, and using output from a version of the CLM4.5 land surface model to remove contributions from soil moisture, snow, canopy storage, and river storage, we conclude that most of the long-term water loss is due to a decline in groundwater storage. By dividing the region into seven mascons outlined along national boundaries and fitting them to the data, we find that the largest groundwater depletion is occurring in Iran, with a mass loss rate of 25±6 Gt/yr during the study period. The conclusion of significant Iranian groundwater loss is further supported by in situ well data from across the country. Anthropogenic contributions to the groundwater loss are estimated by removing the natural variations in groundwater predicted by CLM4.5. These results indicate that over half of the groundwater loss in Iran (14±6 Gt/yr) may be attributed to human withdrawals.

Keywords: GRACE, Middle East, Groundwater, Hydrology Models, Well Observations

1. Introduction

The climate across most of the Middle East is hot and arid. Water scarcity, which has long been a serious problem in the region, has been a particularly challenging issue since the onset of a drought that began in 2007 (see, e.g., Trigo et al, 2010). According to a recent World Bank report [2007], about half the countries in this region are consuming more water on average than they receive in rainfall, and 85% of all water used in the Middle East is used for irrigation. Desertification is occurring throughout the region, especially in Iran, Iraq, Syria, and Jordan. A recent study by Voss et al [2013],

based on time-variable gravity data from the Gravity Recovery and Climate Experiment (GRACE), showed that during 2003-09 the north-central portion of the Middle East lost approximately 143.6 km^3 of total stored fresh water; a volume almost equal to that of the Dead Sea shared by Israel and Jordan. That study showed that the region lost 91.3 ± 10.9 km^3 of groundwater during 2003-09, of which 14.7 ± 9.3 km^3 was lost during 2003-06, and 76.9 ± 10.1 km^3 during 2007- 09 (i.e. since the onset of the 2007 drought).

Quantitative estimates of the temporal and spatial variability of present-day groundwater storage can be useful for managing sustainable water resources in this region. But reliable large-scale values are difficult to obtain from traditional in situ observational methods, due to the difficulty of using a relatively few scattered point measurements to infer regional variability. Satellite gravity data from GRACE [Tapley et al., 2004] can overcome this sampling problem, and can provide a useful tool for groundwater monitoring. In recent years, several research groups have used GRACE data to estimate groundwater depletion rates in various parts of the world (e.g. Tiwari et al. [2009]; Rodell et al. [2009]; Famiglietti et al. [2011]; Voss et al. [2013]). Here, we use 114 months of GRACE data (February, 2003 to December, 2012), to examine groundwater loss across the Middle East. This study extends the study of Voss et al. [2013], by (1) focusing on geographical subregions; (2) using output from an improved global land surface model to (a) remove soil moisture and other non-groundwater hydrological contributions from the GRACE water storage values to obtain groundwater estimates, and (b) to also remove naturally occurring groundwater variability to obtain estimates of anthropogenic contributions; and (3) by extending Voss et al.'s time span by an additional three years. We use a mascon analysis of the GRACE data (Tiwari et al. [2009]; Jacob et al. [2012]) to obtain time series for the variability in total water storage, total groundwater storage, and anthropogenic groundwater storage, in Iran, Iraq, Syria, eastern Turkey (east of 35° longitude), northern and southern Saudi Arabia (north and south of 25° latitude), and the region immediately west of the Caspian Sea. We compare our groundwater results for Iran with independent, Iranian groundwater estimates based on in situ observations of well levels.

2. Data, Models, and Analysis Methods

In this study, we use GRACE satellite gravity data to estimate total water storage (TWS) variability. To obtain total groundwater estimates, contributions from soil moisture, snow, and canopy and river storage estimated from a land surface model are removed from GRACE TWS. Anthropogenic groundwater changes are then estimated by removing the naturally occurring (i.e. climate-driven) groundwater changes predicted by the model, from the total groundwater estimates. Lake storage contributions, which are not estimated by the land surface model, are removed using altimeter lake level observations. For Iran, we compare our groundwater storage estimates with values, based on well data, that are available from the Iran Water Resources Management Company.

2.1. GRACE Data

The GRACE satellite mission was launched in March, 2002 by NASA and the German Aerospace Center (DLR) [Tapley et al., 2004a]. GRACE consists of two satellites, flying at an altitude of 450-500 km in identical near-polar orbits (89.5^{o} inclination), with a separation distance of about 250 km. Continuous microwave measurements of the range between the two satellites, combined with data from on-board accelerometers and Global Positioning System (GPS) receivers, are used by the GRACE Project to determine global, monthly solutions for the Earth's gravity field at scales of a few hundred kilometers and greater. Those fields are derived as monthly sets of spherical harmonic ("Stokes") coefficients, and are made publicly available by the GRACE Project. These coefficients can be used to estimate month-to-month changes in mass stored on or near the Earth's surface, integrated over regions of a few hundred km or larger in scale (e.g. Wahr et al. [1998]). The ability to observe an entire regional mass change without the need of spatial interpolation is a major strength of GRACE. But the lower bound on its resolution means that GRACE cannot determine precisely where the mass change within the region is coming from. In addition, GRACE can only deliver variations in water storage, not the total water storage itself.

This study uses 114 months, from February 2003 to December 2012, of GRACE Release 05 Stokes coefficients, from the Center for Space Research (CSR) at the

University of Texas (data available at http://podaac.jpl.nasa.gov). We replace the GRACE results for the lowest-degree zonal harmonic coefficient, $C_{20,}$ with those obtained from Satellite Laser Ranging [Cheng et al., 2013], and we include degree-one coefficients computed as described by Swenson et al. [2008]. The effects of Glacial Isostatic Adjustment (GIA) are small in this region, but are nevertheless removed by subtracting the GIA Stokes coefficients computed by A et al. [2013].

Figure 1a shows the trend in surface mass across the Middle East, fit over the entire 2003-2012 time span, inferred by simultaneously fitting a trend and seasonal terms to the GRACE data. The results have been smoothed by applying a Gaussian smoothing function with a 350-km radius [Wahr et al., 1998]. There is a positive signal localized over the Black Sea, and a uniform negative signal over the Caspian Sea. The presence of the Black Sea signal was unexpected, because the GRACE Project uses a global ocean model that includes the Black Sea to remove the ocean's gravity contributions from the raw GRACE data before solving for the Stokes coefficients. The Caspian Sea signal is not included in that model, so it is not surprising that Figure 1a shows a non-negligible signal there. Figure 1b is the same as Figure 1a, except with two modifications. One is that we have added the predictions of the ocean model back to the results. Note that the unexpected trend in the Black Sea has now vanished, indicating that it was a spurious trend, artificially introduced by removing an ocean model that evidently has errors in that region. The other modification is that we have removed the signal from the Caspian Sea and from two large lakes in the region: Lake Tharthar in Iraq and Lake Urmiah in Iran. We remove the Caspian Sea signal by computing the Stokes coefficients caused by a uniform one meter rise of the Caspian Sea, and then scaling those coefficients using monthly altimeter estimates (Birkett et al. [2009]; http://www.pecad.fas.usda.gov/cropexplorer/global_reservoir/) of the Caspian Sea surface height (see Swenson and Wahr, [2007]). We use this same procedure for the two lakes. Note, from Figure 1b, that the trend over the Caspian Sea has been dramatically reduced. The remaining trend that appears over the Caspian Sea is presumably caused by leakage from the adjacent land that is introduced by the 350-km Gaussian smoothing function. The trend over Iraq is also reduced. Lake Tharthar experienced a considerable water loss during this time period (see below), that was responsible for much of the

GRACE mass loss that appears over Iraq in Figure 1a. The mass loss from Lake Urmiah was much smaller. The most prominent feature in Figure 1b is the negative trend centered over eastern Iraq and western Iran, that is a clear indication of net water loss in that region. These results are consistent with those of Voss et al. [2013] for a shorter time period.

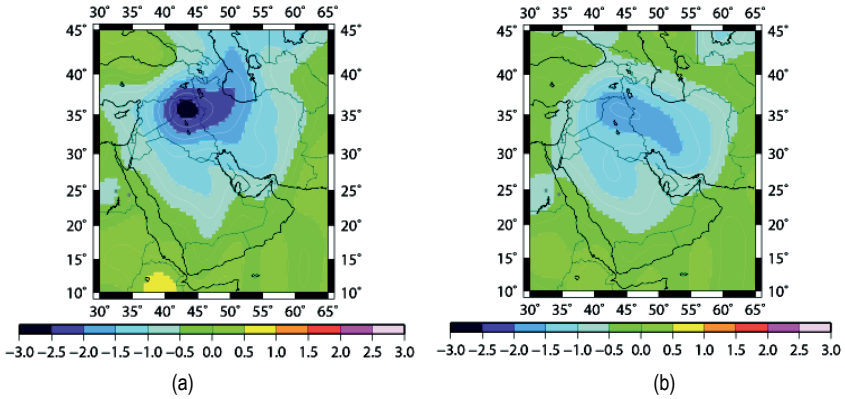

Figure 1. The 2003-2012 secular trend maps (cm/year) over the Middle East before (a) and after (b) removing the mass signals of the Caspian Sea, Lake Tharthar, and Lake Urmiah, and adding back the ocean model contribution that had apparently introduced a spurious positive trend over the Black Sea.

We use the GRACE data to construct time series for specific regions of the Middle East, chosen largely to coincide with political boundaries. The results, which will be described below, are computed by fitting "mascons" to the Stokes coefficients as described by Tiwari et al [2009] and Jacob et al [2012]. We subdivide the entire region into seven mascons: Iran, Iraq, Syria, eastern Turkey, northern Saudi Arabia, southern Saudi Arabia, and the area immediately west of the Caspian Sea, and we fit mass amplitudes for each of these mascons, simultaneously, to the monthly data. We thereby obtain monthly times series of mass variability for each of those regions during 2003-2012. When fitting the mascons to the GRACE Stokes coefficients, Tiwari et al first applied a decorrelation filter to the coefficients and smoothed them with a 250 km Gaussian; Jacob et al did not apply a decorrelation filter, but did use a 150 km Gaussian smoothing function. In this study, we did not use a decorrelation filter, but we did use a 100 km Gaussian smoothing function.

Because GRACE data have finite resolution, it is impossible to obtain a perfect unweighted average of mass variability within a region, no matter what technique is used for the GRACE analysis or what region is considered. A GRACE estimate for the mass change in Iran, for example, will include contamination from mass variations outside Iran, and will not weight every point inside Iran equally.

Results from a mascon fitting method are no exception. Let M be the mass solution for a mascon as inferred by fitting to the GRACE Stokes coefficients, and let $\sigma(\theta,\phi)$ be the true surface mass at co-latitude θ and longitude ϕ. Because the least squares fitting process is linear, there must be a linear relation between M and the point values of $\sigma(\theta,\phi)$:

$$M = \int \Delta\sigma(\theta,\phi)\, A(\theta,\phi)\, a^2 \sin\theta\, d\theta\, d\phi \qquad (1)$$

where the integral is over the entire Earth (a is the Earth's radius), and where the mascon's sensitivity kernel, $A(\theta,\phi)$, describes how the GRACE mass estimate, M, samples the surface mass at any point (θ,ϕ). In the ideal case, $A(\theta,\phi)$ would equal 1 for points inside the mascon and 0 outside. But, given the limitations of GRACE, any actual GRACE analysis will cause $A(\theta,\phi)$ to differ from that ideal. Both Tiwari et al and Jacob et al (see their Supplementary Information) show how to find $A(\theta,\phi)$ when M is obtained by fitting mascons to GRACE Stokes coefficients. Figure 2, for example, shows our sensitivity kernel for the Iran mascon, when fitting all seven mascons to the Stokes coefficients. The kernel's value is small outside Iran and is close to unity inside Iran, but it does depart somewhat from those ideal values. We apply this sensitivity kernel, below, to the well data when comparing those data with our GRACE solutions.

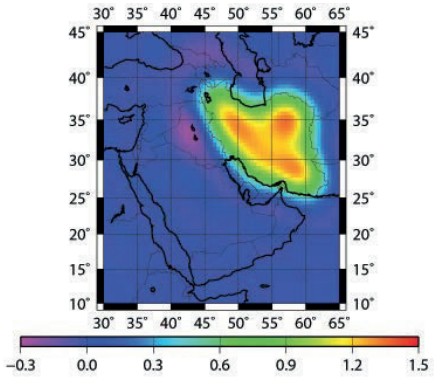

Figure 2. The sensitivity kernel for Iran.

2.2. Land Surface Model

GRACE data have no vertical resolution, in the sense that it is impossible to use the GRACE data alone to determine how much of the mass variability comes from surface water or snow, how much comes from water stored in the soil, and how much comes from water in the sub-soil layers (i.e. from groundwater). Because our primary goal is to isolate the changes in groundwater storage, it is necessary to first remove estimates of the other water storage components. We do this using monthly output from a global, gridded land surface model. For this, we use version 4.5 of the Community Land Model (Oleson et al. [2013]). CLM4.5, the terrestrial component of the Community Earth System Model (CESM1) [Gent et al., 2011], simulates the partitioning of mass and energy from the atmosphere, the redistribution of mass and energy within the land surface, and the export of fresh water and heat to the oceans. To realistically simulate these interactions, CLM4.5 includes terrestrial hydrological processes such as interception of precipitation by the vegetation canopy, throughfall, infiltration, surface and subsurface runoff, snow and soil moisture evolution, evaporation from soil and vegetation and transpiration [Oleson et al., 2013]. The version of CLM4.5 used in this study includes a modified soil evaporative resistance parameterization [Swenson et al. 2013, in prep], and is operated in offline mode, in which the atmospheric inputs are taken from the CRUNCEP dataset [Viovy, N.: CRUNCEP data set V4, http://dods.extra.cea.fr/data/p529viov/cruncep/, last access: 27 July 2013]. The precipitation inputs are bias-corrected using merged satellite- gauge precipitation

analyses from the Global Precipitation Climatology Project (GPCP) (Huffman et al. [1997]). Components of terrestrial water storage output by the model include soil moisture, snow, vegetation canopy storage, channel storage in rivers, and unconfined aquifer storage.

Monthly Stokes coefficients are obtained for the model by transforming the gridded model output into spherical harmonics, and transforming the resulting mass coefficients into gravity coefficients. We combine the model with GRACE to obtain estimates of changes in the total groundwater by subtracting soil moisture + snow + canopy + river storage (SSCR) from the GRACE total water storage results; and we estimate anthropogenic changes in groundwater by further subtracting the model results for naturally occurring groundwater variations.

2.3. Well Data

We compare our GRACE estimates for Iran with Iranian groundwater estimates obtained from 562 active observation wells, used to monitor the level and quality of groundwater across the country. The observations are archived by the Iran Water Resources Management Company and are publicly available at http://wrs.wrm.ir/. The archived data are categorized based on Iran's provinces and are given at yearly intervals, where Iran's water year is defined as the period between October 1st of one year and September 30th of the next. Each well is identified in the data set as representing a single aquifer, and each yearly data value is given as an area-average, computed as the area of the aquifer times the change in aquifer depth.

Taken together, the aquifers reported in the data set do not cover all of Iran, and so the sum of the area-averages for all the wells will underestimate the total change in water storage. Only 13% of the total area of Iran is covered by these reported aquifers. To correct for this undersampling, we add together the area-averages of the well data in each province separately to obtain an initial, but undersampled, estimate of the groundwater change in that province, and we then scale up each provincial estimate by multiplying it by the ratio: $\left(\frac{\text{total area of the province}}{\text{area of all the reported aquifers in that province}}\right)$. We add all these scaled provincial estimates together to obtain estimates for the total Iranian groundwater

change at yearly intervals. It is quite possible that the reported aquifers tend to be those with the most potential for groundwater loss. If so, then our scaling process would result in an overestimate of the mass loss.

We use two methods to add these scaled provincial values together. In one method, we sum them with equal weighting to give a true areal average of the total groundwater change in Iran. In the other method, we weight each provincial estimate using the GRACE Iranian sensitivity kernel shown in Figure 2. The results from this latter method can be compared directly with the GRACE Iranian estimates, since then both the well results and the GRACE results sample the Earth's groundwater storage in the same way. There is a caveat: the GRACE sensitivity kernel for Iran extends outside the country. Because there are no well data from outside Iran, the final well estimates are missing those external contributions. However, because the sensitivity kernel weights are small outside of Iran, we expect these contributions to be small.

3. Results

3.1. Spatial dependence of groundwater storage

Figure 1b shows a large negative trend in the GRACE total water storage estimates, centered over western Iran and eastern Iraq. To isolate the groundwater contributions, we subtract the modeled SSCR, and show the results in Figure 3. This map, which represents the trend in total groundwater storage, still shows large negative values over western Iran and eastern Iraq, indicating that the contribution to the trend in TWS from the SSCR components is relatively small.

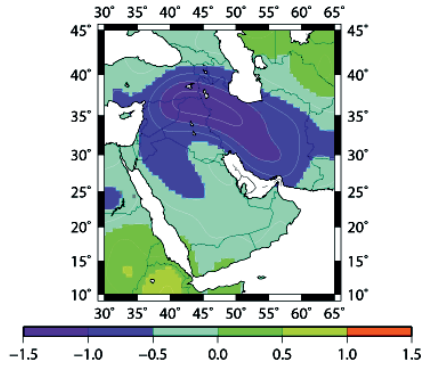

Figure 3. Secular trend in groundwater (cm/yr) during 2003-2012, computed by subtracting CLM4.5 modeled soil moisture + snow + canopy + river storage (SSCR) from the GRACE total water storage results (CLM4.5 groundwater not subtracted).

To separate the groundwater variations into naturally occurring and anthropogenic components, we subtract the CLM4.5 2003-2012 groundwater trend (which does not explicitly model anthropogenic contributions), shown in Figure 4a, from the GRACE-minus- SSCR total groundwater trend shown in Figure 3. The result, shown in Figure 4b, represents anthropogenic groundwater variations.

Note that each map (total water storage, total groundwater, naturally occurring groundwater, and anthropogenic groundwater) shows a notable negative trend over Iran. Negative trends in total water storage and in naturally occurring groundwater storage are indications of drought.

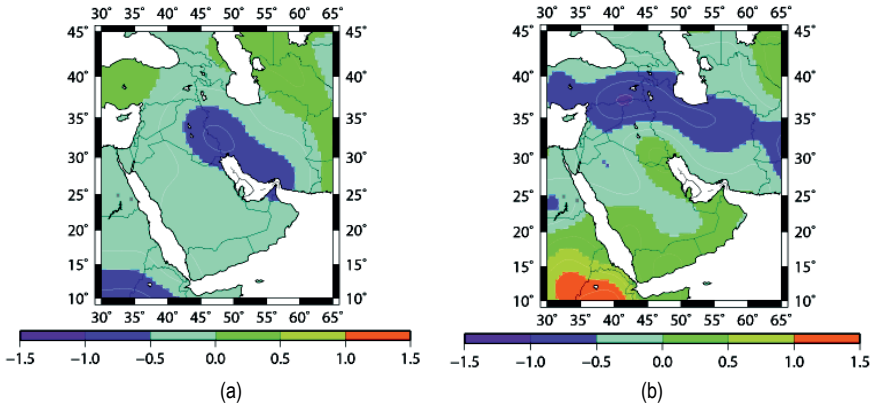

Figure 4. Secular trend (cm/year) in naturally occurring (a) and anthropogenic (b) groundwater during 2003-2012. The naturally occurring trend is estimated from the CLM4.5 groundwater results (which do not include anthropogenic contributions). The anthropogenic trend is estimated by subtracting the CLM4.5 groundwater component from the GRACE-minus-SSCR) total groundwater trend shown in Figure 3.

It is plausible that those negative trends would be accompanied by a negative anthropogenic trend, because when drought occurs in an already dry region, increased groundwater extraction can supply the precipitation deficit required to maintain agricultural productivity. On the other hand, land surface models might not accurately reproduce changes in individual storage components, particularly in ground water, at regional scales. Therefore, it is prudent to question the accuracy of the anthropogenic groundwater trends shown in Figure 4b. This will be discussed below.

3.2. Time series estimates

Figure 5a compares our GRACE estimate of total water storage variability for all Iran, with our corresponding SSCR + groundwater estimate from the CLM4.5 model. The black and red curves show result that have been smoothed to reduce sub-seasonal noise; the blue and green curves show the long-period (i.e. interannual and secular) components of the black and red curves. Note that the GRACE and model results agree well at seasonal periods, and they both show a sharp decrease in water storage that started with the onset of the drought, in 2007. The model results seem to have leveled off, and even recovered some, by 2009. The GRACE results, however, show a continuing water loss. Since CLM4.5 does not include an anthropogenic component, we will interpret (below) the increasing difference between GRACE and CLM4.5 as evidence of post-2007 anthropogenic groundwater loss.

The GRACE results for Iraq, eastern Turkey, and northern and southern Saudi Arabia (Figure 5b) all show a similar abrupt decrease in 2007. In eastern Turkey the GRACE results subsequently recover, though not as rapidly as the CLM4.5 results.

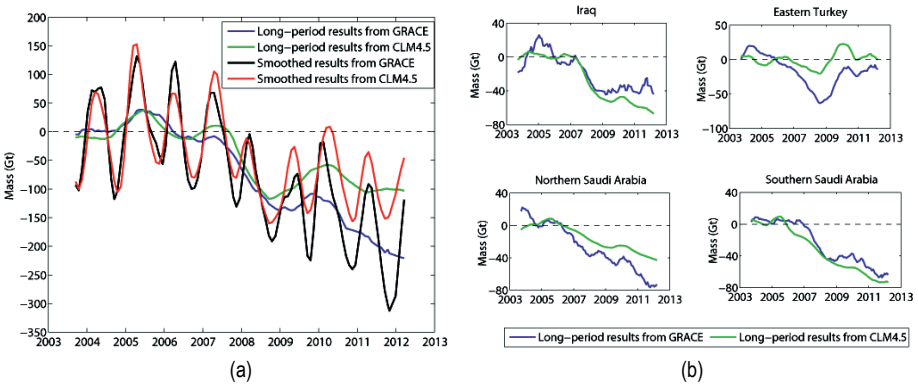

Figure 5. Changes in water storage, in gton, for (a) all Iran; and (b) Iraq, eastern Turkey, and northern and southern Saudi Arabia. The black and red curves show results that have been smoothed to reduce sub-seasonal noise; the blue and green curves show the long-period components of the black and red curves.

Figure 6a shows our estimate of water storage variability, in gtons, for all Iran. As shown in the figure, subtracting the modeled SSCR removes virtually all the seasonal terms in the GRACE estimates of total water storage. The GRACE-minus-SSCR results (red line) consist mainly of short-period, seemingly random fluctuations, superimposed on long-period variability. The short period fluctuations represent the effects of GRACE measurement errors and month-to-month errors in the modeled water storage quantities. The long-period variability, which stands out more clearly after smoothing the GRACE-minus-SSCR results (Figure 6b), represents changes in total groundwater storage. The most obvious characteristic of that variability is a steady groundwater loss during this 10-year period.

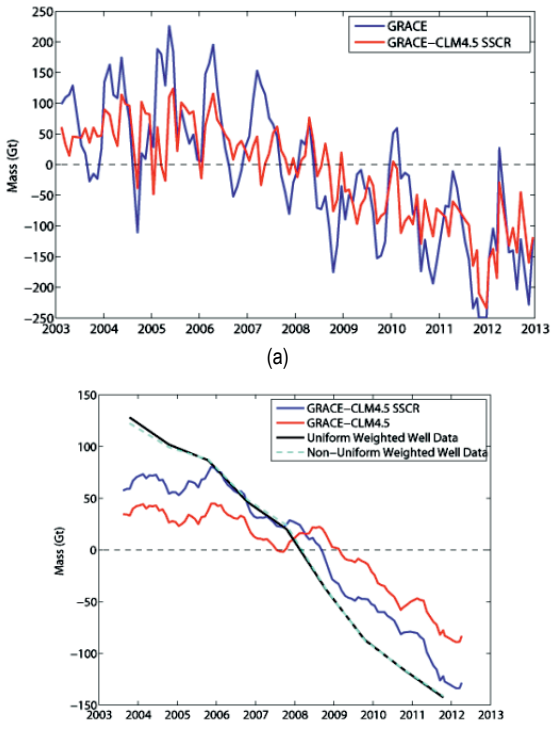

Figure 6. Changes in water storage, for all Iran. (a) monthly values of the total water storage from GRACE, and the groundwater storage inferred from GRACE-minus-(CLM4.5 SSCR). (b) Smoothed monthly values of groundwater storage inferred from GRACE-minus- (CLM4.5 SSCR), compared with the anthropogenic groundwater component (GRACE-CLM4.5), and with yearly values inferred from the well data. The well data values are shown using both uniform weighting, and weighting in a manner that's consistent with the GRACE sensitivity kernel.

The estimates from the well data also show a steady loss of total groundwater during this period, though (see Table 1) the secular trend of the well-based estimates, computed using the GRACE sensitivity kernel, is about 45% more negative than the trend in the GRACE-minus-SSCR results (-36 gt/yr versus -25±6 gt/yr). This difference in trends could be due to errors in the modeled SSCR trends; or, perhaps more importantly, to the overestimate in the trend that could be introduced by our method of scaling the reported aquifer results to correct for their incomplete spatial coverage. Because we have extrapolated the well data to the entire surface area of Iran, the trend from the well data represents an upper bound on the groundwater loss.

The uncertainties given on the GRACE trends in Table 1 are an attempt to account both for measurement errors in the GRACE data, and for errors in the CLM4.5 model output. We assume the GRACE measurement errors are largely uncorrelated from one month to the next, and estimate their contribution to the uncertainty as the 2-sigma formal error of the trend estimate. The land surface model errors are likely to have systematic components, and so are more difficult to estimate. Previous studies have estimated model errors by comparing multiple land surface models (see, e.g. Tiwari et al. [2009]; Jacob et al. [2012]). In this study, we abandoned this approach because the other models we considered performed poorly in this region. Our assessment of model performance was based on how well the model was able to reproduce the seasonal variability in the GRACE data. The CLM4.5 simulation gave a reasonably good match to the GRACE seasonal variability in this region, but this was not true for the other models we examined.

Instead, we use the differences between the CLM4.5 and GRACE seasonal variability to infer an uncertainty on the CLM4.5 trends. To each mascon time series, we fit 12-month and 6-month periodic terms to both the GRACE data and the total CLM4.5 water storage output (SSCR + naturally varying groundwater) across a 13-month sliding window, to extract a seasonally varying time series from both data sets. We subtract the CLM4.5 time series from the GRACE time series, to obtain a seasonally varying residual time series for each mascon. We find the RMS of the seasonal GRACE time series, and the RMS of the residual time series, and form the ratio $R = RMS_{residual} / RMS_{GRACE}$. We make the assumption that there is no seasonal variability in the anthropogenic signal (which is missing from CLM4.5), so that the residual seasonal signal should vanish. In that case, R is a measure of the relative error in the seasonal component of CLM4.5. We assume the relative error of the CLM4.5 trend is given by this same ratio, so that the uncertainty on the trend from the land surface model is $\pm R \times$ trend. Because we are comparing the GRACE results with the total (SSCR + groundwater) CLM4.5 output to obtain this uncertainty, this uncertainty should be interpreted as the uncertainty of the total CLM4.5 water storage. But, we will also use it as the uncertainty on just the SSCR component, alone. The model uncertainty

and the measurement uncertainty are then added in quadrature to get the total uncertainty estimates given in Table 1.

Note, from the dashed light-blue and solid black lines in Figure 6b (see, also, Table 1), that the well data give virtually the same results whether or not the GRACE sensitivity kernel is used when computing the spatial average. So, if the spatial pattern of the signal that is present in the in situ well data is a reasonably accurate representation of the true spatial pattern of groundwater loss, then the fact that the GRACE sensitivity kernel is not an exact kernel probably doesn't significantly impact the GRACE Iran results, either. And it suggests, though does not prove, that the GRACE groundwater estimates for other countries in the region (see below), where there are no in situ groundwater measurements to compare with, might be similarly unaffected by the fact that the GRACE sensitivity kernels differ from the uniformly weighted kernels.

The general agreement between the well data and the GRACE-minus-SSCR estimates for Iran, gives us confidence in the overall trends of our GRACE-minus-SSCR groundwater time series for regions in the Middle East other than Iran. Figure 7 shows the smoothed GRACE-minus-SSCR results for eastern Turkey, Iraq, and northern and southern Saudi Arabia, and Table 1 lists the trends for those regions.

Table 1. Secular trends, in Gt/yr, of the total groundwater storage (GRACE-minus- CLM4.5 SSCR) for Iran and the other regions, for 2003-2012. Results for Iran are compared with estimates based on well data.

Region	GRACE-minus- CLM4.5 SSCR	Non Uniformly Weighted Well Data	Uniformly Weighted Well Data
Iran	-25±6	-36	-35
Iraq	-2±3	N/A	N/A
Eastern Turkey	-5±2	N/A	N/A
Northern Saudi Arabia	-6±5	N/A	N/A
Southern Saudi Arabia	-5±2	N/A	N/A

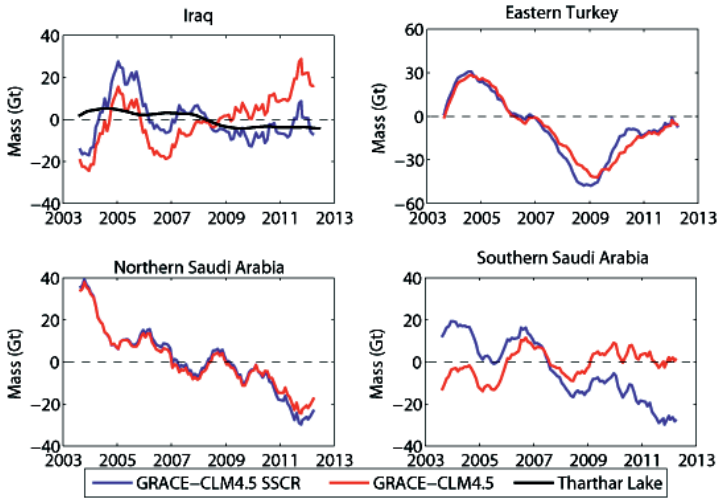

Figure 7. Changes in total groundwater storage, integrated across Iraq, eastern Turkey, and northern and southern Saudi Arabia. Shown are smoothed monthly values of the total groundwater storage inferred from GRACE – minus – (CLM4.5 SSCR), compared with the anthropogenic groundwater component (GRACE-minus-CLM4.5). We have removed the effects of Iraq's Lake Tharthar from the GRACE fields, prior to solving for these mass results. The lake's variable mass is included on the Iraq time series plot, to illustrate the relative amplitude of that signal.

Note that the groundwater loss for Iraq is only -2±3 gt/yr. The GRACE total water storage estimates (Figure 1a), though, do show a notable total water loss over Iraq. The explanation is that the trend in total water loss in Iraq is dominated by water loss in Lake Tharthar. When the contributions from that lake are removed, the trend across Iraq is greatly diminished (Figure 1b), leaving the Iraq results shown in Figure 7 and Table 1. The water loss from Lake Tharthar (as inferred from the altimeter results described above) is included in Figure 6 to show that its long-term variability is roughly the same as the groundwater variability in Iraq. The 2003- 2012 trend in the Lake Tharthar water storage is -2 gt/yr.

3.2. Anthropogenic contributions

Anthropogenic trends during 2003-2012 are shown in Figure 4b, computed by subtracting the total CLM4.5 water storage (SSCR + naturally occurring aquifer storage) estimates from the GRACE results, after the contributions from Lake Tharthar, Lake Urmiah, and the Caspian Sea have been removed. Anthropogenic groundwater

loss is evident across most of the region, focused particularly in a band running across eastern Turkey, northern Iraq, and northern Iran. Note that there are also isolated pockets of groundwater increases, including a positive feature centered near the southern edge of the Iran/Iraq border, where the Shaat al-Arab River in Iraq (formed by the combination of the Tigris and Euphrates Rivers), and the Karun River in Iran, flow into the Persian Gulf. There are also positive trends running along the southern coastline of the Arabian Peninsula. It is reasonable to wonder if these positive features are caused by positive trends in the adjacent ocean, leaking into the solutions over land. This is of particular concern here, because we have added the ocean model predictions back to the GRACE gravity fields to remove the spurious Black Sea trend evident in Figure 1a. But when we compute the anthropogenic trends without adding back the ocean model predictions, the resulting map looks almost identical to Figure 4b. Furthermore, when Figure 4b is re-plotted so that the ocean is not blanked out, the positive features in Figure 4b are seen to be centered over land.

Anthropogenic increases in groundwater are certainly possible. Increased use of river water for broad-scale irrigation, for example, can cause increased groundwater recharge. Perhaps this is the explanation for the positive feature centered near the northern end of the Persian Gulf. In fact, it has been reported that the water table in this area of Iran has been rising by up to 15 cm/yr in places (Agriculture Bank of Iran, 2009). Still, the presence of these apparent anthropogenic increases, combined with the difficulty of modeling the naturally occurring groundwater variability that has been subtracted from GRACE to produce the results shown in Figure 4b, suggest caution when interpreting the apparent anthropogenic results in this region.

Keeping that caveat in mind, we show time series (Figures 6b and 7) for the anthropogenic groundwater over each region, computed by fitting mascons to the GRACE-minus-CLM4.5 Stokes coefficients, where “CLM4.5” in this case refers to the sum of the SSCR and naturally occurring groundwater components. As always, the effects of the Caspian Sea, Lake Tharthar, and Lake Urmiah, have been removed. Trends for 2003-2012 are given in Table 2. The only regions where the anthropogenic change differs from zero by more than the uncertainty are eastern Turkey and Iran. Both those regions show anthropogenic mass loss.

Note that although we have fit a secular trend to each time series, some of those time series are dominated by long-period signals that don't look much like a trend. The most obvious case is eastern Turkey, where the long-period total groundwater and anthropogenic groundwater signals appear to consist mostly of a decadal-scale periodic term. The origin of this term can be seen in the eastern Turkey GRACE and CLM4.5 total water storage results shown in Figure 5b. Note that the GRACE water storage results decrease rapidly in 2007, and recover slowly; but they do recover, in contrast to the results from the other regions. The CLM4.5 results show a much milder decrease in 2007, followed by a quick recovery. One interpretation is that because eastern Turkey has a relatively high precipitation rate, its natural and anthropogenic groundwater losses can be replenished more rapidly than those in, say, Iran, where the average precipitation rates are lower.

Table 2. Secular trends, in Gt/yr, of anthropogenic groundwater (GRACE – CLM4.5) during 2003-2012.

Region	Secular Trend
Iran	-14 ± 6
Iraq	3 ± 3
Eastern Turkey	-6 ± 2
North Saudi Arabia	-5 ± 5
South Saudi Arabia	2 ± 2

Summary and Conclusion

Irrigation is heavily used in the Middle East to increase agricultural productivity during times of drought. A recent drought occurring in 2007 highlighted the need for sustainable management of water resources. When precipitation is insufficient, surface water stored in rivers, lakes, and reservoirs may provide additional water for irrigation. However, these resources are not available throughout the region, and in their absence, groundwater can be used to reduce water deficits. In many cases, groundwater resources are non-renewable, and monitoring the rates at which they are utilized is important for planning purposes.

In this study, GRACE data are used to monitor monthly changes in total water storage (groundwater plus soil moisture plus surface water and snow) across the Middle East. Results from February 2003 to December 2012 show a prominent, negative trend

in total water storage centered over western Iran and eastern Iraq. This had been noted earlier by Voss et al [2013], using 2003-09 GRACE data. After subtracting soil moisture + snow + canopy storage + river storage changes predicted by a modified version of the CLM4.5 hydrological model, and removing contributions from the Caspian Sea and from two large lakes in the region, we find that most of the long-term, sub-surface water loss is due to a decline in groundwater storage.

By dividing the Middle East into regions outlined along national boundaries, and solving for the rate of change of groundwater volume within each region, we find that Iran experienced considerable groundwater loss during this period, at an average rate of 25±6 Gt/yr. An analysis of in situ well data from across Iran further supports the conclusion of significant groundwater loss. In fact, our well data estimate of groundwater loss is roughly 45% larger than our GRACE estimate; though we suspect that our well-based rate is overestimated due to the scaling method we use to correct the well data for spatial undersampling.

The GRACE-minus-model results show that other regions in the Middle East lost groundwater during 2003-2012. Our estimated rates of groundwater loss in Iraq, eastern Turkey (east of 35° longitude), northern Saudi Arabia, and southern Saudi Arabia (north and south of 25° latitude), are 2±3 Gt/yr, 5±2 Gt/yr, 6±3 Gt/yr, and 5±2 Gt/yr, respectively.

These estimates represent the combined effects of natural climate variability (e.g. drought) and human activities. Because CLM4.5 also includes an unconfined aquifer store, we can estimate anthropogenic groundwater trends by subtracting the CLM4.5 predictions of naturally occurring groundwater change from our total groundwater change estimates. Although the relative uncertainty in the residual time series is higher, the results tentatively suggest that there was significant anthropogenic groundwater loss in Iran and eastern Turkey during 2003-2012, much of which occurred during and after 2007. In eastern Turkey, where annual precipitation is greater, groundwater appears by 2013 to have nearly recovered to pre-2007 levels. In contrast, groundwater levels in Iran do not appear to have attained pre-2007 levels, implying that a subsequent drought will further reduce groundwater resources in that region.

Acknowledgements. This work was conducted while G.J. was on an extended visit to the University of Colorado (CU), supported by the Norwegian University of Science and Technology (NTNU). We thank Geruo A for providing GIA corrections to the GRACE data. This project was partially supported by NASA GRACE funding, and by NASA's 'Making Earth Science Data Records for Use in Research Environments (MEaSUREs) Program'.

References

A, G., J. Wahr, and, S. Zhong (2013), Computations of the viscoelastic response of a 3-D compressible Earth to surface loading: an application to Glacial Isostatic Adjustment in Antarctica and Canada. Geophysical Journal International, 192:557–572, doi: 10.1093/gji/ggs030.

Agriculture Bank of Iran (2009), Weather, climate and water resources in Khuzestan province, The Economic Studies and Analysis Department (ESAD) report.

Birkett, C. M., Reynolds, C., Beckley, B. and Doorn, B. 2009. "From research to operations: The USDA global reservoir and lake monitor". In *Coastal altimetry*, Heidelberg: Springer Verlag.

Cheng, M.K., B. D. Tapley, and J. C. Ries (2013), Deceleration in the Earth's oblateness, Journal of Geophysical Research, V118, 1-8, doi:10.1002/jgrb.50058.

Famiglietti, J. S., M. Lo, S. L. Ho, J. Bethune, K. J. Anderson, T. H. Syed, S. C. Swenson, C. R. de Linage, and M. Rodell (2011), Satellites measure recent rates of groundwater depletion in California's Central Valley, Geophysical Research Letter, 38, L03403, doi: 10.1029/2010GL046442.

Gent, P.R. et al., 2011, The Community Climate System Model version 4, J. Clim., 24 4973-91.

Huffman, G. J., R. F. Adler, P. Arkin, A. Chang, R. Ferraro, A. Gruber, J. Janowiak, A. McNab, B. Rudolf and U. Schneider, The Global Precipitation Climatology Project (GPCP) Combined Precipitation Dataset, Bull. Amer. Meteor. Soc., 78(1), p5-20,1997.

Jacob, T., J. Wahr, W. Tad Pfeffer, and S. Swenson (2012), Recent contributions of glaciers and ice caps to sea level rise, Nature, 482, 514–518 doi: 10.1038/nature10847.

Oleson, K.W., D.M. Lawrence, G.B. Bonan, B. Drewniak, M. Huang, C.D. Koven, S. Levis, F. Li, W.J. Riley, Z.M. Subin, S.C. Swenson, P.E. Thornton, A. Bozbiyik, R. Fisher, C.L. Heald, E. Kluzek, J.-F. Lamarque, P.J. Lawrence, L.R. Leung, W. Lipscomb, S. Muszala, D.M. Ricciuto, W. Sacks, Y. Sun, J. Tang, and Z.-L. Yang, 2013: Technical description of version 4.5 of the Community Land Model (CLM), NCAR Technical Note NCAR/TN-503+STR, 434 pp.

Oleson, K. W., G. Y. Niu, Z. L. Yang, D. M. Lawrence, P. E. Thornton, P. J. Lawrence, R. Stockli, R. E. Dickinson, G. B. Bonan, S. Levis, A. Dai, and T. Qian (2008), Improvements to the Community Land Model and their impact on the hydrological cycle, Journal of Geophysical Research, 113, G01021, doi: 10.1029/2007JG000563.

Qian, T.T., Dai, A., Trenberth, K.E., & Oleson, K.W., Simulation of global land surface conditions from 1948 to 2004. Part I: Forcing data and evaluations. Journal of Hydrometeorology 7, 953-975 (2006).

Rodell, M., P. R. Houser, U. Jambor, J. Gottschalck, K. Mitchell, C. J. Meng, K. Arsenault, B. Cosgrove, J. Radakovich, M. Bosilovich, J. K. Entin, J. P. Walker, D. Lohmann, and D. Toll (2004), The Global Land Data Assimilation System, American Meteorological Society, doi: 10.1175/BAMS-85-3-381.

Rodell, M., I. Velicogna, and J.S. Famiglietti (2009), Satellite-based estimates of groundwater depletion in India, Nature, 460, 999-1002, doi: 10.1038/460789a.

Swenson, S., and J. Wahr (2007), Multi-sensor analysis of water storage variations of the Caspian Sea, Geophysical Research Letter, 34, L16401, doi: 10.1029/2007GL030733.

Swenson, S., D. Chambers, and J. Wahr (2008), Estimating geocenter variations from a combination of GRACE and ocean model output, J. Geophys. Res., 113, B08410, doi: 10.1029/2007JB005338.

Tapley, B. D., S. Bettadpur, M. Watkins, and C. Reigber (2004a), The gravity recovery and climate experiment: Mission overview and early results, Geophysical Research Letter, 31, L09607, doi: 10.1029/2004GL019920.

Tapley B.D., S Bettadpur, J. C. Ries, P. F. Thompson, and M. M. Watkins (2004b), GRACE measurements of mass variability in the Earth system. Science, 305:503-505.

Tiwari, V. M., J. Wahr, and S. Swenson (2009), Dwindling groundwater resources in northern India, from satellite gravity observations, Geophysical Research. Letter, 36, L18401, doi: 10.1029/2009GL039401.

Trigo, R.M., C.M. Gouveia, and D. Barriopedro (2010). The intense 2007–2009 drought in the Fertile Crescent: Impact and associated atmospheric circulation. Agric For Meteorol 150, 1245–1257.

Voss, K. A., J. S. Famiglietti, M. Lo, C. de Linage, M. Rodell, and S. C. Swenson (2013), Groundwater depletion in the Middle East from GRACE with implications for transboundary water management in the Tigris-Euphrates-Western Iran region, Water Resource Research, 49, doi:10.1002/wrcr.20078.

Wahr, J., M. Molenaar, and F. Bryan (1998), Time-Variability of the Earth's Gravity Field: Hydro- logical and Oceanic Effects and Their Possible Detection Using GRACE, Journal of Geophysical Research, 103, 30205-30230.

Wahr, J., S. Swenson, and I. Velicogna (2006), The Accuracy of GRACE Mass Estimates. Geophys. Res. Lett., 33, L06401, doi:10.1029/2005GL025305.

World Bank (2007), Making the Most of Scarcity Accountability for Better Water Management Results in the Middle East and North Africa, The MENA Development report.